UNIVERSITY OF SANTIAGO DE COMPOSTELA

SCHOOL OF ENGINEERING (E.T.S.E.)

Department of Chemical Engineering

DESULFURIZATION OF FUELS WITH IONIC LIQUIDS BY EXTRACTION AND OXIDATIVE EXTRACTION PROCESSES

A thesis submitted by BORJA RODRÍGUEZ CABO for the degree of Doctor in Chemical and Environmental Engineering to the University of Santiago de Compostela

Santiago de Compostela, November 2013

Authorization for submission by the thesis directors (in Spanish)

Alberto Arce Arce, Catedrático de Ingeniería Química, **Ana M. Soto Campos**, Catedrática de Ingeniería Química, y **Eva Rodíl Rodríguez**, Profesora titular de Ingeniería Química

INFORMAN:

Que la presente memoria titulada *"Desulfurization of fuels with ionic liquids by extraction and oxidative extraction processes"*, que para optar al grado de Doctor en Ingeniería Química, Programa de Doctorado de Ingeniería Química y Ambiental, presenta **Borja Rodríguez Cabo,** fue realizada bajo nuestra inmediata dirección en el Departamento de Ingeniería Química de la Universidad de Santiago de Compostela.

Considerando que constituye trabajo de Tesis, autorizan su presentación al Centro de Postgrado de la Universidad de Santiago de Compostela.

Y para que así conste, firman el presente informe en Santiago de Compostela a 4 de Noviembre de 2013

Alberto Arce Arce Ana Soto Campos Eva Rodíl Rodríguez

Acknowledgements

Five years. Probably the best five years in my life. And it is mainly due to this thesis work. In the end of 2008 I had the honor of joining a leading research group in its field not only in Spain but also in the world. The Group of Phase Equilibria and Separation Processes from the University of Santiago de Compostela has taken me in, becoming my second family. Thus, I want to express my acknowledgements to all the people that somehow were part of this amazing period.

In first place I would like to thank Professors Alberto Arce and Ana Soto. They gave me the great opportunity of being part of this ship they always crew with good judgment and professionalism. When someone teaches you principles like rigor, sacrifice and honesty, you are not only being formed as a good worker, but also as a good person. Moreover, they trusted me to let me help in the organization of the 24th European Symposium on Applied Thermodynamics, what was assumed by me as a challenge and a sign of confidence. Thank you.

Of course this acknowledgement is also extended to Eva Rodíl. Thanks to her I had the opportunity to (slightly) go into the nanotechnology world (completely unknown for me until that moment), which is one of the things I appreciate the most of this period. Coffees, advices and confidences don't need to be mentioned. I especially thank Héctor Rodríguez, who always was there to offer his valuable help and to try to make things work. Thanks to all of them I discovered the ionic liquids, an amazing and interesting field that I already really love.

When I arrived to this group I had the pleasure to coincide with María Francisco for more than one year. She took my hand for my first steps in the research world, showing me how to get along in the lab. But during these years I also was lucky to know other many people that have passed through the group: Alfonsina, Yamil, Magda, Kasia, Cristina, Jara, María, Oscar and Alberto. Alicia and Iago, who besides being my thesis-period lab mates, are very good friends. They always cheer the lab up and make the work easier. Elio, Adrián and Iria arrived to the group not too long ago, but we quickly had a very nice harmony that led to a good friendship. And of course, the person who I must strongly thank is Sara. She accompanied me since the beginning, being the best friend, the best workmate. A person who always is happy and makes people around her feel the same. She never let me give up.

All the help and good moments shared with the people in the Department are also very valuable for me. I want to thank Susana for her inestimable help and patience with the patent application. Thanks to the RIAIDT staff who perfectly knew the urgency of many analysis and always treated me with generosity.

In the last period I also had the opportunity to spend three amazing months in the Delft University of Technology (TU Delft), Netherlands. Professor Andreas Schmidt-Ott allowed me to form part

of his excellent group for this period, from which I learned many things. Jicheng and Marco were my best friends and advisors in the group, but I can't forget Tobias, George, Julien, Luyi, Isaac, Aaike, Anne and Kostis.

But the support received during these years does not only come from the work. Thus I want to acknowledge Toño for his understanding and patience, as well as all my friends from Lugo, Santiago, Sanxenxo and Delft. They were able to forgive my absences in many evenings, weekends or holidays.

Finally, but very, very important I want to thank my family. An especial mention is referred to my parents. This thesis work is now finished thanks to and for them. It wouldn't have made sense without them by my side.

Closing these lines, I want to express my acknowledge to the University of Santiago de Compostela, and to the Ministry of Economy and Competitiveness of the Spanish Government for financial support through project CQT2012-33359, and for having awarded me with a FPI grant (ref. BES-2010-033448). Thanks to Repsol and CYTEC for kindly supplying the fuel samples and some ionic liquids, respectively.

B. Rodríguez Cabo

Santiago de Compostela, November 2013.

ABSTRACT

The excessive emission of pollutants to the atmosphere has been a problem during the last few decades due to, among other reasons, the massive use of transports. In order to avoid this problem, many methods are being investigated as an alternative to the classical hydrodesulfurization technique, such as adsorption, biodesulfurization, extraction and oxidation. The extractive desulfurization is one of the most promising alternatives. Moreover, its enhancement with selective oxidation of sulfur compounds has been a trending field of research over the last years.

Ionic liquids have turned into perfect solvents for many different tasks. Since they are composed by a cation and an anion, plenty combinations are possible, giving to these designer solvents different and defined properties. Among them, the negligible vapor pressure make these solvents easily recoverable while also avoiding atmospheric contamination. Amid other applications, ionic liquids are being proposed for the extraction of sulfur from fuels.

In this work four ionic liquids, 1-hexyl-2,4-dimethylpyridinium bis(trifluoromethylsulfonyl)imide, $[C_6^{2,4}mmpy][NTf_2]$, 1-ethyl-3-methylimidazolium bis(trifluoromethylsulfonyl)imide, $[C_2mim][NTf_2]$, 1-ethyl-3-methylimidazolium acetate, $[C_2mim][OAc]$ and 1-ethyl-3-methylimidazolium diethylphosphate, $[C_2mim][DEP]$, were studied for the desulfurization of fuels. Liquid-liquid equilibrium data were obtained for the systems ionic liquid + thiophene + toluene, ionic liquid + thiophene + hexane and ionic liquid + pyridine + hexane at 298.15 K and atmospheric pressure. The obtained data were correlated using the UNIQUAC and NRTL models. The suitability of the ionic liquids as solvents was evaluated in terms of solute distribution ratio and selectivity.

Then, the ionic liquids were tested in a three-stage extractive desulfurization using synthetic samples of fuels (gasoline and diesel oil). With the aim of enhancing the process, an oxidative desulfurization was also studied. Besides the traditional oxidative system for desulfurization (acetic acid and hydrogen peroxide), different ionanofluids, formed by the ionic liquid and metallic oxide nanoparticles (Cr_2O_3, Al_2O_3, TiO_2), were tested as oxocatalytic system. In the case of H_2O_2-AcOH system, the research on the model fuels was carried out to optimize the operation conditions (ratio of oxidant and catalyst, temperature, extraction times and operation mode).

Finally, the extractive and oxidative desulfurization methods were tested using the four ILs with real gasoline and diesel oil samples. Based on the results, $[C_2mim][OAc]$ is suggested for the desulfurization of gasoline in an extractive desulfurization process, whereas $[C_2mim][NTf_2]$ is preferred for the oxidative desulfurization of diesel oil.

CONTENTS

1. OBJECTIVES....1
2. INTRODUCTION....5
2.1. IONIC LIQUIDS....7
2.2. IONANOFLUIDS....12
2.3. DESULFURIZATION OF FUEL OILS....14
2.4. IONIC LIQUIDS IN DESULFURIZATION OF FUEL OILS....19
2.4.1. EXTRACTIVE DESULFURIZATION....19
2.4.2. OXIDATIVE DESULFURIZATION....21
3. EXPERIMENTAL....25
3.1.1. IONIC LIQUIDS SYNTHESIS....29
3.1.2. IONANOFLUIDS SYNTHESIS....30
3.1.1.1. METHODS....31
3.1.1.2. NANOPARTICLES CHARACTERIZATION....31
3.2. EQUIPMENT....33
3.3. EXPERIMENTAL PROTOCOL....38
3.3.1. LIQUID-LIQUID EQUILIBRIA....38
3.3.2. DESULFURIZATION OF SYNTHETIC FUELS....38
3.3.2.1. EXTRACTIVE DESULFURIZATION....40
3.3.2.2. OXIDATIVE DESULFURIZATION....41
3.3.3. DESULFURIZATION OF REAL FUELS....41
4. RESULTS AND DISCUSSION....43
4.1. LIQUID-LIQUID EQUILIBRIA....45
4.1.1. CORRELATION....61
4.2. DESULFURIZATION OF SYNTHETIC FUELS....79
4.2.1. EXTRACTIVE DESULFURIZATION....79

4.2.1.1. SYNTHETIC GASOLINE 79
4.2.1.2. SYNTHETIC DIESEL OIL 81
4.2.2. OXIDATIVE DESULFURIZATION 84
4.2.2.1. SYNTHETIC GASOLINE 84
4.2.2.2. SYNTHETIC DIESEL OIL 84
4.3. DESULFURIZATION OF REAL FUELS 93
4.3.1. EXTRACTIVE DESULFURIZATION 93
4.3.1.1. GASOLINE 93
4.3.1.2. DIESEL OIL 94
4.3.2. OXIDATIVE DESULFURIZATION 94
4.3.2.1. GASOLINE 94
4.3.2.2. DIESEL OIL 94
5. CONCLUSIONS 97
LIST OF SYMBOLS 103
Symbols 105
Greek letters 106
Subscripts 107
Superscripts 107
Symbols on top 107
REFERENCES 109
APPENDIX A (List of publications) 127
APPENDIX B (Summary in Spanish, Resumen) 131

1. OBJECTIVES

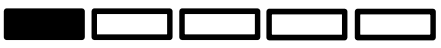

As it is well-known, the growing use of sulfur-containing fuels in the industry and in the transport sector is leading to serious pollution problems. In an effort to invert this tendency, authorities are approving each time more severe directives aimed at obtaining ultra-low sulfur fuels. The adaptation of refineries to those requirements implies high operation costs and less safe processes.

The main objective of this thesis is to define a system for the desulfurization of fuels by using Ionic Liquids (ILs). In particular, two different operations are going to be studied, the extractive desulfurization and the oxidative desulfurization, so as to look for a suitable solvent and find the optimal operational conditions for the process.

The first part of this study is the analysis of the viability of using several ILs for the desulfurization of fuels by liquid-liquid extraction. The objective is to complete a previous work, carried out in our research group, where the IL 1-hexyl-3,5-dimethylpyridinium bis(trifluoromethylsulfonyl)imide, $[C_6^{3,5}mmpy][NTf_2]$, was proposed for that aim, but there were some outstanding issues. Now, the experiments intend to analyze the effect of the position of the cation substituents on the desulfurization process. Taking this into account, the IL 1-hexyl-2,4-dimethylpyridinium bis(trifluoromethylsulfonyl)imide, $[C_6^{2,4}mmpy][NTf_2]$, having asymmetric substituents, will be tested. Moreover, the IL 1-ethyl-3-methylimidazolium bis(trifluoromethylsulfonyl)imide, $[C_2mim][NTf_2]$, was not previously studied for this purpose despite the fact that it showed preliminary good results. For this reason, this IL will also be evaluated. On the other hand, as no solubility of the IL was observed in the hydrocarbon phase in the extraction process, the presence of sulfur in the anion should not be a problem. Nonetheless, since undetectable traces of the IL could increase the sulfur content of the raffinate, we decided to continue with the study of ILs based on this last cation (cheaper than the pyridinium one) and to avoid the presence of sulfur in the anion. Accordingly, the ILs 1-ethyl-3-methylimidazolium acetate, $[C_2mim][OAc]$, and 1-ethyl-3-methylimidazolium diethylphosphate, $[C_2mim][DEP]$, will also be assessed.

For all chosen solvents, the liquid-liquid equilibria of the systems {IL + hexane + thiophene}, {IL + toluene + thiophene}, and {IL + hexane + pyridine} will be determined. Thermodynamic parameters will be used for the evaluation of the efficacy of the solvents in the desulfurization process, paying attention to parallel and relevant processes that may also take place, such as the denitrogenation or dearomatization of the fuel. The obtained data will be correlated in order to facilitate their use in processes simulation and design.

As a following step, the extractive desulfurization (EDS) of synthetic fuels (gasoline and diesel oil) will be carried out in a three step extraction process. The fuels are simulated as a mixture of aliphatics, aromatics, and nitrogen and sulfur containing compounds.

In the case of the diesel oil model, heavier alkanes and a more refractive sulfur component will be used. Composition of feed and raffinate after each one of the extraction steps will be analyzed with the aim of following the evolution of fuel constituents along the process. In spite of being a forgotten matter in most bibliographic studies, the effect of the desulfurization in all the fuel compounds is a key factor to be considered during the implementation of the process in real refineries.

As the next goal, and in order to enhance the desulfurization yield, the possibility of combining the extraction with an oxidation step (oxidative desulfurization process, ODS) will be evaluated. The oxidation of sulfur compounds makes them easier to be extracted. The highly effective AcOH + H_2O_2, will be tested as an oxocatalytic system. However, another objective of this thesis is to find a method to synthetize stable ionanofluids of metal oxides (nanoparticles of Al_2O_3, TiO_2 and Cr_2O_3 dispersed in an IL). These oxides can be used as catalytic agents with H_2O_2, since the specific area of the solid is increased due to the nanometer size, and, thus, its catalytic activity is improved.

The best oxocatalytic system will be selected, and an optimization of the oxidative conditions will be carried out. Several parameters, such as the ratios of catalyst and oxidizing agent, the temperature, the mixing technique, or the stirring and settling down times will be studied. Afterwards, the three steps extraction process will be carried out with the optimized oxidesulfurization system and the results will be compared to those obtained for the EDS.

Finally, samples of real diesel oil and gasoline will be subjected to the three stages of desulfurization and oxidesulfurization. The evolution of the total sulfur content in the fuel will be determined, to verify the conclusions obtained in the previous stages of development of this thesis.

2. INTRODUCTION

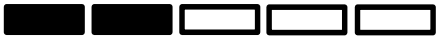

2.1. IONIC LIQUIDS

ILs are salts with a melting point below 373.15 K [1]. This brief definition does not shed light on their properties or characteristics, but on their ionic nature: since they are liquid salts, they are formed by at least one cation and one anion. There are many possible combinations of these two ions, what leads to an enormous number of ILs. It was estimated that 10^{18} potential ILs could be created by varying their constituent ions and their substitutions [2]. The asymmetry of the organic cations compared to their counterpart lowers the lattice energy, disrupting the ion-ion packing, thus decreasing the melting point. This is why these salts can be liquid at 373.15 K and below, unlike other ionic compounds that have really higher melting points (like NaCl and other traditional salts). When the ILs are in liquid state at ambient temperature they are called Room-Temperature Ionic Liquids (RTILs). Some properties of these salts depend on the anion (like thermal stability or miscibility), and others, such us viscosity or density, depend on the anion-cation combination.

The most common cations are those based on imidazole and pyridine rings or polysubstituted atoms such as phosphorus or nitrogen. Nevertheless, there are many more cations (Figure 2.1): piperidinium, sulfonium, pyrrolidinium, guanidinium, etc. They are usually organic species, and different alkyl chains and functional groups can be added to them. Regarding to the anion, its nature can be organic or inorganic. In most cases they have a small size, but we can also find big anions. They vary from monoatomic halogens to alkylic polyatomic groups. In Figure 2.1 the most used anions are also presented.

The ILs can be protic (PILs) or aprotic (APILs). The former are synthesized by proton transfer from an acid to a base, (i.e. ethylammonium nitrate). The latter are salts with a not protonated cation and an anion (for example, 1-hexyl-3-methylimidazolium hexafluorophosphate). Other way, ILs can be named as task-specific ionic liquids (TSILs), referring to the chance of design the IL [3]. Since they are composed by anions and cations, and many combinations are possible, it is achievable to create an IL with certain physical and chemical properties that make it being suitable for a specific application. They can thus be designed in our interest!

The ILs can also be chiral [4]. The most frequent examples are ILs with a chiral cation, and few works are on the case of a chiral anion. In 2005, it was reported an IL (1-methyl-3-[(S)-2′-methylbutyl]imidazolium (S)-camphorsulfonate) with both chiral anion and cation [5].

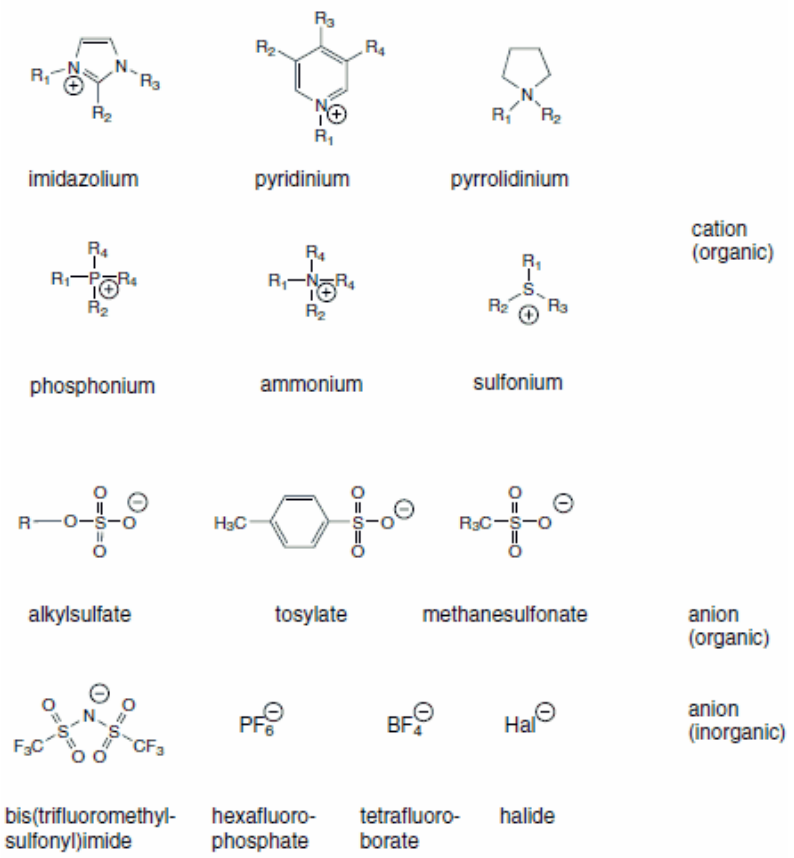

Figure 2.1. Some common cations and anions of ILs.

ILs' history evolved really fast in a short period of time. Actually, their progress can be classified in three general and broad stages [6]. A first generation of ILs comprises the haloaluminate ILs. The first RTILs on this category were the dialkylimidazolium chloroaluminates, reported by Wilkes and co-workers in 1982 [7]. Despite they have been studied as solvent media, they react with water and need to be handled in a dry-box. The second generation is formed by non-haloaluminate ILs, as the first examples reported once more by Wilkes and Zaworotko in 1992 [8], having anions such as hexafluorophosphate or tetrafluroborate. They were originally thought to be stable in air and water, but it was demonstrated they can hydrolyze under certain conditions, forming hydrogen fluoride. Nevertheless, ILs stability in water and air was achieved by Bonhôte [9] in 1996 by using the bis(trifluoromethylsulfonyl)imide anion. Finally, the recent chiral and task-specific ILs constitute the third generation. It must be highlighted that this classification does not imply a chronological order in the appearance of these designer solvents.

The origins of ILs go back to the nineteenth century, when Friedel and Crafts noticed the formation of a "red oil" during their alkylation and acylation reactions [10]. It was not known yet what it was, and it was necessary to wait until 1976 for the determination of its composition by Nambu et al. [11]: an alkylated aromatic ring cation with a chloroaluminate anion, *ergo*, an IL! Despite this fact took place in 1877, the birthdate of ILs is considered to be in 1914, when Walden published the synthesis of the IL ethylammonium nitrate [12], the first RTIL, with a melting point of 285.65 K. The great explosion in the research with ILs took place in the late 90s, as it can be seen in Figure 2.2.

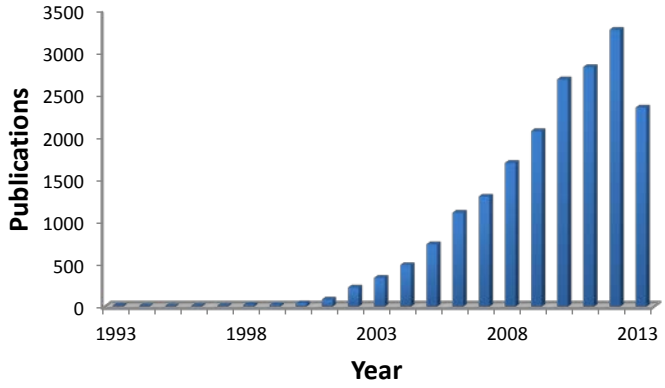

Figure 2.2. Number of papers in the last 20 years (until 2013 October). Entry for the query: ionic liquid, as entered (source: SciFinder®).

Once the ILs are well-defined, the next question must be answered: why are they so important? The answer lies in their properties. Their physical and chemical behavior make possible that ILs can be thought as an alternative to traditional organic solvents, enhancing performances and environmental effects in different processes. Among these properties the following ones stand out [13]:

- They are generally non-flammable and most of them are highly thermally stable. This reduces the risks in their handling and storage, and allows working under high temperatures. The degradation temperatures for the less stable ILs (i.e.1-ethyl-3-methylimidazolium acetate) start from 473.15 K.

- By definition, their melting point or glass transition is placed below 373.15 K, having a wide range of temperatures in which they are liquids (sometimes ranges over 573.15 K).

- ILs have a great capacity as solvents. They can dissolve a wide range of organic and inorganic gases, liquids and solutes (both polar and non-polar solutes). In general, their solvating ability is stronger than for conventional organic molecular solvents. For example, ILs can dissolve kerogen [14], insoluble in all known solvents except the hazardous hydrofluoric acid.

- Their vapor pressure is negligible, what confers them a great potential as "green solvents" [15]. Since they have not vapor pressure they are not volatile, and then they do not generate air pollution events. This is, probably, their most important and appreciated characteristic.
- ILs also have a wide electrochemical window [16].
- Brønsted, Lewis and Franklin acidity, as well as superacidity, can be found in them [17].
- They are easy to synthesize and most of them easy to handle.
- ILs can, depending on their substitutions and functional groups, act not only as solvent media but also as catalytic agents in many processes [18,19], developing a double role.
- There is, as previously explained, a huge number of possible ILs in comparison with traditional organic solvents. Moreover, and taking into account the possibility of designing their properties by means of tuning their ions, an appropriate IL can be searched for an specific task.
- Miscibility with water depends on their constituent ions. Hydrophobic ILs can be used in biphasic processes as water-immiscible phase. In general, the hydrophobicity of ILs increases when decreasing the coordination ability of the anion.

The toxicity of ILs is also an important factor to consider. Despite the existence of several works warning about their toxicity for aquatic environments and animals [20,21], it is possible to design less toxic and more biodegradable ILs [22,23]. ILs have been even proposed as active pharmaceutical ingredients [24].

The whole of these properties and characteristics make ILs very interesting solvents for the industry. Their absence of atmospheric emissions in comparison to the common volatile organic solvents, and their amazing properties as solvent media caused a great interest in the researching activities world-wide. With this aim, the use of ILs for different processes has been studied during last decades.

For example, they have been widely used in electrochemistry: an IL electrolyte was useful to create a lithium ion cell with a good performance and at a level of practical utility [25]. RTILs have also been thought as solvents in lithium batteries [26], showing promising results. The metal and alloy depositions (sometimes in the nanoscale) in ILs [27] or the films deposits of ILs on electrode surfaces [28] have been also reported. Other related usages are as electrolytes in electrochemical synthesis of conducting polymers [29] and electromechanical actuators [30], or as electrochemical sensors to detect fire or ethanol [31,32].

Due to the capacity of ILs to solve polar and non-polar compounds, they were also studied as alternative phase for gas chromatography columns [33,34] and as suitable candidates for replacement of volatile organic solvents in extraction processes. In this sense, ILs can be used for separation of chiral substances,

biological agents or even as able entrainers to break a variety of azeotropic systems [35-37]. The study of ILs for liquid-liquid extraction became necessary and there are, thus, a big number of works dealing with this issue [38-41]. The extraction of metal ions from aqueous solutions was achieved with ILs, showing partitioning values in agreement with traditional liquid-liquid separations [42-44].

Other interesting possible applications studied are: solvents for cellulose [45,46], fluids for the storage of solar thermal energy [47], reprocessing agents for nuclear fuels [48,49], lubricants [50,51], fluids for the synthesis of enhanced thermometers [52], etc. The capture of pollutant gases in ILs has been extensively studied during last years. CO_2, SO_2 and SH_2 are probably de most studied gases [53-56]. The enhanced oil recovery (EOR) by using ILs is also gaining great attention by the researchers [57,58]. Moreover, there is also a huge amount of samples of researching activity with ILs focused on their use as synthesis media [59-61], acting in some cases as catalyst too [62,63].

Nonetheless, and besides the endless researching work, the use of ILs in the industry is still quite limited nowadays. The BASIL [64] and DIFASOL [65] are probably, the best known examples of use of ILs for industrial processes. The former, Biphasic Acid Scavenging utilizing Ionic Liquids of BASF, is used for the production of the generic photoinitiator precursor alkoxyphenylphosphine with an increased yield in comparison with the traditional process. Moreover, the volume of the reactor needed is reduced. The latter, from the Institut Français du Pétrole, uses chloroaluminate (III) ILs for biphasic dimerization reactions, and they achieved with this new procedure a smaller reactor, and a higher yield and dimer selectivity. Moreover, Eastman Chemical Company was using an IL-based process since 1996 for the isomerization of 3,4-epoxybut-1-ene to 2,5-dihydrofuran [66]. Other companies, such as IoLiTec, Air Products or Central Glass Company, also use ILs technology. Recently, Petronas (with the support of QUILL Research Center) has developed an interesting method (HycaPure Hg) for scrubbing toxic and corrosive mercury from natural gas streams by using ILs [67]. Taking into account the unstoppable research in this field it would be logic to think that the list of real industrial applications will carry on growing.

2.2. IONANOFLUIDS

Nanotechnology is a growing and very important researching field. Since the first time this word was used by Taniguchi [68], a remarkable tenacity was put by the scientific community on the development of this area. Nevertheless, the unlimited possibilities of nanotechnology could already be imagined some years before, when Feynman enlightened the world with his famous talk entitled "There's plenty of room at the bottom" [69]. Nanotechnology can be defined, so, as the science to manipulate matter on the molecular or atomic scale [70].

The great importance of working at the nanoscale is that at this level matter can interact in a different way with what surrounds it. This means that the physical and/or chemical properties of materials in the nanoscale are different from those shown in the bulk solids [71].

There is no need to delve into the numerous applications of nanotechnology in the present industry, as varied as: catalysis, electronics, medicine, food, batteries and cells, sports, environmental treatment, cosmetics, textiles or military uses [72-81]. The methods for synthesizing nanomaterials (either nanofilms or nanowires or nanoparticles) are also plentiful and very different. They can be divided in top-down and bottom-up processes. The former (litographic and milling methods) consist in the reduction of the solid to the nanoscale. The "bottom-up" techniques (colloids, sol-gel, epitaxy…) are based on the chemical synthesis and/or the controlled deposition and growing of the material. Among them, the chemical synthesis in liquid phase is probably the most used method and the easiest to upscale. It normally consists in the reaction of two precursors or the reduction of a precursor within a liquid medium, and many kinds of nanomaterials have been synthesized by this method [82-86].

But the preparation of isolated solid materials is not the only objective of nanotechnology. Nanofluids are dispersions of nanomaterials in a conventional base fluid (water, oil, glycol, etc). This term was used for the first time by Choi in 1995 [87], and due to the enhanced properties of this new kind of material, its popularity and interest grew very fast. They are mainly fluids in which certain properties are enhanced because of the nanosolid they contain. The advantages of working with a solid material in the nanosize instead of a bulky solid lie in a better flow and better interaction of the particle with the fluid: the specific area is increased and a physical property can more easily be transmitted if needed [88]. Moreover the size of the particles avoids corrosion phenomena.

Nanofluids can be obtained by two different methods. When the nanoparticles are directly synthesized within the fluid which will form the nanofluid we will talk about one-pot synthesis. This technique allows much more stable nanofluids. The other option is to synthesize the nanomaterial and then transfer it to the fluid base. This is called a "two-pot synthesis" method. These special materials are mostly used

as thermal fluids [89-92], but other applications are also found for nanofluids. For example, Zhang [93] dispersed a Mo-S nanocluster in mineral oils for automotive lubrication applications, reducing wear and friction. Huang *et al.* [94] prepared biocompatible and bioconjugatable magnetite nanofluids which could be applied to several bioapplications including magnetic resonance imaging, highly efficient magnetic bioseparation, or targeted drug delivery.

But, could ILs be useful for the synthesis of nanofluids? Actually, they are. These solvents form extent bonding systems in the liquid state and they are highly structured [95]. This allows the obtaining of well-defined and ordered nanostructures. The dispersion of nanostructured materials within an IL as base fluid is an ionanoluid [96]. As it was explained before, the formed nanoparticles can be dispersed in an IL (what would be a two-pot synthesis) or they can be directly formed inside the IL, where they will be stabilized (one-pot method).

The main advantages of ionanofluids in comparison with other nanofluids are those related to the important properties of ILs. Thus, dispersions of nanoparticles can be achieved with enhanced applications, due to higher thermal stabilities as well as wider ranges of temperatures in which the nanofluid will be liquid. There is a thriving growth of publications of ionanofluids [97-101], but most of them are related to the dispersion of other-way formed nanoparticles in an IL [97-99]. Just some of them are prepared in the IL itself [100,101], involving a reaction step between precursors.

2.3. DESULFURIZATION OF FUEL OILS

With the industrialization and development of many countries, serious atmospheric pollution episodes started to appear worldwide. It is usual to make the assumption that the only cause of air pollution is big factories, but the truth is that automobile emissions are a big contributor to this phenomenon facing the entire world. With the number of vehicles on the road and the number of vehicle miles traveled, it is needed to control this problem. These "mobile sources" include cars, motorcycles, trucks, buses, non-road recreational vehicles, farm and construction machines, lawn and garden equipment, marine engines, aircraft, locomotives…

One of the sadly most known air pollution problems is the acid rain [102]. It is produced when the emissions of SO_2 and NO_x react with the water molecules in the atmosphere, leading to acidic species. Then, they are spread by the effect of winds for hundreds of miles, and when they reach the land they sink into the soil and go to water sources. This way lakes, streams and aquatic systems become acidic and, thus, toxic for many aquatic animals. But the acid rain also affects forests, where trees are less able to take up water and nutrients, and their leaves and needles are harmed by the acid. Materials and structures are affected by these depositions, which obviously can damage humans. Moreover, sulfur inhibits the use of advanced technology to control total pollutant emissions, including NO_x, CO, and particulate matter.

All these reasons make evident the necessity of diminishing the sulfur content in fuels, and many countries established directives for this effect. The European Union fixed the maximum content of sulfur in gasoline and gasoil to 10 ppm, starting from 2009 [103], and for non-road mobile machinery, agricultural and forestry tractors and recreational craft from 2011 [104]. As for the Unites States of America, the regulations established a maximum of 15 ppm of sulfur in diesel from 2006 and of 30 ppm for gasoline from 2005 [105].

The current industrial process for the desulfurization of fuels is the hydrodesulfurization (HDS). It consists in the reaction of the hydrocarbons present in the untreated fuel with hydrogen, leading to the cleavage of the C-S bonds. Hydrogen sulfide is formed as by-product, and normally it is treated to obtain sulfur-free gas (rich-hydrogen gas) which is used again in the hydrogenolysis. The reaction takes place in a catalytic fixed-bed reactor working at high pressures (20 – 70 atm) and temperatures (between 543.15 and 673.15 K). The catalyst is, typically, a sulfide of molybdenum supported on alumina and promoted by either cobalt or nickel [106]. With this process it is expected to remove the organic sulfur compounds, such as mercaptans, sulfides and disulfides, thiophenes, dibenzothiophenes and their alkyl-substituted derivatives, present in the fuels due to the natural formation of the crude oil. The presence of each compound varies in each type of fuel (the main three transportation fuels are gasoline, diesel and jet fuels), and their reactivity in the HDS process

diminishes when increasing the size of the molecule (Figure 2.3). Thus, the most difficult components to remove by the HDS process are the refractory dibenzothiophenes, especially those with substitutions in the positions 4 and 6.

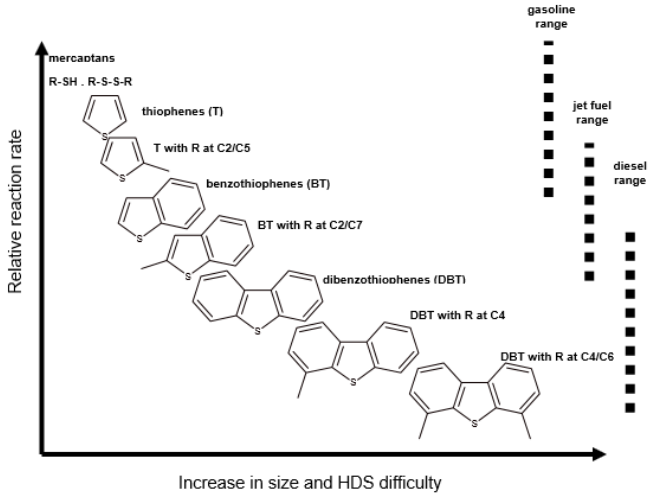

Figure 2.3. Reactivity of the sulfur containing compounds of transportation fuel versus their size.

The thiophenic compounds are reactive to the HDS process depending on both the electron structure and the steric hindrance of alkyl groups. The HDS reactivity is higher for thiophene and benzothiophene than for dibenzothiophene due to a higher π-electron density [107,108]. Moreover, the more substituted the rings are, the more difficult to extract, since the steric hindrance is stronger. The sulfur-containing compounds that dominantly remain in the diesel fuels after the hydrodesulfurization are dibenzothiophenes with alkyl substituents at the 4- and/or 6- positions [109-112]. The HDS process implies the denitrogenation of the fuels in a certain extension, too. The hydrogenolysis reaction also transforms N-containing compounds, as pyridine, to alkanes and ammonia. A certain rate of dearomatization also takes place, but this elimination has to be controlled, since the total elimination of aromatic compounds can be bad for the fuel.

The adaptation of refineries to the each time more strict legislative requisites is being carried out through a change in their processes. Several desulfurization steps, recycling, more severe pressure and temperature conditions, high hydrogen consumptions... are the pathways to achieve the demanded desulfurization levels. Nonetheless, these proposals imply high operation costs and less safe processes.

With the aim of solving these limitations and enhancing the extraction of sulfur from fuels several alternative techniques were

studied during last years to replace or to be coupled to the HDS process. Most studied methods are:

- Reactive alkylation: if the boiling point of the sulfur compounds is increased, it will be easier to separate these components by distillation. This can be achieved by inserting alkylic groups in the molecule, what is known as reactive alkylation. British Petroleum patented this technology under the olefinic alkylation thiophenic sulfur process (OATS) [113]. This technique allowed obtaining high desulfurization yields with a minimal octane loss [114].
- Precipitation: this technique is based on the formation and later precipitation of insoluble-in-fuel sulfur compounds. The original sulfur derivatives are mixed with a π-acceptor, forming insoluble charge-transfer complexes, which precipitate and are withdrawn [115,116]. Other option is to form insoluble crystalline powders of the sulfur compound by, for example, methylation with iodomethane [117-119].
- Biodesulfurization: it consists in the use of biological agents to metabolize the sulfur compounds and transform them into sulfur-free molecules or easier extractable ones. This technique uses mild conditions and it can be used accompanying other desulfurization methods. Different kinds of microorganisms and/or enzymes can be used for the biodesulfurization of fuels, such as *Rhodococcus rhodochrous*, *Sulfolobus acidocaldarius*, *Pseudomonas* or the catalytic system Dsz protein-flavin reductase [120-123].
- Adsorption: adsorptive techniques are based on the ability of certain solids to adsorb the sulfur containing compounds [124-126]. This mechanism can be carried out by physical interactions, physisorption, or by means of chemical interactions between sulfur compounds and the adsorbent, chemisorption. In the first case the selectivity of the adsorbent is lower, but they can be more easily recovered. Nevertheless, when chemical interactions take place the behavior is the opposite, and the selectivity and efficiency of the adsorbent is higher bur they are much more difficult to regenerate.
- Extractive desulfurization (EDS): the desulfurization of fuels via extraction implies the use of a solvent in which the sulfur compounds are more soluble than in the fuel. Then, they are transferred into the solvent phase, which is immiscible with the fuel. Distillation is used to separate the organosulfur compounds and to recycle the solvent. A general process flow is shown in Figure 2.4 [112].

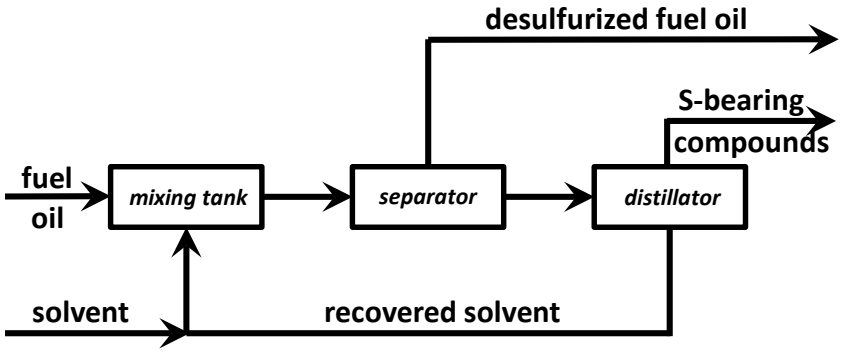

Figure 2.4. General process for the EDS of fuels.

Many solvents were tested to carry out a high-performance extraction. The solubility of sulfur compounds is not the only important parameter to select the appropriate solvent: its capability to extract the desired compounds and not the rest is also decisive. A lot of organic solvents such as polyalkyleneglycol, acetone or ethers were tested but the performances of the extraction were not satisfactory. Best results when using common organic solvents were achieved by means of mixtures of solvents: acetone–ethanol, tetraethyleneglycol–methoxytriglycol, etc [127,128]. These "solvent cocktails" enhanced the solubility of the sulfur compounds, making easier their extraction.

- Oxidative desulfurization (ODS): one way to improve the extraction of the sulfur containing compounds is to oxidize these extracted components and then, the solvent can carry on extracting more sulfur components. This is the basis of the ODS. It is, thus, a complementary technique to adsorption, extraction, thermal decomposition… The selection of a suitable oxidizing agent to convert the sulfur compounds into sulfoxides and then to sulfones (Figure 2.5) is a critical factor. To get the process more efficient, a catalyst for the oxidation reaction will be needed.

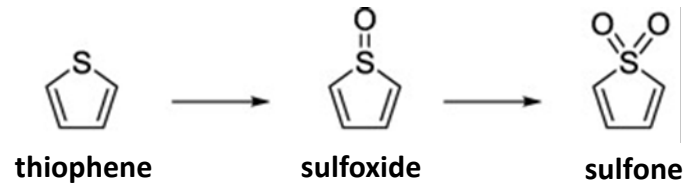

Figure 2.5. Oxidation of sulfur containing compounds.

An important feature for application of the ODS is that its relative efficiency is different from that of HDS. The oxidative

reactivity seems to increase when the electron density of the sulfur specie is higher [130]: dibenzothiophene > 4,6-dimethyldibenzothiophene > benzothiophene >> thiophene [129-131]. As consequence, refractory sulfur compounds in HDS are easily removed by ODS [132].

The most used oxidant is hydrogen peroxide, H_2O_2, and the usual catalyst is a carboxylic acid, like acetic or formic acid. These two components form a peroxycarboxylic acid, which is the real responsible for the oxidation [133-136]. But other oxidants and catalysts were also studied, thus leading to different yields of oxidation and to different performances of desulfurization [137-141].

Among all these techniques, EDS and ODS are probably the most studied methods due to, in part, the huge amount of possible solvents for an extraction process, as well as to the effectiveness of combining both methods. Nonetheless, the lack of a solvent with the suitable requirements means that none of these techniques could be an industrial reality nowadays.

2.4. IONIC LIQUIDS IN DESULFURIZATION OF FUEL OILS

The research about the use of ILs to desulfurize fuels is quite widespread because of their excellent properties as solvents for extraction purposes, being an alternative to traditional organic solvents. As it will be explained below, they have been widely studied for EDS processes as extracting agents. But moreover, due to the endless possibilities and complexity of ILs, they were also studied for oxidation of sulfur containing compounds, acting in some cases as a solvent that can contain oxidizing and/or catalytic systems within itself, showing a great value for ODS processes.

2.4.1. EXTRACTIVE DESULFURIZATION

The use of ILs for the selective extraction of sulfur from fuels was reported for first time by the group of Wassercheid [142] in 2001. Lewis (1-butyl-3-methylimidazolium chloride with $AlCl_3$) and Brønsted (a mixture of diethyl(hexyl)ammonium methanesulfonate and tributylammonium methanesulfonate) acidic ILs were studied and compared to a neutral one (1-butyl-3-methylimidazolium octylsulfate). The Lewis-acidic IL showed a much higher efficiency in sulfur extraction from real diesel than the other two. The effect of the extraction of dibenzothiophene was analyzed using the same acidic IL but with $FeCl_3$ instead of $AlCl_3$ [143]. The amount of dibenzothiophene extracted increased with an increasing molar ratio of $FeCl_3$/IL. The high extraction ability of these ILs was suggested to be due to the π-complexation bonding of these species with the aromatic sulfur compounds. Despite the good desulfurization performances, these ILs are sensitive to water [144] and they can generate HCl, being unstable in air and not applicable to real processes.

Zhang and coworkers [145] used imidazolium ILs with hexafluorophosphate and tetrafluroborate anions. They found that a butyl chain in the cation enhanced the desulfurization in comparison to an ethyl one, obtaining best results when using the hexafluorophosphate anion. They also observed that the sulfur extraction is higher when the density of aromatic π electrons is increased. Other authors worked with this kind of ILs [146,147] obtaining promising results. Once more it was checked that the desulfurization rate increased with the length of the alkyl chain of the cation, but this time for pyridinium-based ILs [148]. This work also revealed the negligible solubility of these ILs in the fuel, and that the extraction is favored for sulfur compounds with higher density of aromatic π-electrons. The extraction mechanism was postulated to be due to the π-π interactions between the aromatic sulfur compounds and the pyridinium ring of the IL. Nevertheless, these anions imply the possible formation of their hydrolysis products such as HF [149], which is observed in presence of water at moderate temperatures.

Halogen-free ILs were, then, thought to be the solution to these decomposition problems. Anions based in alkylsulfates were considered to be a good alternative. 1-ethyl-3-methylimidazolium octylsulfate and 1-ethyl-3-methylimidazolium ethylsulfate were studied as water-stable and relatively cheap ILs [150]. The influence of the number and length of substituents was analyzed for these ILs [151]. The extraction yield of dibenzothiophene increased linearly with the number of carbons of the alkyl group in the ILs. Nevertheless, the extraction of sulfur compounds is limited with this anion and cross-solubility of hydrocarbons takes place. Other anion option is the bis(trifluoromethylsulfonyl)imide [152-156]. The very high prices and toxicity of this anion can be potential limiting factors for its use. Other different anions and cations were also tested with no very different results [157-160].

An important step in the screening of ILs for this specific task was carried out by Holbrey *et al.* [161], who studied different anions and cations for the extraction of dibenzothiophene from dodecane, being able to establish a ranking of ILs for desulfurization depending on the cation: alkylpyridinium ≥ pyridinium ≈ imidazolium ≈ pyrrolidinium.

Besides the already explained limitations of these ILs, there was an alarming absence of studies concerning the content of the other compounds of the fuels during the desulfurization process. Most of studies in the bibliography are just based in the solubility of a sulfur compound (normally dibenzothiophene) in the IL. Other studies focus on the liquid-liquid equilibrium of systems composed by an IL, a sulfur-containing compound, and an aliphatic hydrocarbon [162-164]. The denitrogenation of the fuel is also an important parameter to take into account, as well as the dearomatization process, which directly affects the fuel properties. With this in mind, an exhaustive research work was started in 2006 by our group studying the fuel desulfurization with four ILs [165]. In a first moment, the liquid-liquid equilibrium with sulfur containing compound and an aromatic or aliphatic was studied for these ILs [166-170]. Later, their extraction capacity was evaluated using synthetic models and real fuels. For these experiments a polysubstituted pyridinium IL (which was supposed to have great performances on desulfurization) and three imidazolium ILs were tested as solvents for the sulfur extraction in model and real fuels. In agreement with Holbrey's ranking [161], it was found that the IL 1-hexyl-3,5-dimethylpyridinium bis(trifluoromethylsulfonyl)imide was the one extracting more sulfur from both gasoline and gasoil.

Nonetheless, at the end of that work, there were still several issues to be investigated. The influence of the number of substituents (and their position in the pyridinium ring) on the extraction ability of the IL should be studied. On the other hand, the liquid-liquid equilibrium for the system 1-ethyl-3-methylimidazolium bis(trifluoromethylsulfonyl)imide + thiophene + heptane was found to be very promising [171], but the desulfurization of fuels with this IL was not studied yet.

Moreover, many of the proposed ILs for desulfurization (in bibliography and by our group) have sulfur atoms in the anion. This should not be a problem because our studies showed that the IL content in the oil phase after the separation was non-existing. Nevertheless, since a really small contamination with the IL (several ppms) can be decisive, there is a high risk on the use of this kind of anions as desulfurizing agents. During last years, new anions (such as acetate or dialkylphosphate) have appeared, being environmentally benign and really cheap ions. For instance, some solubility tests of sulfur compounds in model fuels were performed studying the influence of the alkyl chain of the alkylphosphate anion of the IL [172-174]. The possibility of using ILs with these anions as extracting agents for the desulfurization of fuels must be analyzed, taking also into account the behavior of the other components in the fuel.

2.4.2. OXIDATIVE DESULFURIZATION

The oxidizing-catalytic systems used for the ODS with ILs are very varied. While not many different oxidants were studied (only few works can be found using sodium hypoclorite, dioxygen or ozone [175-177] and most of them use H_2O_2), the possible catalysts used are quite numerous.

Some experimental works are based on the use of polyoxometalates (POMs). This polyatomic species showed high performances when acting as catalysts for the oxidation of dibenzothiophene and other sulfur-containing compounds to sulfones and sulfoxides. These POMs can be added to the mixture of fuel and IL or they can directly be part of the first. In the first case, most studies are based on tungstophosphoric acids or peroxomolybdenum amino acids complexes mixed with hexafluorophospahte or tetrafluoroborate alkylmethylimidazolium ILs [178-180]. When the catalyst is contained in the IL itself, quaternary ammonium cations are usually used, but some works with pyridinium and imidazolium-based ILs can be also found [181-184]. This type of catalysts enhances the desulfurization ability of ILs, achieving promising oxidation yields that lead to very good performances. Nonetheless, these complex species are quite expensive and its application to real desulfurization processes can be very questionable, thus. Furthermore, it is well-known that these catalysts are difficult to separate from their reaction products limiting their recyclability, and it can be found recontamination in the oil from the dissolution of traces of catalysts.

Other solid catalysts were also used for the oxidation of fuels. For example V_2O_5 was used by Xu *et al.* [185] with the imidazolium-based ILs and tetrafluoroborate and hexafluorophsphate anions. D. Liu and co-workers [186] used Na_2WO_4 catalyst in the oxidizing system, which seemed to form a complex with the IL, giving place to a POM-based ODS.

The advantage of being able to design the IL can also help to introduce classical catalytic groups in the solvent medium. For instance, Lissner *et al.* [187] synthesized ILs with a carboxylate group attached to an imidazolium cation, which acted as catalyst (instead of acetic acid) and oxidized the sulfur compounds in presence of hydrogen peroxide. A coordinated IL (a tetraalkylammomium salt reacted with caprolactam) was presented [188] acting as phase transfer catalysts, whose role is to accelerate the oxidation reaction in the biphasic system oil (fuel) – water (formic acid, hydrogen peroxide and IL catalyst) [189]. These complex ILs can balance out results achieved with traditional ones, but they are usually more expensive and difficult to synthesize or purchase.

The use of acidic ILs has been widely reported during these last years. The ODS conditions with Fenton-like ILs were studied. This kind of systems consists in an IL with metallic chlorides and the oxidant (hydrogen peroxide). Most of them are based on imidazolium or ammonium cations [190-192], and the chloride counterpart can be very varied ($CrCl_3$, $CuCl_2$, $NiCl_2$, $FeCl_3$, $ZnCl_2$…). Some of them, as the ones with $AlCl_3$ are extremely sensitive to moisture and must be handled either in vacuo or under inert atmosphere at all times [18]. Corrosion problems can occur with this acidic ILs. Then it was proposed to use acidic halogen-free ILs. A series of Brønsted acidic ILs was evaluated as both catalyst and extracting agent for the ODS of fuels [193-200]. First studies were carried out using the IL N-methyl-pyrrolidium tetrafluoroborate [193-195]. Although high removal of dibenzothiophene was obtained, these ILs could hydrolize under certain conditions. Moreover, fluoroboric acid, a strong acid with extreme corrosion and high toxicity [149], was required in the preparation of this acidic IL. So, “greener” acidic ILs were searched and studied. Hydrogen sulfate and dihydrogen phosphate substituted the fluorinated anions (with imidazolium, pyridinium and pyrrolidinium cations), leading to very promising results in ODS [196-200]. But despite the good performances, these ILs lose their protons in aqueous solutions to form acidic by-products [201]. Moreover, corrosive and harmful acids are used for their synthesis.

The use of the most common oxidizing system, H_2O_2 and AcOH, seems to be one of the most suitable alternatives for the ODS with ILs. Nevertheless it is necessary to ponder on the enhancement achieved by using these difficult to handle and recycle systems and to evaluate if it is really worth the effort to use this technique in comparison to the EDS with ILs. Other huge lack in the bibliography is the use of oxides as catalysts. Moreover, the effect of the size of the solid catalysts is still not studied. Since nanoparticles show a huge specific area in comparison with bulk solids, they could catalyze the oxidation of sulfur compounds with better performances.

As in the case of the EDS, a lack in the study of the behavior of the other compounds of the fuel is total for the ODS. This implies that a researching work must be done regarding this issue, taking special care of aromatics and N-containing compounds evolution.

For all these reasons, more research is needed in the ODS technique. It is necessary to find more effective, stable and cheap solvents (ILs) as well as to optimize the catalytic reactions that take place by means of a suitable oxidant-catalyst system.

3. EXPERIMENTAL

3.1. MATERIALS

For the fuel models, hexane (>99 wt%), heptane (>99.5 wt%), isooctane (≥99.5 wt%), dodecane (>99 wt%), hexadecane (99 wt%), toluene (≥99.5 wt%), thiophene (>99 wt%) and dibenzothiophene (98 wt%) were purchased from Sigma-Aldrich and used without purification. Pyridine was obtained from Riedel-de Haën (≥99.5 wt%). Samples of real gasoline and diesel oil were kindly supplied by Repsol.

For the oxidation of the sulfur compounds, hydrogen peroxide (30 wt%), acetic acid (≥99 wt%), anatase TiO_2 (99.8 wt%), Cr_2O_3 (≥98 wt%) and Al_2O_3 (99.7 wt%) were purchased from Sigma-Aldrich and used without purification.

The structure of the four ILs used in this work is showed in Figure 3.1. The IL [C_2mim][OAc] was purchased from Iolitec (>95 wt%) and purified under vacuum ($5 \cdot 10^{-3}$ mbar) for 48 h at 343.15 K. The ILs [$C_6^{2,4}$mmpy][NTf_2], [C_2mim][NTf_2] and [C_2mim][DEP] were synthesized in our laboratory.

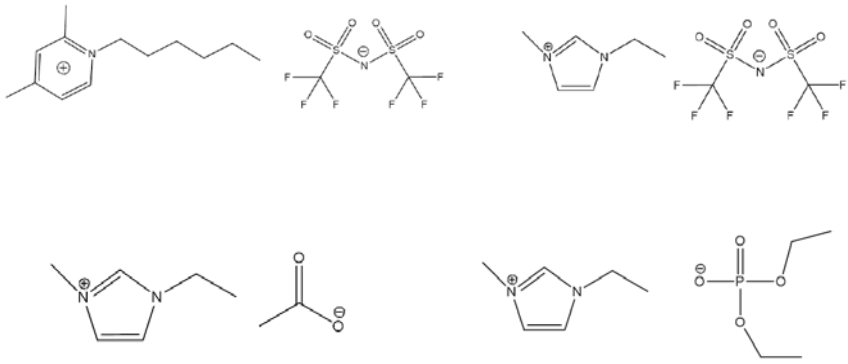

Figure 3.1. Studied ILs. Upper row: [$C_6^{2,4}$mmpy][NTf_2] (left) and [C_2mim][NTf_2] (right). Lower row: [C_2mim][OAc] (left) and [C_2mim][DEP] (right).

The materials needed for the synthesis of the ILs were purchased from Sigma-Aldrich: 1-bromohexane (98 wt%), 1-bromoethane (≥99 wt%), acetonitrile (99.8 wt%), ethyl acetate (99.7 wt%), 2,4-lutidine (99 wt%), triethylphosphate (≥99.8 wt%) and 1-methylimidazole (≥99 wt%). Diethylether (99.5 wt%) was acquired from Panreac. The salt lithium bis(trifluoromethylsulfonyl)imide (99.9 wt%) was acquired from Solvionic. The synthesis of each IL is detailed below. The purity of all ILs, commercial and synthesized, was verified by ^{1}H NMR and ^{13}C NMR spectroscopy.

The water content of the pure components, along with their experimental densities and refractive indices are showed in Table 3.1 and compared to bibliographic data [202-212].

Table 3.1
CAS-register numbers, water content (ω_{H2O}), densities (ρ) and refractive indices (n_D) of the pure components at 298.15 K and atmospheric pressure

Component	CAS	ω_{H2O} (ppm)	ρ (g cm^{-3})		n_D	
			Exp.	Lit.	Exp.	Lit.
Hexane	110-54-3	40	0.65511	0.65484 [202]	1.37243	1.37226 [202]
Heptane	142-82-5	5	0.67947	0.67946 [202]	1.38517	1.38511 [202]
iso-Octane	540-84-1	5	0.68784	0.68778 [203]	1.38921	1.3895 [203]
Dodecane	112-40-3	31	0.74532	0.74518 [202]	1.42011	1.41952 [202]
Hexadecane	544-76-3	7	0.77115	0.77003 [203]	1.43232	1.4325 [203]
Toluene	108-88-3	18	0.86215	0.86219 [203]	1.49352	1.49413 [203]
Thiophene	110-02-1	257	1.05858	1.05887 [202]	1.52519	1.52572 [202]
Pyridine	110-86-1	358	0.97811	0.97824 [202]	1.50663	1.50745 [202]
Acetic acid	64-19-7	440	1.04397	1.0446 [206]	1.37072	1.3720 [206]
[$C_6^{2,4}$mmpy][NTf_2]	Not found	285	1.33939	Not found	1.45336	Not found
[C_2mim][NTf_2]	174899-82-2	115	1.51842	1.518 [207]	1.42306	1.42251 [208]
[C_2mim][OAc]	143314-17-4	1300	1.09902	1.0993 [209]	1.50069	1.4992 [210]*
[C_2mim][DEP]	848641-69-0	215	1.14840	1.1464 [211]	1.47304	1.4789 [212]

*Interpolated value

3.1.1. IONIC LIQUIDS SYNTHESIS

– 1-hexyl-2,4-dimethylpyridinium bis(trifluoromethylsulfonyl)imide, [$C_6^{2,4}$mmpy][NTf_2].

Following the procedure previously published [156], 1-bromohexane was reacted with 2,4-lutidine (1.05:1 in mass) for 48 hours at 353.15 K, as explained in Figure 3.2. Some ml of acetonitrile were added to the resulting brown solid, and it was washed several times with ethyl acetate. Then the mixture was left to separate in a decanting funnel and the excess of solvents were removed by a rotary evaporator firstly, and by high vacuum later.

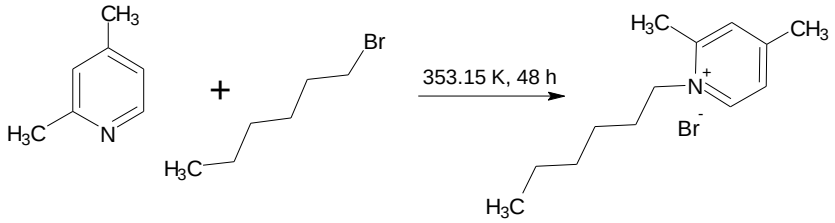

Figure 3.2. Alkylation of the pyridinium ring.

In a second step (see Figure 3.3), the formed IL, 1-hexyl-2,4-dimethylpyridinium bromide, [$C_6^{2,4}$mmpy]Br, was reacted with lithium bis(trifluoromethylsulfonyl)imide (1:1.02 in mass). For that purpose, both solids were solved in distilled water and then the two aqueous solutions were mixed for 12 hours at room temperature.

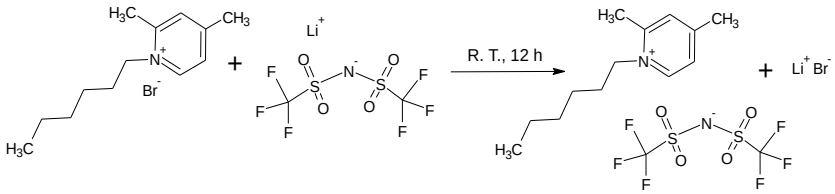

Figure 3.3. Metathesis with Li[NTf_2] salt.

The obtained IL was washed several times with fresh distilled water and separated by decanting. The aqueous phase contained the salt excess and the LiBr by-product. The water content in the IL was decreased under 300 ppm by using a rotary evaporator and afterwards high vacuum ($5 \cdot 10^{-3}$ mbar) for 48 hours at 343.15 K.

– Synthesis of 1-ethyl-3methylimidazolium bis(trifluoromethylsulfonyl)imide, [C_2mim][NTf_2].

The synthesis of this IL (Figure 3.4) follows a classical metathesis reaction [9] similar to the above-explained one. 1-Bromoethane was reacted for 48 hours with 1-methylimidazole (mass ratio of 1.05:1) at 313.15 K. The obtained IL was then purified in the rotary evaporator and solved in water to be reacted with an aqueous solution of lithium

bis(trifluoromethylsulfonyl)imide (1:1.02 in mass) for 12 hours at room temperature.

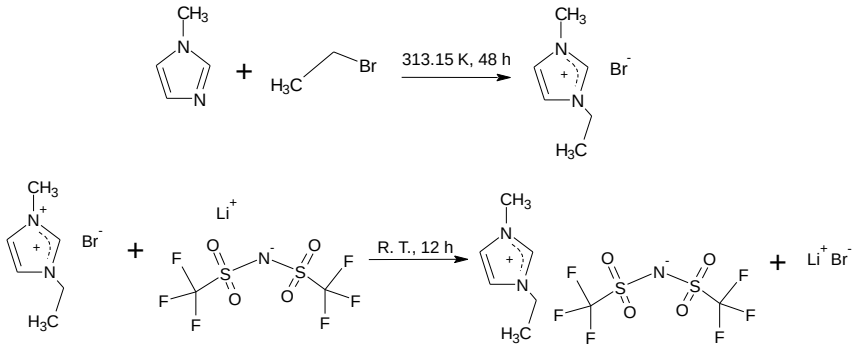

Figure 3.4. Steps for the synthesis of the IL [C_2mim][NTf_2].

Afterwards the IL was washed with water several times and separated in a decanting funnel. As in the previous case, the LiBr by-product and the excess of lithium bis(trifluoromethylsulfonyl)imide were eliminated with the aqueous phase. A rotary evaporator and high vacuum ($5 \cdot 10^{-3}$ mbar) for 48 hours at 343.15 K were used to purify the obtained IL.

– Synthesis of 1-ethyl-3-methylimidazolium diethylphosphate, [C_2mim][DEP].

In this case, the 1-methylimidazole was reacted for 3 days at 393.15 K with triethylphosphate (mass ratio of 1:1), as described by Kuhlmann *et al.* [213]. The reaction is showed in Figure 3.5.

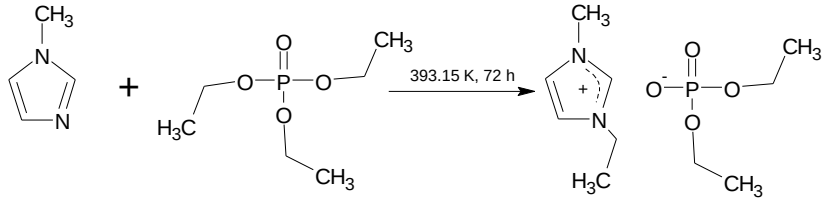

Figure 3.5. Synthesis of the IL [C_2mim][DEP].

The resulting IL was washed with diethylether for three times to remove the possible excess of reactants. After extraction, water content of the IL was decreased by using a rotary evaporator and a further purification under high vacuum ($5 \cdot 10^{-3}$ mbar) for 48 h at 343.15 K.

3.1.2. IONANOFLUIDS SYNTHESIS

Ionanofluids of titanium dioxide (TiO_2), aluminum oxide (Al_2O_3) and chromium oxide (Cr_2O_3) in the IL ([$C_6^{2,4}$mmpy][NTf_2]) were prepared.

3.1.1.1. METHODS

a) Disolution-reprecipitation method

This method, developed in this thesis and recently patented [214], does not need any volatile solvent or solid precursor, avoiding air pollution and the formation of by-products. Thus, the technique permits a "greener fabrication" of nanoparticles/nanofluids. Moreover, high temperatures or pressures are not needed, and the method is quite simple. The bulk powder was added to the IL (1 wt%) in a round-bottomed flask at room temperature, and the reaction mixture was heated at 393.15 K and vigorously stirred for 4 h in an argon atmosphere (Figure 3.6).

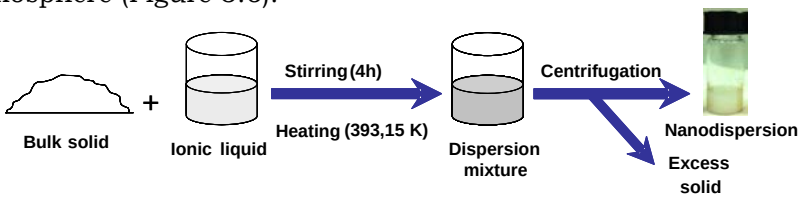

Figure 3.6. Procedure for the formation of the ionanofluids (dissolution-reprecipitation method).

The resulting colored mixture was allowed to cool down to room temperature, and then it was centrifuged at 4000 rpm for 15 min, to separate the excess bulk solid from the nanodispersion.

b) Spark discharge method

The other method used in the preperation of the ionanofluid was the spark discharge, introduced in 1988 [215] and widely studied by Schmidt-Ott group [216,217].

A spark was generated between two electrodes of the target material within an inert gas flow. This spark breakdowns the gas (nitrogen) and generates a plasma channel. So, the electrode material evaporates in the vicinity of the spark, obtaining primary particles in the vapor phase. This gas flow was then mixed with an air current to obtain the oxide of the metal. Then, the gas containing the formed nanoparticles was bubbled into the IL so that the solid was retained transferred to it.

3.1.1.2. NANOPARTICLES CHARACTERIZATION

The optical properties of the synthesized nanoparticles were measured by UV–Vis absorption spectroscopy. An aliquot taken from the nanodispersion was dissolved in acetone. The blank consisted in the same volume of pure IL also dispersed in acetone. Each sample was measured after having done a wavelength screening between 200 and 1000 nm, to obtain the maximum absorption peak. The distributions of sizes of the nanoparticles were determined by the Dynamic Light Scattering (DLS) technique. The suitable parameters (viscosity, absorption, dielectric constant, and refractive index) were needed for the nanomaterial and dispersant. Histograms with the distributions of sizes were recorded. Moreover, in order to know the approximate

concentration of the metal oxide nanoparticles in the IL, a sample of the ionanofluid was analysed by ICP-MS.

For some characterization techniques it is necessary to separate the solid material from the liquid medium. Precipitation and isolation of the nanoparticles was carried out according to the procedure in Figure 3.7. Dodecanethiol (50 μL/mL of sample) was added as a capping agent to the nanodispersion, and the sample was mixed with a vortex mixer. Then, to facilitate the precipitation of the nanoparticles, ethanol (20 mL) was added. The nanoparticles were isolated by centrifugation at 3000 rpm for ca. 10 min, and then allowed to dry under ambient conditions for 48 h.

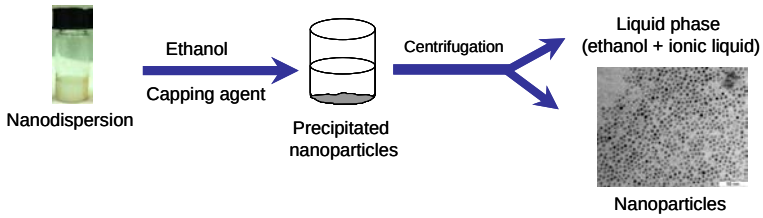

Figure 3.7. Procedure for the precipitation of the nanoparticles.

The structure of the nanoparticles was corroborated by X-ray powder diffraction (XRPD). The precipitated solid was diluted in ethanol on a sample tray and left to evaporate. A screening in the diffraction angle was done to obtain the X-ray patterns.

The size and the shape of the nanoparticles were also determined by transmission electron microscopy (TEM). The precipitated nanoparticles were dispersed in acetone. One drop was added on a copper grid covered with Formvar, which was manually shaken for few seconds and left to evaporate overnight. Several micrographs of the nanoparticles were collected from different parts of the grid with different magnification degrees.

3.2. EQUIPMENT

For the synthesis of ILs a Velp Scientifica Arex heater and magnetic stirrer plate was used with temperature control. It was also used for the purification of the ILs, which were dried in a glass-made vacuum line with capacity for four samples at the same time (Figure 3.8).

Figure 3.8. Synthesis of ILs (left) and high vacuum line (right).

For the preparation of the ionanofluids by the dissolution-reprecipitation method, a Selecta Agimatic-E hotplate stirrer was used (Figure 3.9).

Figure 3.9. Arex heating plate with magnetic stirring.

For the generation of nanoparticles with a spark discharge method, a GFG 1000 PALAS spark generator was used (Figure 3.10 shows the setup).

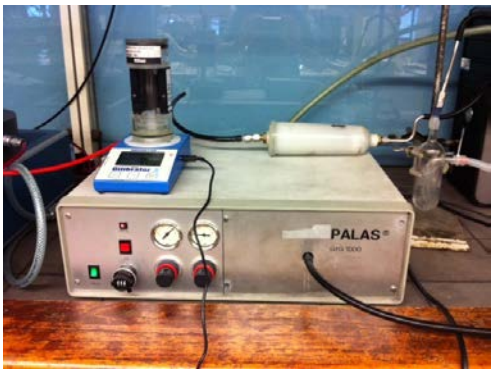

Figure 3.10. PALAS used spark generator.

In order to precipitate the nanoparticles from the ionanofluid for their characterization, a Selecta Mixtasel centrifuge with a rotor allowing to work up to 4400 rpm, and a Reax Top vortex mixer from Heidolph were used. They are showed in Figure 3.11.

Figure 3.11. Selecta Mixtasel centrifuge (left) and a Heidolph Reax Top vortex mixer (right).

The optical characterization of the nanoparticles was carried out using an Agilent 8453 UV-visible spectrophotometer with a wavelength range of 190-1100 nm, with an accuracy of ± 0.5 nm. Quartz 10 mm cuvettes were used for the measurements. For the morphological study a PHILIPS CM-12 transmission electronic microscope (TEM) with acceleration voltages from 20 to 120 kV was used. The interlinear resolution is 0.3 nm, and zooms up to 730000x can be achieved. The distribution of sizes was also studied by means of a Malvern Zen3600 ZetaSizer Nano ZS using glass cuvettes. In order to check the composition and concentration of the nanoparticles, a Siemens X-ray powder diffractometer with copper anode and a quadrupole VARIAN 820-MS ICP mass spectrometer (ICP-MS) were used, respectively. All these equipment are shown in Figure 3.12.

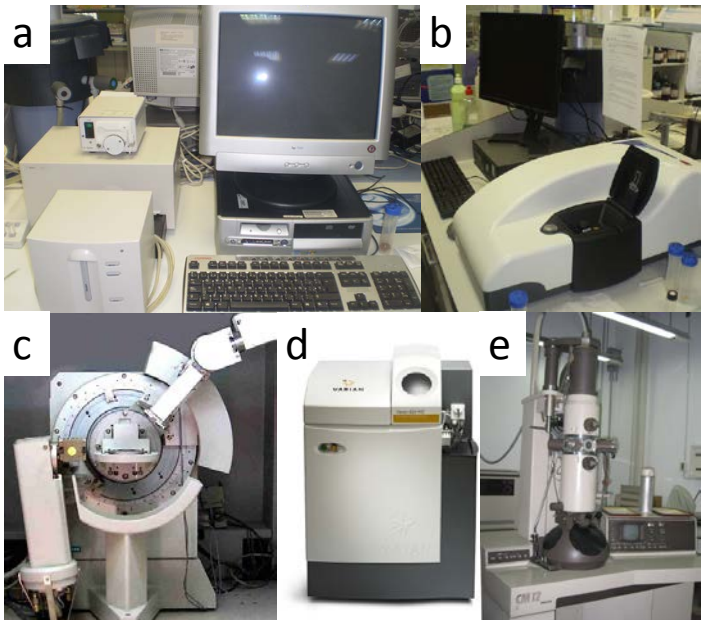

Figure 3.12. Agilent 8453 UV-visible spectrophotometer (a); Malvern Zen3600 ZetaSizer Nano ZS (b); Siemens X-ray powder diffractometer (c); ICP-MS VARIAN 820-MS (d); PHILIPS CM-12 TEM (e).

The water content of the pure compounds was measured using a Metrohm 737 coulometer (see Figure 3.13) by a Karl-Fischer titration method. The uncertainty in the measurements is 5 μg when the water content is lower than 10^3 μg and 0.5 wt% for higher mass of water.

Figure 3.13. Metrohm 737 coulometer.

The densimeter used was an Anton Paar DMA with an uncertainty of 3 ± 10^{-5} g·cm^{-3}. For the measurement of the refractive indices an ATAGO RX-5000 refractometer was used (uncertainty of $\pm 4 \cdot 10^{-5}$). Figure 3.14 shows this equipment.

Figure 3.14. Anton Paar DMA densimeter (left) and ATAGO RX-5000 refractometer (right).

All weighing was carried out by means of a Mettler Toledo AE 240 balance with an uncertainty in the measurement of $\pm 10^{-4}$ g. It is showed in Figure 3.15.

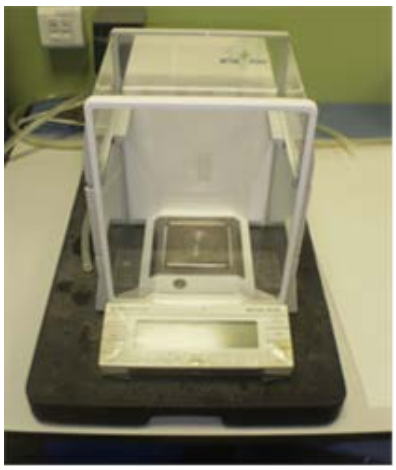

Figure 3.15. Mettler Toledo AE 240 balance.

To ensure that the temperature was kept constant during each experiment, a Selecta Ultraterm 200 thermostatic bath, showed in Figure 3.10, was used. The uncertainty in the temperature measurement is ± 0.05 K.

Figure 3.15. Thermostatic bath from Selecta.

The compositions of the samples were determined by gas chromatography with a HP 6890N series chromatograph (see Figure 3.16, left), equipped with a flame ionization detector (FID) and a flame photometric detector (FPD). The capillary column used was a SUPELCO SPBTM-1 SULFUR (30 m × 0.32 mm × 0.4 μm). The total sulfur content of samples was measured with an OXFORD Lab-X3500s sulfur analyzer, showed in Figure 3.16 (right).

Figure 3.16. HP 6890N gas chromatograph with automatic sampler (left) and OXFORD Lab-X3500s sulfur analyzer (right).

3.3. EXPERIMENTAL PROTOCOL

3.3.1. LIQUID-LIQUID EQUILIBRIA

To determine the experimental tie-lines for each ternary system, mixtures of their components in the immiscible region were mixed in 30 mL glass jacketed vessels (Figure 3.17). The temperature was kept constant at 298.15 K by means of a Selecta Ultraterm 200 thermostatic bath. The mixtures were magnetically stirred for 2 h, and then settled down for a minimum of 4 h. These times were enough to ensure a good mixture degree and the posterior achievement of equilibrium.

Figure 3.17. View of a jacketed cell (left), and different cells connected to the thermostatic bath (right).

Then, samples from both layers were withdrawn with syringes. Compositions of hydrocarbons and nitrogen or sulfur compounds were determined by gas chromatography. The IL composition was calculated by difference. The operational conditions for the analysis are shown in Table 3.2.

3.3.2. DESULFURIZATION OF SYNTHETIC FUELS

In order to simulate the behavior of real fuels, gasoline and diesel oil models were prepared and used to study the extraction of sulfur compounds with ILs. The synthetic gasoline is composed by hexane (26 wt%), heptane (26 wt%), isooctane (26 wt%), toluene (10% wt%), pyridine (6 wt%) and thiophene (6 wt%). In the case of the diesel oil model, the alkanes become heavier and the sulfur proportion in the fuel is shared with a more refractive compound, resulting the following mixture: heptane (26 wt%), dodecane (26 wt%), hexadecane (26 wt%), toluene (10 wt%), pyridine (6 wt%), thiophene (3 wt%) and dibenzothiophene (3 wt%).

Table 3.2
Gas chromatograph operational conditions.

Column	SPB™-1 SULFUR (30m x0.32mm x4µm)
Injection volume	4 µL
Carrier gas	Helium
Liquid-Liquid Equilibria	
Flow rate	1.5 ml·min^{-1} for 14 min
Oven temperature	373 K for 10 min → 473.15 K (50 K·min^{-1}) for 2 min
Injector temperature	473.15 K
Split ratio	75:1
Detector temperature	548.15.15 K
Detector	FID
Synthetic gasoline	
Flow rate	4 ml·min^{-1} for 8 min → 6 ml·min^{-1} (1 ml·min^{-1}) for 4 min
Oven temperature	343.15 K for 9 min → 553.15 K (100 K·min^{-1}) for 2 min
Injector temperature	548.15 K
Split ratio	25:1
Detector temperature	523.15 K
Detector	FID
Synthetic diesel oil	
Flow rate	4 ml·min^{-1} for 14 min
Oven temperature	413.15 K for 4 min → 553.15 K (100 K·min^{-1}) for 8 min
Injector temperature	548.15 K
Split ratio	25:1
Detector temperature	523.15 K
Detector	FID and FPD

3.3.2.1. EXTRACTIVE DESULFURIZATION

With the aim of studying the EDS of the fuel models with ILs, three extraction steps were carried out. The synthetic fuel was added to a thermostated cell (at 298.15 K) with the corresponding IL. The proportion was 1:1 in weight. The mixture was stirred for 12 hours (Figure 3.18) to ensure equilibrium conditions between both phases. Then, the stirring was stopped and the phases were left to settle down. After 12 hours of separation, a sample from the model (upper phase) was withdrawn and analyzed by GC. The IL was removed, and the rest of the organic phase was stirred with fresh IL for the second extraction step, and later the process was repeated for the third one (see Figure 3.19). This protocol was followed for both synthetic gasoline and diesel oil.

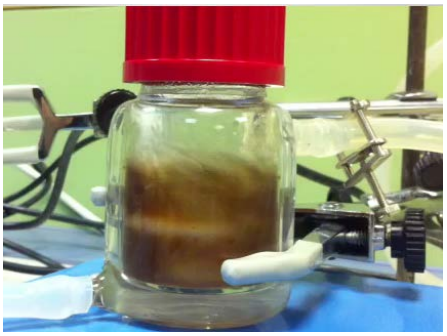

Figure 3.18. Jacketed cell with IL and synthetic fuel.

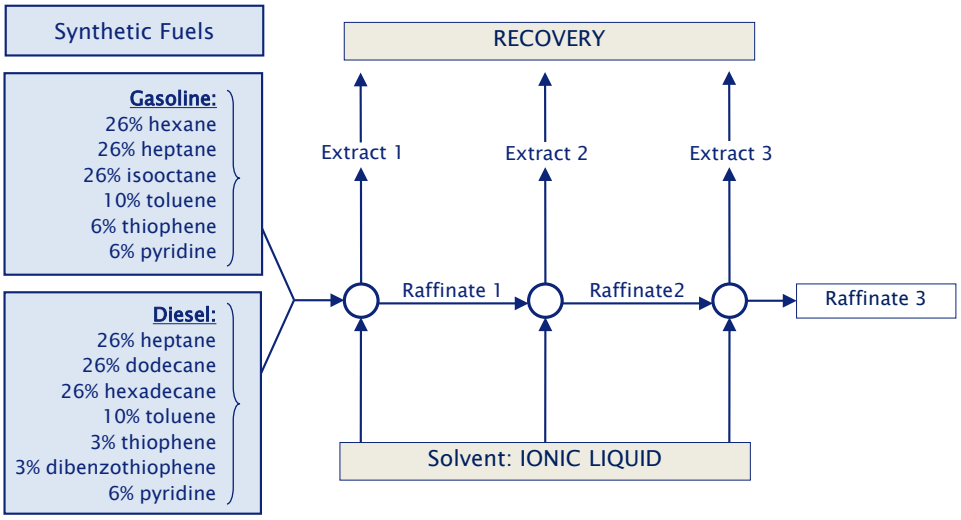

Figure 3.19. Three steps EDS process.

3.3.2.2. OXIDATIVE DESULFURIZATION

Regarding the ODS experiments, firstly an optimization of the parameters in the oxidation process was carried out. For this optimization, the IL $[C_6^{2,4}mmpy][NTf_2]$ was used, due to the high solubility of sulfur compounds in it.

Hydrogen peroxide was selected as oxidizing agent, and the use of two possible catalysts was analyzed: acetic acid (AcOH) and metal oxide nanoparticles (TiO_2, Al_2O_3 or Cr_2O_3). With the former, different molar ratios of acetic acid and of H_2O_2 to the sulfur content in the synthetic oil were tested. In the case of the metal oxide nanoparticles, their concentration in the IL was the maximum allowed to have a stable ionanofluid.

Once the best oxidizing-catalytic system was selected, an optimization of the most suitable temperature for the ODS process was carried out. The influence of a one-pot operation (IL, model oil, oxidant, and catalyst added all together) versus a two-step operation (first mixing the IL and the model oil to carry out the extraction, and then adding the oxidant and the catalyst) was also studied. Finally, the stirring and settling down times for equilibration and phases separation were optimized by analyzing (by gas chromatography) the evolution of the sulfur components in the raffinate at different times.

With the optimized oxocatalytic system, operation mode, temperature, and stirring and settling down times for the ODS procedure, a protocol similar to that described previously for EDS was carried out.

3.3.3. DESULFURIZATION OF REAL FUELS

EDS and ODS processes carried out with synthetic fuels were subsequently repeated with real gasoline and diesel oil. In this case, due to the large number of components in the real fuels, the oil-rich phases were studied using a total sulfur analyzer (as it is usually done in refineries), following the decrease of sulfur in the fuel.

4. RESULTS AND DISCUSSION

4.1. LIQUID-LIQUID EQUILIBRIA

LLE data for the ternary systems consisting in {IL + thiophene + hexane}, {IL + thiophene + toluene}, and {IL + thiophene + pyridine} were obtained at 298.15 K and atmospheric pressure. Tables 4.1 to 4.12 show the compositions of the tie-lines ends for each IL and each system. The corresponding triangular diagrams are shown in Figures 4.1 to 4.12.

From the experimental LLE data, the solute distribution ratio, β, and selectivity, S, were calculated for each tie-line as follows:

$$\beta = \frac{x_2^{II}}{x_2^{I}} \quad (1)$$

$$S = \frac{x_2^{II}}{x_2^{I}} \cdot \frac{x_1^{I}}{x_1^{II}} \quad (2)$$

where x is the mole fraction. Subscripts *1* and *2* indicate hydrocarbon (inert) and thiophene or pyridine (solute). Superscripts *I* and *II* refer to the hydrocarbon-rich phase and the IL-rich phase, respectively. These parameters are related to the amount of solvent needed for the separation (solute distribution ratio) and to the number of needed stages to carry it out (selectivity). Thus, they are decisive parameters to determine the suitability of a solvent as extracting agent. Tables 4.1 to 4.12 also show the β and S values obtained for the LLE data of studied ternary systems. These values are plotted versus the solute molar fraction in the hydrocarbon-rich phase in Figures 4.1 to 4.12.

As it can be seen (Figures 4.1, 4.4, 4.7 and 4.10) the systems containing thiophene and hexane show a Type II behavior, with two pairs of partially immiscible compounds and one biphasic region. The slope of the tie-lines in the lowest part of the diagram (interesting region for practical applications) is positive, but this tendency changes in the upper part of the ternary diagram, showing a solutropic behavior.

In the case of the systems {IL+ thiophene + toluene} the diagrams are also Type II, as it is showed in Figures 4.2, 4.5, 4.8 and 4.11. The slope of tie-lines are negative through all the diagram. Nevertheless, when studying the IL [C_2mim][DEP] (Figure 4.11) it can be seen that the slope of the tie-lines is higher than the unity for the lower part of the diagram, and it becomes negative when increasing the fraction of thiophene (solutropic behavior).

For the systems with pyridine, the obtained ternary diagrams show a Type I behavior, with only one pair of components partially immiscible and one immiscible region (see Figures 4.3, 4.6, 4.9 and 4.12). All the systems have positive slopes in all the range of compositions, except in the case of the [C_2mim][OAc] IL, whose diagram presents a solutropic behavior and the slope of the tie-lines becomes negative in the upper region.

Table 4.1

Experimental LLE data for the ternary system {[$C_6^{2,4}$mmpy][NTf_2] (1) + thiophene (2) + hexane (3)} at 298.15 K and atmospheric pressure.

Hydrocarbon-rich phase			IL-rich phase			β	S
x_1^I	x_2^I	x_3^I	x_1^{II}	x_2^{II}	x_3^{II}		
0.000	0.000	1.000	0.833	0.000	0.167		
0.000	0.039	0.961	0.704	0.140	0.156	3.59	22.1
0.000	0.072	0.928	0.627	0.230	0.143	3.19	20.7
0.000	0.167	0.833	0.464	0.402	0.134	2.41	15.0
0.000	0.273	0.727	0.366	0.515	0.119	1.89	11.5
0.000	0.414	0.586	0.290	0.608	0.102	1.47	8.44
0.000	0.481	0.519	0.261	0.636	0.103	1.32	6.66
0.000	0.568	0.432	0.225	0.670	0.105	1.18	4.85
0.000	0.655	0.345	0.202	0.702	0.096	1.07	3.85
0.000	0.745	0.255	0.172	0.743	0.085	1.00	2.99
0.000	0.892	0.108	0.135	0.815	0.050	0.91	1.97
0.000	1.000	0.000	0.108	0.892	0.000	0.89	

Standard uncertainties: $u(p)$ = 5 kPa; $u(T)$ = 0.05 K; $u(x^I)$ = 0.003; $u(x^{II})$ = 0.005.

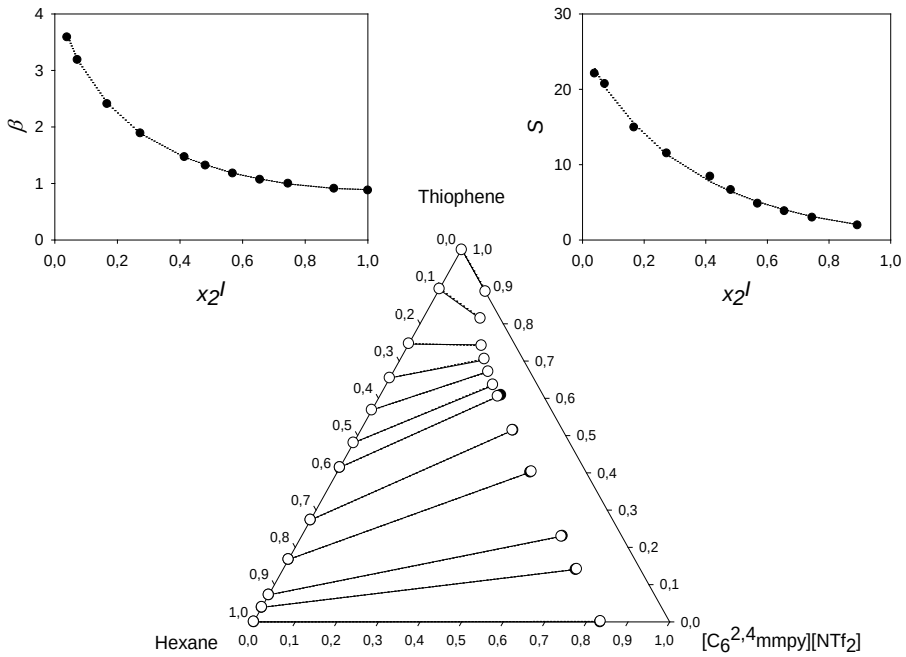

Figure 4.1. Down: Experimental (●, solid line) and correlated with UNIQUAC model (○, dotted line) tie-lines for the LLE of the ternary system {[$C_6^{2,4}$mmpy][NTf_2] + thiophene + hexane} at 298.15 K and atmospheric pressure. Up: Experimental (●) and correlated (dotted line) solute distribution ratios (β) and selectivities (S).

Table 4.2

Experimental LLE data for the ternary system {[$C_6^{2,4}$mmpy][NTf_2] (1) + thiophene (2) + toluene (3)} at 298.15 K and atmospheric pressure.

Hydrocarbon-rich phase			IL-rich phase			β	S
x_1^I	x_2^I	x_3^I	x_1^{II}	x_2^{II}	x_3^{II}		
0.000	0.000	1.000	0.167	0.000	0.833		
0.000	0.031	0.969	0.169	0.030	0.801	0.97	1.17
0.000	0.093	0.907	0.181	0.088	0.731	0.95	1.18
0.000	0.180	0.820	0.166	0.172	0.662	0.96	1.18
0.000	0.282	0.718	0.161	0.265	0.574	0.94	1.18
0.000	0.411	0.589	0.152	0.380	0.468	0.92	1.16
0.000	0.523	0.477	0.137	0.484	0.379	0.92	1.16
0.000	0.570	0.430	0.138	0.522	0.340	0.92	1.16
0.000	0.669	0.331	0.131	0.610	0.259	0.91	1.17
0.000	0.766	0.234	0.124	0.692	0.184	0.90	1.15
0.000	0.847	0.153	0.116	0.762	0.122	0.90	1.13
0.000	0.913	0.087	0.114	0.818	0.068	0.90	1.15
0.000	0.956	0.044	0.115	0.850	0.035	0.89	1.12
0.000	1.000	0.000	0.108	0.892	0.000	0.89	

Standard uncertainties: $u(p)$ = 5 kPa; $u(T)$ = 0.05 K; $u(x^I)$ = 0.002; $u(x^{II})$ = 0.003.

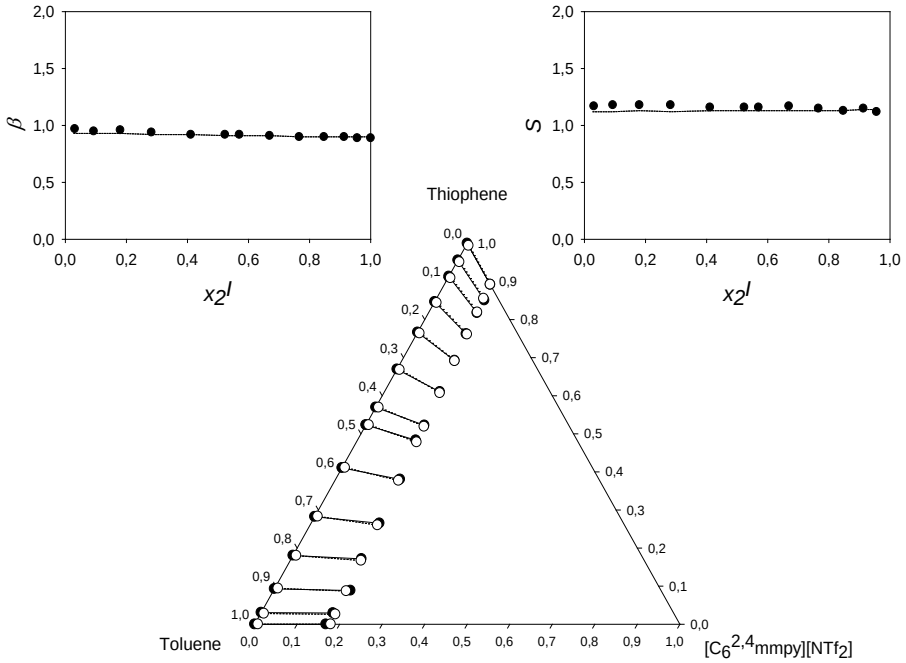

Figure 4.2. Down: Experimental (●, solid line) and correlated with UNIQUAC model (○, dotted line) tie-lines for the LLE of the ternary system {[$C_6^{2,4}$mmpy][NTf_2] + thiophene + toluene} at 298.15 K and atmospheric pressure. Up: Experimental (●) and correlated (dotted line) solute distribution ratios (β) and selectivities (S).

Table 4.3
Experimental LLE data for the ternary system {[$C_6^{2,4}$mmpy][NTf_2] (1) + pyridine (2) + hexane (3)} at 298.15 K and atmospheric pressure.

Hydrocarbon-rich phase			IL-rich phase			β	S
x_1^I	x_2^I	x_3^I	x_1^{II}	x_2^{II}	x_3^{II}		
0.000	0.000	1.000	0.833	0.000	0.167		
0.005	0.001	0.994	0.714	0.145	0.141	145	1022
0.004	0.030	0.966	0.605	0.262	0.133	8.73	63.4
0.005	0.059	0.936	0.489	0.378	0.133	6.41	45.1
0.005	0.089	0.906	0.407	0.467	0.126	5.25	37.7
0.003	0.126	0.871	0.312	0.562	0.126	4.46	30.8
0.003	0.168	0.829	0.241	0.638	0.121	3.80	26.0
0.004	0.244	0.752	0.177	0.688	0.135	2.82	15.7
0.002	0.334	0.664	0.109	0.732	0.159	2.19	9.16
0.000	0.411	0.589	0.085	0.736	0.179	1.79	5.89

Standard uncertainties: υ(p) = 5 kPa; υ(T) = 0.05 K; υ(x^I) = 0.005; υ(x^{II}) = 0.008.

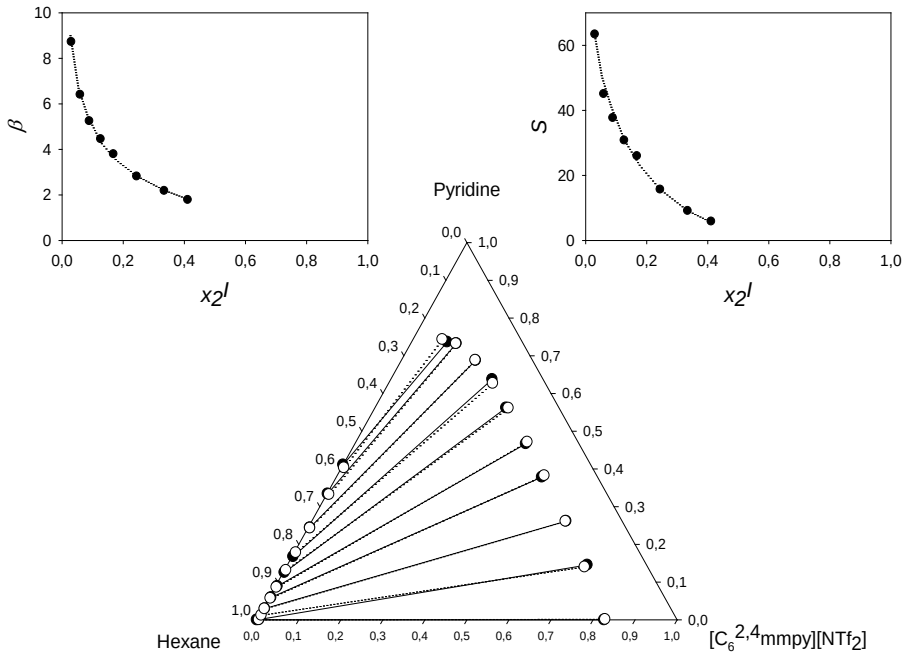

Figure 4.3. Down: Experimental (●, solid line) and correlated with NRTL model and α=0.1 (○, dotted line) tie-lines for the LLE of the ternary system {[$C_6^{2,4}$mmpy][NTf_2] + pyridine + hexane} at 298.15 K and atmospheric pressure. Up: Experimental (●) and correlated (dotted line) solute distribution ratios (β) and selectivities (S).

Table 4.4
Experimental LLE data for the ternary system {[C_2mim][NTf_2] (1) + thiophene (2) + hexane (3)} at 298.15 K and atmospheric pressure.

Hydrocarbon-rich phase			IL-rich phase			β	S
x_1^I	x_2^I	x_3^I	x_1^{II}	x_2^{II}	x_3^{II}		
0.000	0.000	1.000	0.961	0.000	0.039		
0.000	0.049	0.951	0.873	0.088	0.039	1.80	43.8
0.000	0.113	0.887	0.769	0.192	0.039	1.70	38.6
0.000	0.192	0.808	0.673	0.289	0.038	1.51	32.0
0.000	0.277	0.723	0.588	0.377	0.035	1.36	28.1
0.000	0.405	0.595	0.499	0.464	0.037	1.15	18.4
0.000	0.420	0.580	0.480	0.483	0.037	1.15	18.0
0.000	0.549	0.451	0.414	0.551	0.035	1.01	13.0
0.000	0.644	0.356	0.364	0.601	0.035	0.93	9.48
0.000	0.768	0.232	0.318	0.653	0.029	0.85	6.79
0.000	0.897	0.103	0.257	0.719	0.024	0.80	3.44
0.000	1.000	0.000	0.213	0.787	0.000	0.79	

Standard uncertainties: u(p) = 5 kPa; u(T) = 0.05 K; u(x^I) = 0.004; u(x^{II}) = 0.005.

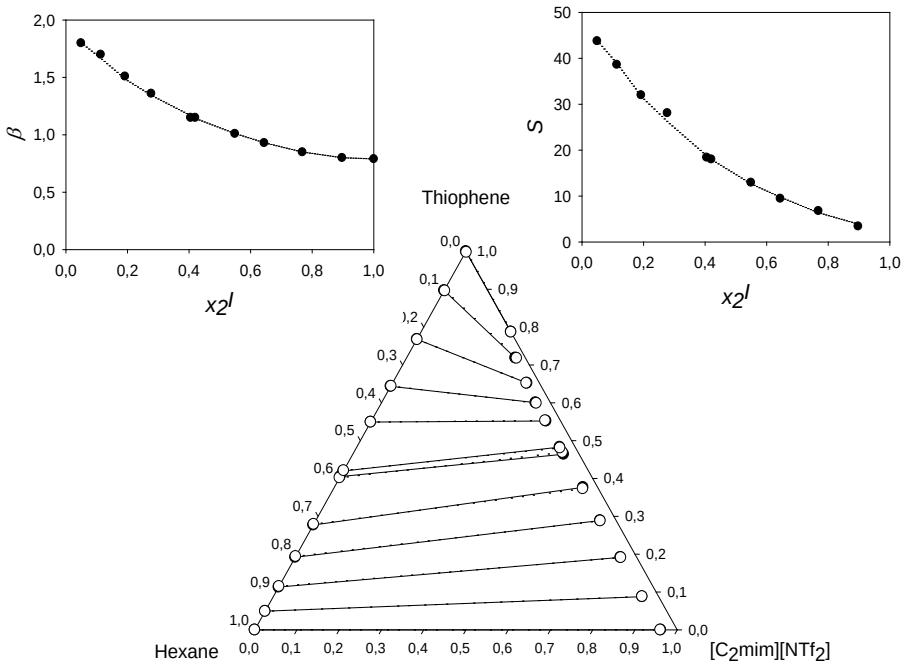

Figure 4.4. Down: Experimental (●, solid line) and correlated with UNIQUAC model (○, dotted line) tie-lines for the LLE of the ternary system {[C_2mim][NTf_2] + thiophene + hexane} at 298.15 K and atmospheric pressure. Up: Experimental (●) and correlated (dotted line) solute distribution ratios (β) and selectivities (S).

Table 4.5

Experimental LLE data for the ternary system {[C_2mim][NTf_2] (1) + thiophene (2) + toluene (3)} at 298.15 K and atmospheric pressure.

Hydrocarbon-rich phase			IL-rich phase			β	S
x_1^I	x_2^I	x_3^I	x_1^{II}	x_2^{II}	x_3^{II}		
0.000	0.000	1.000	0.370	0.000	0.630		
0.000	0.077	0.923	0.351	0.066	0.583	0.86	1.36
0.000	0.131	0.869	0.341	0.113	0.546	0.86	1.37
0.000	0.257	0.743	0.314	0.220	0.466	0.86	1.36
0.000	0.346	0.654	0.303	0.293	0.404	0.85	1.37
0.000	0.464	0.536	0.282	0.387	0.331	0.83	1.35
0.000	0.556	0.444	0.266	0.461	0.273	0.83	1.35
0.000	0.654	0.346	0.255	0.534	0.211	0.82	1.34
0.000	0.773	0.227	0.241	0.621	0.138	0.80	1.32
0.000	0.887	0.113	0.225	0.706	0.069	0.80	1.30
0.000	0.941	0.059	0.215	0.749	0.036	0.80	1.30
0.000	1.000	0.000	0.213	0.787	0.000	0.79	

Standard uncertainties: $u(p)$ = 5 kPa; $u(T)$ = 0.05 K; $u(x^I)$ = 0.004; $u(x^{II})$ = 0.005.

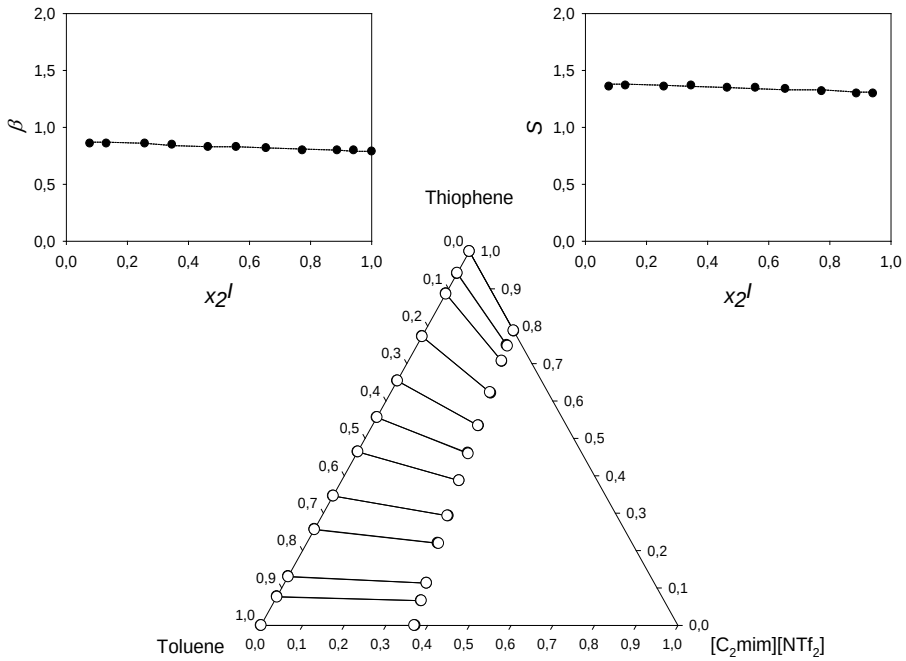

Figure 4.5. Down: Experimental (●, solid line) and correlated with UNIQUAC model (○, dotted line) tie-lines for the LLE of the ternary system {[C_2mim][NTf_2] + thiophene + toluene} at 298.15 K and atmospheric pressure. Up: Experimental (●) and correlated (dotted line) solute distribution ratios (β) and selectivities (S).

Table 4.6

Experimental LLE data for the ternary system {[C_2mim][NTf_2] (1) + pyridine (2) + hexane (3)} at 298.15 K and atmospheric pressure.

Hydrocarbon-rich phase			IL-rich phase			β	S
x_1^I	x_2^I	x_3^I	x_1^{II}	x_2^{II}	x_3^{II}		
0.000	0.000	1.000	0.961	0.000	0.039		
0.000	0.010	0.990	0.899	0.062	0.039	6.20	157
0.002	0.032	0.966	0.771	0.184	0.045	5.75	123
0.000	0.053	0.947	0.671	0.281	0.048	5.30	105
0.000	0.078	0.922	0.557	0.383	0.060	4.91	75.4
0.000	0.109	0.891	0.458	0.481	0.061	4.41	64.5
0.001	0.138	0.861	0.377	0.556	0.067	4.03	51.8
0.005	0.169	0.826	0.286	0.638	0.076	3.78	41.0
0.001	0.252	0.747	0.205	0.699	0.096	2.77	21.6
0.000	0.395	0.605	0.138	0.714	0.148	1.81	7.39

Standard uncertainties: $u(p)$ = 5 kPa; $u(T)$ = 0.05 K; $u(x^I)$ = 0.004; $u(x^{II})$ = 0.004.

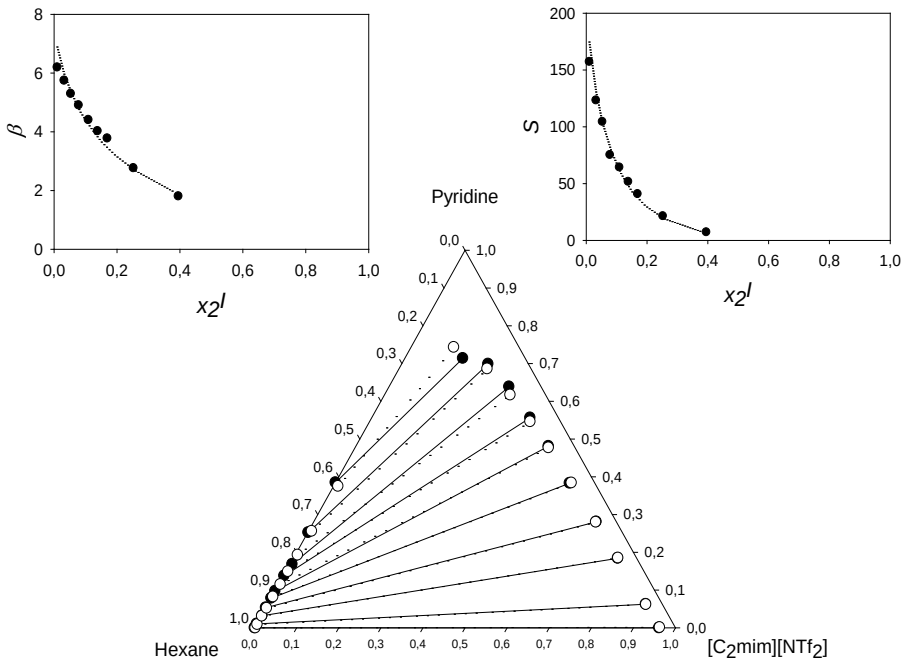

Figure 4.6. Down: Experimental (●, solid line) and correlated with NRTL model and α=0.3 (○, dotted line) tie-lines for the LLE of the ternary system {[C_2mim][NTf_2] + pyridine + hexane} at 298.15 K and atmospheric pressure. Up: Experimental (●) and correlated (dotted line) solute distribution ratios (β) and selectivities (S).

Table 4.7

Experimental LLE data for the ternary system {[C_2mim][OAc] (1) + thiophene (2) + hexane (3)} at 298.15 K and atmospheric pressure.

Hydrocarbon-rich phase			IL-rich phase			β	S
x_1^{I}	x_2^{I}	x_3^{I}	x_1^{II}	x_2^{II}	x_3^{II}		
0.000	0.000	1.000	0.990	0.000	0.010		
0.000	0.059	0.941	0.901	0.088	0.011	1.49	127
0.000	0.176	0.824	0.767	0.223	0.010	1.27	104
0.000	0.340	0.660	0.675	0.316	0.009	0.93	68.2
0.000	0.488	0.512	0.600	0.391	0.009	0.80	45.6
0.000	0.645	0.355	0.521	0.469	0.010	0.73	25.8
0.000	0.745	0.255	0.487	0.503	0.010	0.68	17.3
0.000	0.821	0.179	0.428	0.561	0.011	0.68	11.1
0.000	0.922	0.078	0.367	0.625	0.008	0.68	6.62
0.000	0.983	0.017	0.327	0.671	0.002	0.68	5.79
0.000	1.000	0.000	0.293	0.707	0.000	0.71	

Standard uncertainties: $u(p)$ = 5 kPa; $u(T)$ = 0.05 K; $u(x^{I})$ = 0.004; $u(x^{II})$ = 0.007.

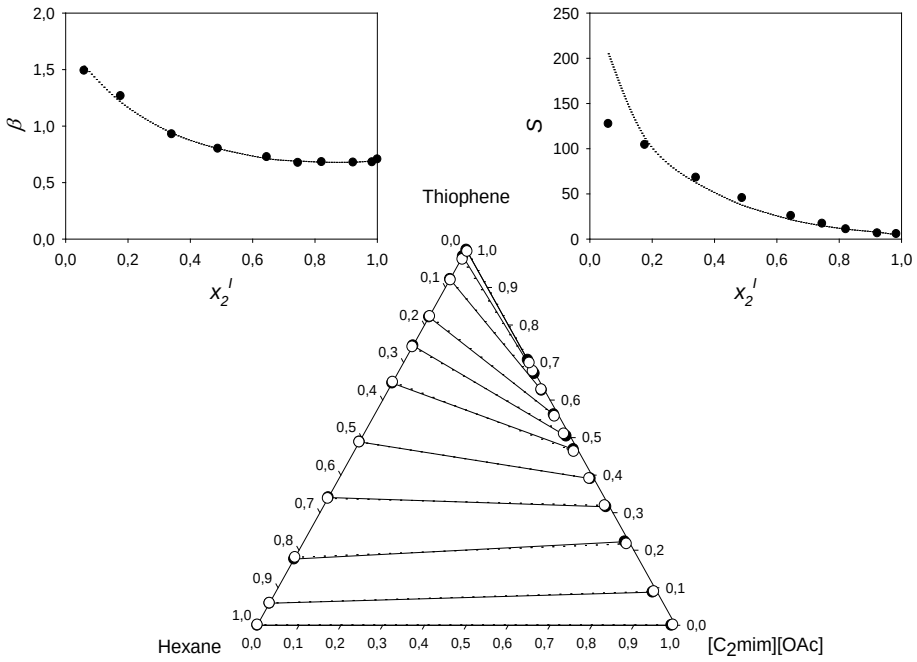

Figure 4.7. Down: Experimental (●, solid line) and correlated with UNIQUAC model (○, dotted line) tie-lines for the LLE of the ternary system {[C_2mim][OAc] + thiophene + hexane} at 298.15 K and atmospheric pressure. Up: Experimental (●) and correlated (dotted line) solute distribution ratios (β) and selectivities (S).

Table 4.8

Experimental LLE data for the ternary system {[C_2mim][OAc] (1) + thiophene (2) + toluene (3)} at 298.15 K and atmospheric pressure.

Hydrocarbon-rich phase			IL-rich phase			β	S
x_1^{I}	x_2^{I}	x_3^{I}	x_1^{II}	x_2^{II}	x_3^{II}		
0.000	0.000	1.000	0.793	0.000	0.207		
0.000	0.035	0.965	0.772	0.032	0.196	0.91	4.50
0.000	0.141	0.859	0.712	0.115	0.173	0.82	4.05
0.000	0.304	0.696	0.639	0.212	0.149	0.70	3.26
0.000	0.474	0.526	0.537	0.329	0.134	0.69	2.72
0.000	0.652	0.348	0.452	0.450	0.098	0.69	2.45
0.000	0.791	0.209	0.376	0.558	0.066	0.71	2.23
0.000	0.946	0.054	0.311	0.669	0.020	0.71	1.91
0.000	1.000	0.000	0.293	0.707	0.000	0.71	

Standard uncertainties: υ(p) = 5 kPa; υ(T) = 0.05 K; υ(x^{I}) = 0.004; υ(x^{II}) = 0.007.

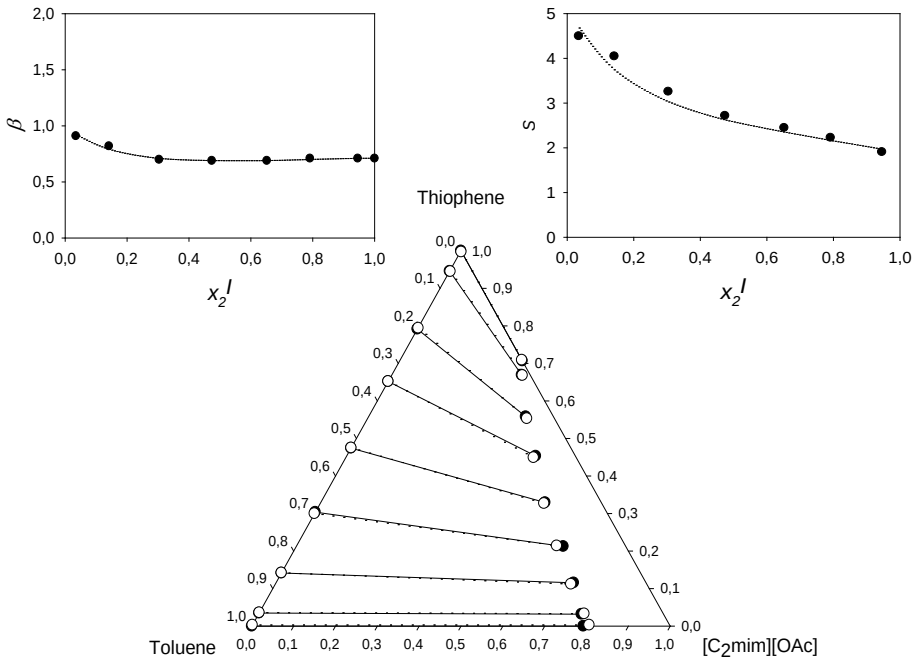

Figure 4.8. Down: Experimental (●, solid line) and correlated with UNIQUAC model (○, dotted line) tie-lines for the LLE of the ternary system {[C_2mim][OAc] + thiophene + toluene} at 298.15 K and atmospheric pressure. Up: Experimental (●) and correlated (dotted line) solute distribution ratios (β) and selectivities (S).

Table 4.9

Experimental LLE data for the ternary system {[C_2mim][OAc] (1) + pyridine (2) + hexane (3)} at 298.15 K and atmospheric pressure.

Hydrocarbon-rich phase			IL-rich phase			β	S
x_1^{I}	x_2^{I}	x_3^{I}	x_1^{II}	x_2^{II}	x_3^{II}		
0.000	0.000	1.000	0.998	0.000	0.002		
0.000	0.051	0.949	0.889	0.108	0.003	2.12	670
0.000	0.129	0.871	0.737	0.252	0.011	1.95	155
0.000	0.204	0.796	0.658	0.332	0.010	1.63	130
0.000	0.325	0.675	0.503	0.482	0.015	1.48	66.7
0.000	0.454	0.546	0.426	0.551	0.023	1.21	28.8
0.000	0.618	0.382	0.342	0.626	0.032	1.01	12.1
0.000	0.726	0.274	0.312	0.654	0.034	0.90	7.26
0.000	0.798	0.202	0.253	0.712	0.035	0.89	5.16

Standard uncertainties: $u(p)$ = 5 kPa; $u(T)$ = 0.05 K; $u(x^{I})$ = 0.006; $u(x^{II})$ = 0.007.

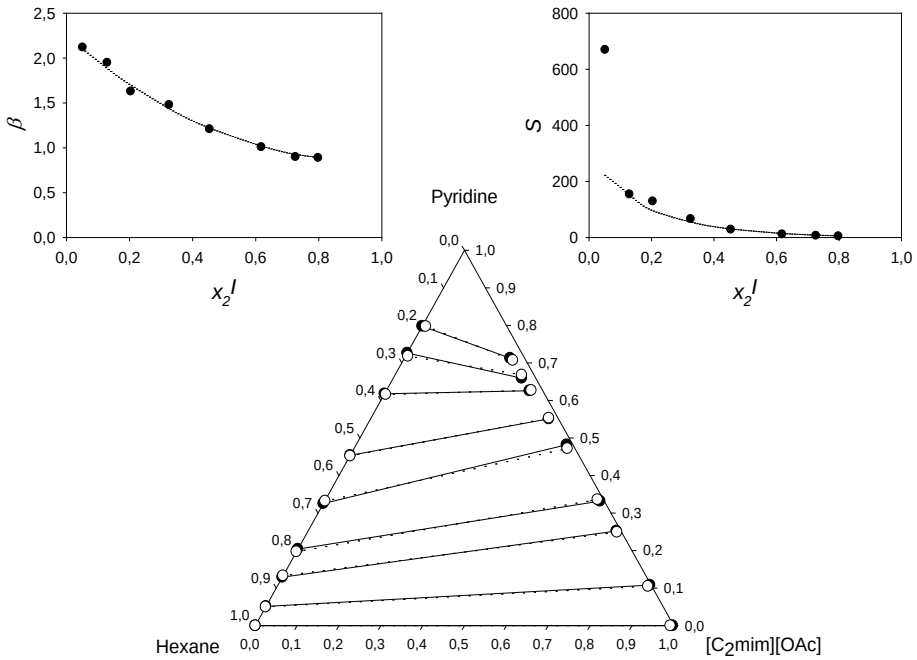

Figure 4.9. Down: Experimental (●, solid line) and correlated with UNIQUAC model (○, dotted line) tie-lines for the LLE of the ternary system {[C_2mim][OAc] + pyridine + hexane} at 298.15 K and atmospheric pressure. Up: Experimental (●) and correlated (dotted line) solute distribution ratios (β) and selectivities (S).

Table 4.10
Experimental LLE data for the ternary system {[C2mim][DEP] (1) + thiophene (2) + hexane (3)} at 298.15 K and atmospheric pressure.

Hydrocarbon-rich phase			IL-rich phase			β	S
x_1^{I}	x_2^{I}	x_3^{I}	x_1^{II}	x_2^{II}	x_3^{II}		
0.000	0.000	1.000	0.942	0.000	0.058		
0.000	0.016	0.984	0.896	0.046	0.058	2.88	48.8
0.000	0.090	0.910	0.735	0.210	0.055	2.33	38.6
0.000	0.168	0.832	0.611	0.340	0.049	2.02	34.4
0.000	0.304	0.696	0.506	0.450	0.044	1.48	23.4
0.000	0.431	0.569	0.405	0.540	0.055	1.25	13.0
0.000	0.608	0.392	0.332	0.617	0.051	1.01	7.80
0.000	0.710	0.290	0.269	0.678	0.053	0.95	5.23
0.000	0.804	0.196	0.239	0.712	0.049	0.89	3.54
0.000	0.917	0.083	0.166	0.802	0.032	0.88	2.27
0.000	1.000	0.000	0.116	0.884	0.000	0.87	

Standard uncertainties: υ(p) = 5 kPa; υ(T) = 0.05 K; υ(x^{I}) = 0.004; υ(x^{II}) = 0.007.

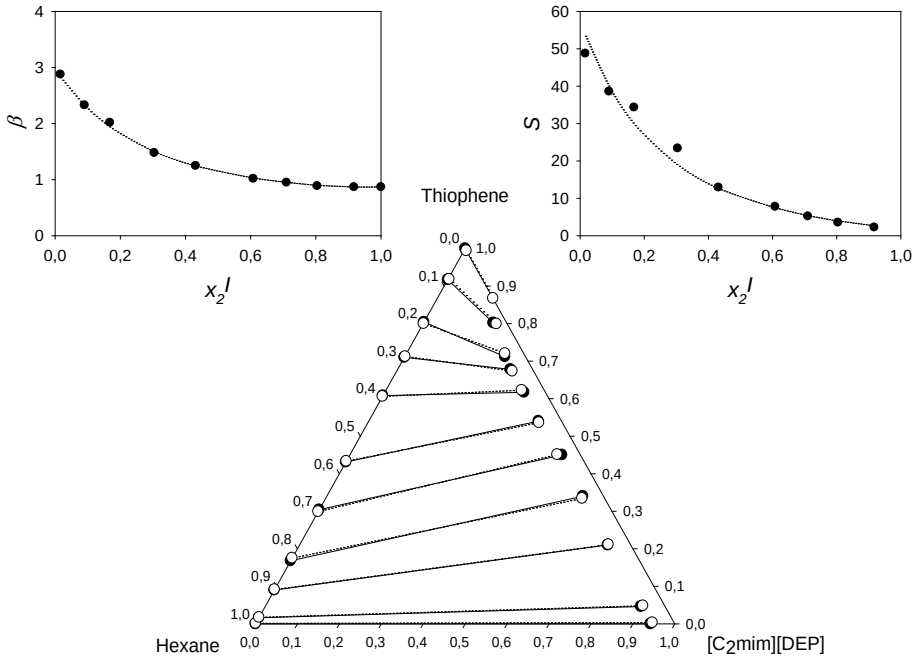

Figure 4.10. Down: Experimental (●, solid line) and correlated with UNIQUAC model (○, dotted line) tie-lines for the LLE of the ternary system {[C2mim][DEP] + thiophene + hexane} at 298.15 K and atmospheric pressure. Up: Experimental (●) and correlated (dotted line) solute distribution ratios (β) and selectivities (S).

Table 4.11
Experimental LLE data for the ternary system {[C$_2$mim][DEP] (1) + thiophene (2) + toluene (3)} at 298.15 K and atmospheric pressure.

Hydrocarbon-rich phase			IL-rich phase			β	S
x_1^{I}	x_2^{I}	x_3^{I}	x_1^{II}	x_2^{II}	x_3^{II}		
0.000	0.000	1.000	0.471	0.000	0.529		
0.000	0.112	0.888	0.420	0.123	0.457	1.10	2.14
0.000	0.226	0.774	0.385	0.217	0.398	0.96	1.87
0.000	0.311	0.689	0.360	0.291	0.349	0.94	1.85
0.000	0.452	0.548	0.309	0.409	0.282	0.91	1.76
0.000	0.597	0.403	0.270	0.511	0.219	0.86	1.58
0.000	0.712	0.288	0.236	0.603	0.161	0.85	1.51
0.000	0.870	0.130	0.191	0.724	0.085	0.83	1.27
0.000	1.000	0.000	0.134	0.866	0.000	0.87	

Standard uncertainties: $u(p)$ = 5 kPa; $u(T)$ = 0.05 K; $u(x^{I})$ = 0.004; $u(x^{II})$ = 0.007.

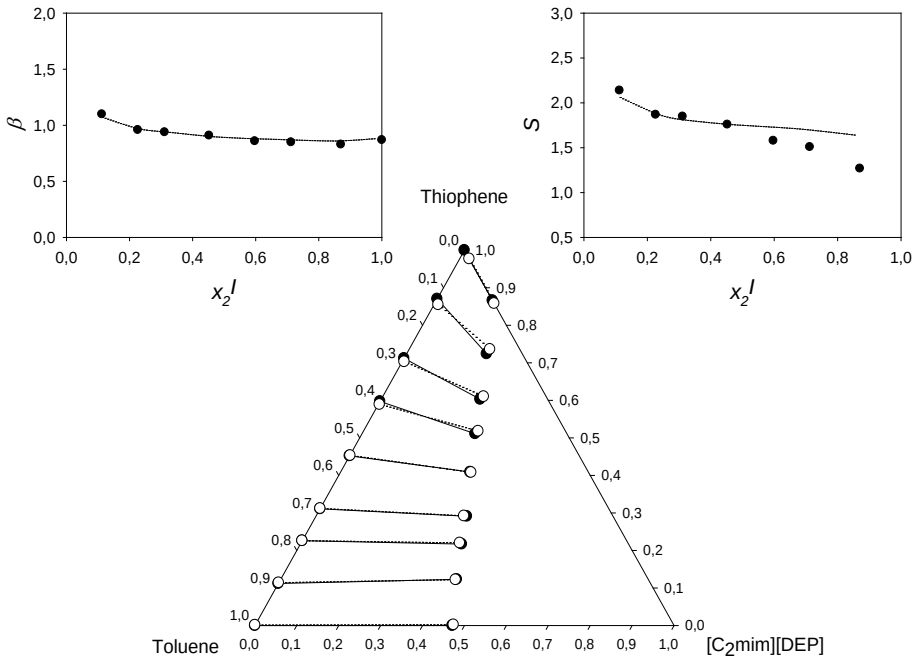

Figure 4.11. Down: Experimental (●, solid line) and correlated with UNIQUAC model (○, dotted line) tie-lines for the LLE of the ternary system {[C$_2$mim][DEP] + thiophene + toluene} at 298.15 K and atmospheric pressure. Up: Experimental (●) and correlated (dotted line) solute distribution ratios (β) and selectivities (S).

Table 4.12
Experimental LLE data for the ternary system {[C$_2$mim][DEP] (1) + pyridine (2) + hexane (3)} at 298.15 K and atmospheric pressure.

Hydrocarbon-rich phase			IL-rich phase			β	S
x_1^{I}	x_2^{I}	x_3^{I}	x_1^{II}	x_2^{II}	x_3^{II}		
0.000	0.000	1.000	0.940	0.000	0.060		
0.000	0.020	0.980	0.851	0.100	0.049	5.13	103
0.000	0.049	0.951	0.758	0.196	0.046	4.00	82.7
0.000	0.084	0.916	0.671	0.274	0.055	3.26	54.3
0.000	0.143	0.857	0.552	0.397	0.051	2.78	46.7
0.000	0.274	0.726	0.420	0.529	0.051	1.93	27.5
0.000	0.322	0.678	0.377	0.572	0.051	1.78	23.6
0.003	0.427	0.570	0.299	0.650	0.051	1.52	17.0
0.000	0.555	0.445	0.209	0.706	0.085	1.27	6.66

Standard uncertainties: $u(p)$ = 5 kPa; $u(T)$ = 0.05 K; $u(x^{I})$ = 0.006; $u(x^{II})$ = 0.007.

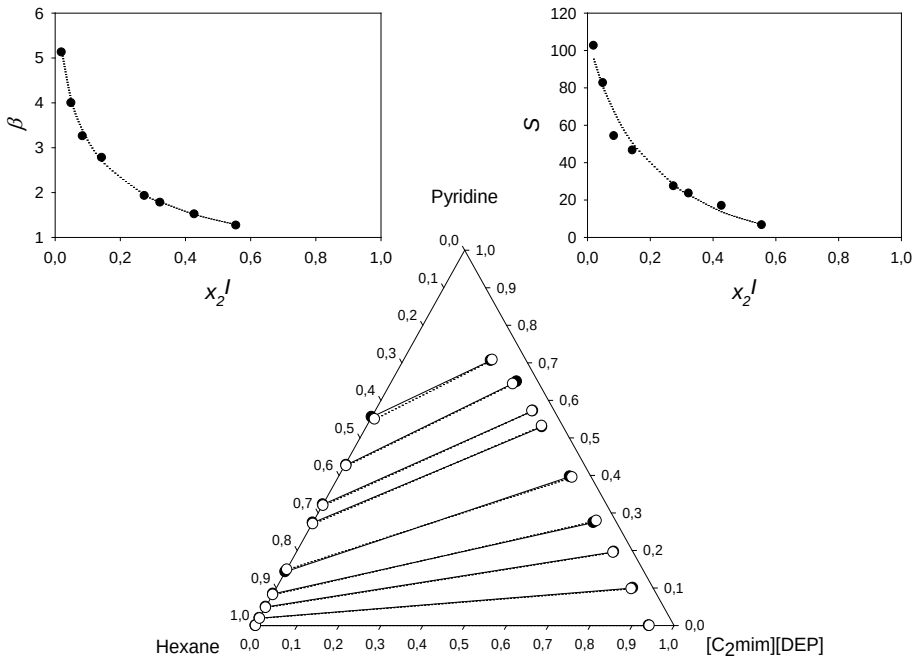

Figure 4.12. Down: Experimental (●, solid line) and correlated with NRTL model and α=0.1 (○, dotted line) tie-lines for the LLE of the ternary system {[C$_2$mim][DEP] + pyridine + hexane} at 298.15 K and atmospheric pressure. Up: Experimental (●) and correlated (dotted line) solute distribution ratios (β) and selectivities (S).

Practical applications of desulfurization process correspond to lowest sulfur concentrations. Taking into account the slopes of the tie-lines in the lowest part of the diagrams, thermodynamic parameters for all the tested ILs indicate a favorable separation of thiophene and pyridine from hexane. Nonetheless, separation of the sulfur compound from toluene becomes more difficult. A better comparison among solvents can be carried out through solute distribution ratios, β, and selectivities, S.

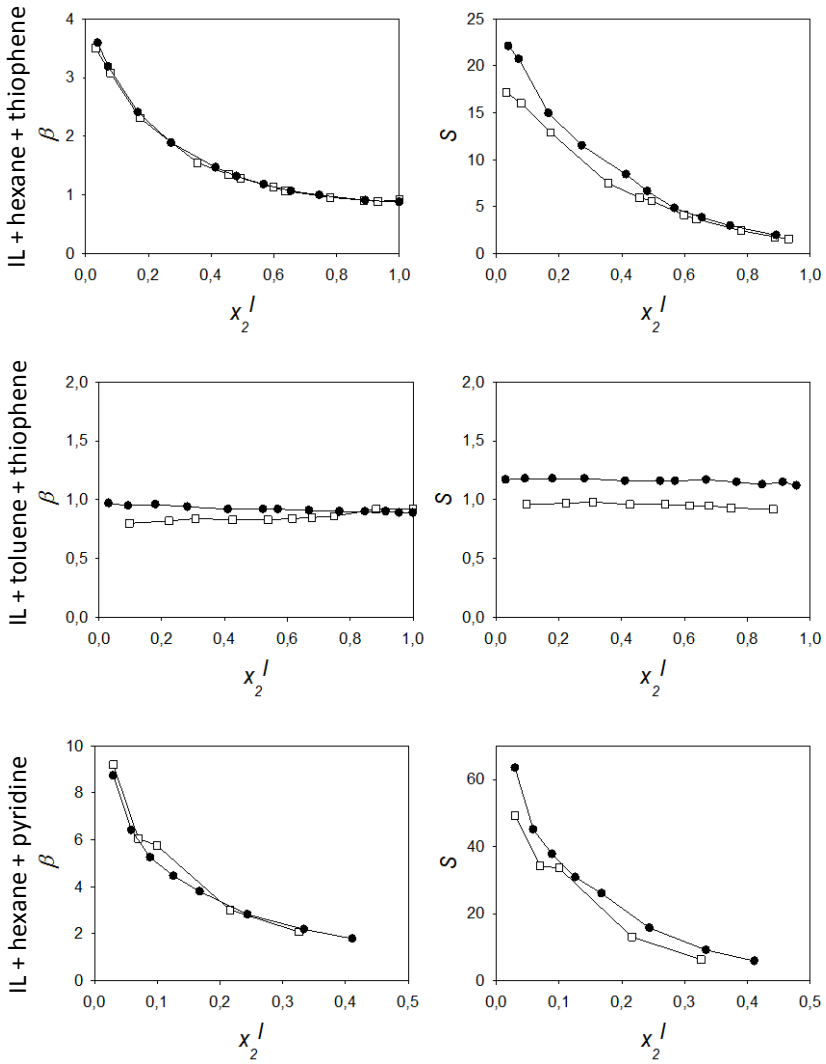

Figure 4.13. β and S values, as a function of the solute concentration in the hydrocarbon-rich phase, for the ternary systems {[C$_6$mmpy][NTf$_2$] + hexane + thiophene} (up), {[C$_6$mmpy][NTf$_2$] + toluene + thiophene} (middle) and {[C$_6$mmpy][NTf$_2$] + hexane + pyridine} (down). The compared ILs are [C$_6^{2,4}$mmpy][NTf$_2$] (●) and [C$_6^{3,5}$mmpy][NTf$_2$] (□).

As the first goal of this work is to analyze the effect of the position of the cation substituents on the desulfurization process, a comparison between the results obtained with the previously studied 1-hexyl-3,5-dimethylpyridinium bis(trifluoromethylsulfonyl)imide IL [156], [$C_6^{3,5}$mmpy][NTf_2], and with the 1-hexyl-2,4-dimethylpyridinium bis(trifluoromethylsulfonyl)imide, [$C_6^{2,4}$mmpy][NTf_2], is going to be carried out.

Figure 4.13 shows β and S, as a function of the solute concentration in the hydrocarbon-rich phase, for the {[C_6mmpy][NTf_2] + thiophene + hexane}, {[C_6mmpy][NTf_2] + thiophene + toluene}, and {[C_6mmpy][NTf_2] + thiophene + pyridine} ternary systems. It can be seen that values and trends of β and S are really similar for both ILs. This figure demonstrates that the separation of thiophene from hexane with these ILs is favorable in terms of solubilities and selectivities, especially at low mole fractions of thiophene. The values of this last parameter are slightly higher in the case of [$C_6^{2,4}$mmpy][NTf_2]. In the separation of thiophene from toluene, also slightly higher values of β and S were found in the case of IL with methyls asymmetrically placed in the pyridinium cation ring. Nonetheless, the low values of these parameters indicate that desulfurization would be accompanied with a certain degree of aromatic compound removal. Figure 4.13 also shows that with desulfurization a good denitrogenation would be achieved, with no appreciable differences between both ILs.

In Figures 4.14 to 4.16, β and S values can be observed as a function of the solute concentration in the hydrocarbon-rich phase for the different ternary systems and the four ILs studied in this work.

When studying the solubilities and selectivities of the systems with hexane and thiophene (Figure 4.14) it can be noticed that they are higher than the unity for the four ILs, what means they are good candidates for desulfurization. The ranking of solubilities is [$C_6^{2,4}$mmpy][NTf_2] > [C_2mim][DEP] > [C_2mim][NTf_2] > [C_2mim][OAc]. This results agree with the establishments done by Holbrey *et al.* [161], which state the dialkylpyridinium as the best solvents to extract sulfur compounds. Taking into account that the IL could be recovered, the selectivity becomes a decisive parameter to the evaluation of the ILs as solvents for the extraction. This parameter is related to the ability of extracting the target (sulfur) compound while keeping the other fuel components. For the extraction of thiophene from hexane the ranking of selectivities is [C_2mim][OAc] > [C_2mim][NTf_2] ≈ [C_2mim][DEP] > [$C_6^{2,4}$mmpy][NTf_2]. The best selectivity values are obtained for the IL [C_2mim][OAc] while the pyridinium IL achieves the worst results.

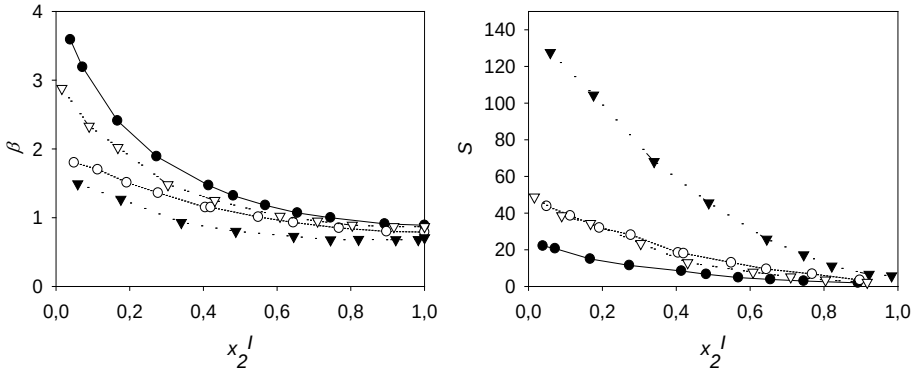

Figure 4.14. β (left) and S (right) values, as a function of the solute concentration in the hydrocarbon-rich phase, for the ternary system {IL + thiophene + hexane} at 298.15 K and atmospheric pressure. The compared ILs are: [$C_6^{2,4}$mmpy][NTf_2] (●, solid line), [C_2mim][NTf_2] (○, dotted line), [C_2mim][OAc] (▼, dashed line), and [C_2mim][DEP] (▽, dash-dotted line).

For the separation of thiophene from toluene, the solubilities ranking is [C_2mim][DEP] ≈ [$C_6^{2,4}$mmpy][NTf_2] > [C_2mim][NTf_2] ≈ [C_2mim][OAc], being all values too close (see Figure 4.15). β values close to the unity point out that a high amount of solvent is needed, but selectivity values, which are higher than the unity (especially in the case of the IL with acetate anion), ensure the viability of the separation. In the case of the selectivities, the ILs are ranked as follows: [C_2mim][OAc] > [C_2mim][DEP] > [C_2mim][NTf_2] > [$C_6^{2,4}$mmpy][NTf_2]. They are higher than the unity, but in the two latter they are too close to this value. Once more, the highest selectivities values are found for the [C_2mim][OAc] IL.

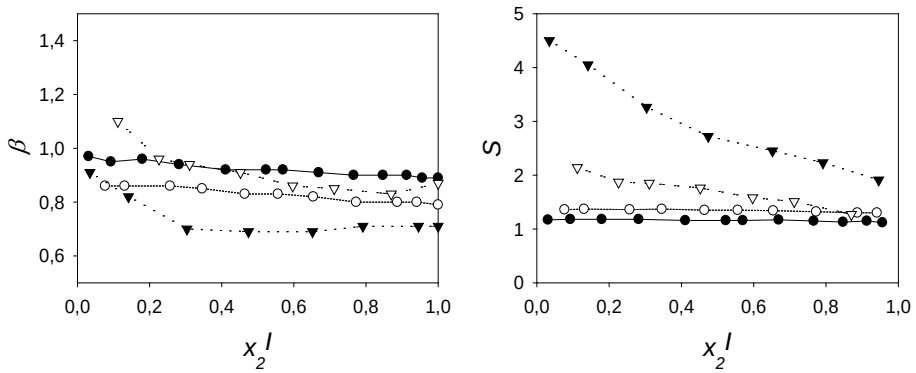

Figure 4.15. β (left) and S (right) values, as a function of the solute concentration in the hydrocarbon-rich phase, for the ternary system {IL + thiophene + toluene} at 298.15 K and atmospheric pressure. The compared ILs are: [$C_6^{2,4}$mmpy][NTf_2] (●, solid line), [C_2mim][NTf_2] (○, dotted line), [C_2mim][OAc] (▼, dashed line), and [C_2mim][DEP] (▽, dash-dotted line).

Finally, the values of solubilities and selectivities are higher than one for all the ILs when studying the separation of pyridine from hexane. This would imply a denitrogenation process simultaneous to the desulfurization. As it can be seen in Figure 4.16, the ranking for the solubilities is $[C_6^{2,4}mmpy][NTf_2]$ > $[C_2mim][NTf_2]$ ≈ $[C_2mim][DEP]$ >$[C_2mim][OAc]$. The ability of the ILs to preferentially extract pyridine ranks $[C_2mim][OAc]$ > $[C_2mim][NTf_2]$ ~ $[C_2mim][DEP]$ > $[C_6^{2,4}mmpy][NTf_2]$.

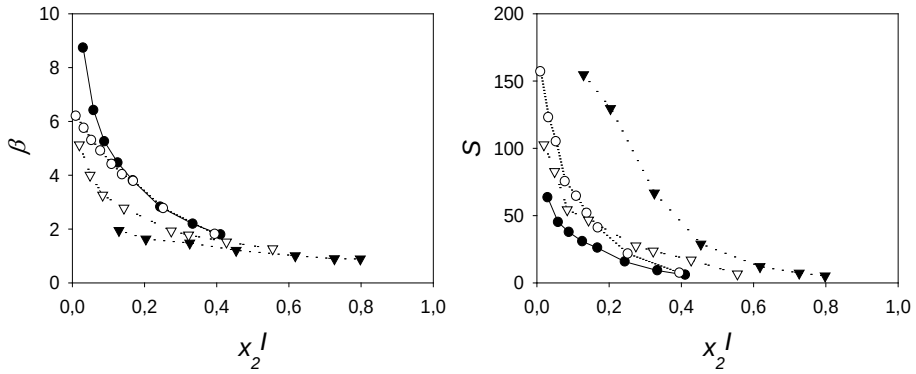

Figure 4.16. β (left) and S (right) values, as a function of the solute concentration in the hydrocarbon-rich phase, for the ternary system {IL + pyridine + hexane} at 298.15 K and atmospheric pressure. The compared ILs are: $[C_6^{2,4}mmpy][NTf_2]$ (●, solid line), $[C_2mim][NTf_2]$ (○, dotted line), $[C_2mim][OAc]$ (▼, dashed line), and $[C_2mim][DEP]$ (▽, dash-dotted line).

4.1.1. CORRELATION

Equilibrium conditions are deduced from the First and Second Laws of Thermodynamics. A closed system, heterogeneous and multicomponent, is at equilibrium when at constant temperature (T) and pressure (P), the Gibbs free energy (G) is a minimum. Mathematically:

$$d(G)_{T,P} = 0 \tag{3}$$

and this expression can be considered as a criteria or definition of equilibrium.

From this equation, equilibrium conditions can be established in terms of activities. For a multi-phasic and multi-component system, the equilibrium conditions are:

$$T^{(1)} = T^{(2)} = \cdots = T^{(m)} \tag{4}$$

$$P^{(1)} = P^{(2)} = \cdots = P^{(m)} \tag{5}$$

$$a_i^{(1)} = a_i^{(2)} = \cdots = a_i^{(m)} \quad (6)$$

where i refers to all the components of the system and the superscripts make reference to all the distinct phases. The activity is related to composition through the activity coefficient, which is defined as the ratio of the two, hence the expression turns into:

$$(x_i.\gamma_i)^1 = (x_i.\gamma_i)^{(2)} = \cdots = (x_i.\gamma_i)^{(m)} \quad (7)$$

which is probably the most practical expression of the equilibrium criterion.

To correlate the experimental data, a model of the activity coefficient as function of composition and temperature is needed. The experimental obtained data for the compositions of the equilibria systems were correlated using two well-known models, NRTL (*Non Random, Two-Liquid)* [218] and UNIQUAC (*UNIversal QUAsi Chemical*) [219].

The NRTL equation was developed by Renon and Prausnitz (1968) [218]:

$$\ln \gamma_i = \frac{\sum x_i \tau_{ji} G_{ji}}{\sum x_k G_{ki}} + \sum \frac{x_j G_{ij}}{\sum x_k G_{kj}} \left(\tau_{ij} - \frac{\sum x_m G_{mj} \tau_{mj}}{\sum x_k G_{kj}} \right) \quad (8)$$

$$\tau_{ij} = (g_{ij} - g_{jj})/RT = \Delta g_{ij}/RT \quad (9)$$

$$G_{ij} = exp(-\alpha_{ij}\tau_{ij}) \quad (10)$$

where g_{ij} is the residual Gibbs free energy and $\alpha_{ij} = \alpha_{ji}$ is the parameter that takes into account the non-randomness aleatory disposition of the molecules. In principle, the non-randomness parameter can be specified (from 0.2 to 0.47) according to a set of rules devised by the authors [218] that depend on the chemical nature of the components in the mixture, but it is usually given fixed value in an empirical way. The NRTL equation is applicable to multicomponent systems with only binary parameters (Δg_{ij}).

Abrams and Prausnitz [219] combined the theoretical concepts of the NRTL equation background with the quasi-chemical lattice model. The resulting UNIQUAC equation for the excess Gibbs energy consists of two parts, the first is a combinatorial part that attempt to describe the dominant entropic contribution, and the second is a residual part that is primarily due to intermolecular forces that are responsible for the enthalpy of mixing. For any component i, the expression of the activity coefficient provided by the UNIQUAC model is:

$$\ln \gamma_i = \ln \frac{\emptyset_i}{x_i} + \frac{z}{2} q_i ln \frac{\theta_i}{\emptyset_i} + l_i - \frac{\emptyset_i}{x_i} \sum x_j l_j - q_i \ln\left(\sum_{j=1}^{m} \theta_j \tau_{ji}\right) + q_i - q_i \sum_{j=1}^{m} \left(\frac{\theta_j \tau_{ij}}{\sum_{k=1}^{m} \theta_k \tau_{kj}}\right) \quad (11)$$

$$l_j = \frac{z}{2}(r_j - q_j) - (r_j - 1) \quad (12)$$

where z is the lattice coordination number, arbitrarily given a value of 10; and the segment fraction Φ, the area fraction θ and the parameter τ are given by:

$$\emptyset_i = \frac{r_i x_i}{\sum_{j=1}^{m} r_j x_j} \quad (13)$$

$$\theta_i = \frac{q_i x_i}{\sum_{j=1}^{m} q_j x_j} \quad (14)$$

$$\tau_{ij} = exp\left(-\frac{u_{ij} - u_{jj}}{RT}\right) \quad (15)$$

where $(u_{ij}–u_{jj}) = \Delta u_{ij}$ are the adjusting parameters of the model and represent the description of the energy interaction between a molecule of i and a molecule of j; and the parameters r and q are pure-component molecular-structure constants depending on molecular size and external surface areas. These structural parameters can be obtained from crystallographic data, although it is also possible to estimate them through a group contribution method, using the Van der Waals volumes and areas of the functional groups and making them dimensionless by reference to the volume or area of a methylene element in an infinite hydrocarbon chain.

In the NRTL correlation, the non-randomness parameter, α, was pre-fixed at the values of 0.1, 0.2 and 0.3. For the UNIQUAC model, the structural parameters, r and q, for the hydrocarbons are obtained using the molecular volume and area calculated by Bondi [220], and for the ILs from group contribution data [221, 222]. They are showed in Table 4.13.

Table 4.13
Structural parameters for the UNIQUAC model.

Component	r	q	Ref.
Hexane	4.4998	3.856	[220]
Toluene	3.9228	2.968	[220]
Thiophene	2.8569	2.140	[220]
Pyridine	2.9993	2.113	[220]
$[C_6^{2,4}mmpy][NTf_2]$	11.8990	9.975	[221]
$[C_2mim][NTf_2]$	9.8900	8.780	[222]
$[C_2mim][OAc]$	6.0191	5.576	[221,222]
$[C_2mim][DEP]$	8.2841	6.616	[221,222]

The binary interaction parameters were obtained by using the program of Sørensen and Arlt [223]. Two objective functions are used to fit the experimental phase compositions. Firstly the experimental data are fitted using F_a as objective function. After convergence, the obtained parameters are used in the second fit with F_b as objective function. These parameters are defined as:

$$F_a = \sum_k \sum_i [(a_{ik}^I - a_{ik}^{II})/(a_{ik}^I + a_{ik}^{II})]^2 + Q \sum_n P_n^2 \qquad (16)$$

$$F_b = \sum_k min \sum_i \sum_j (x_{ijk} - \hat{x}_{ijk})^2 + Q \sum_n P_n^2 + [\ln \left(\frac{\hat{\gamma}_{S\infty}^I}{\hat{\gamma}_{S\infty}^{II}} \beta_\infty\right)]^2 \qquad (17)$$

where a_i is the activity, x_i is the experimental composition in mole fraction, and $\hat{x}_i$ the corresponding calculated composition for component i. Other subscripts and superscripts are: j for phases (I, II) and k for tie-lines. With the aim of reducing the risks related to multiple solutions when using parameters of high value, a penalty term is introduced in both functions (second term). Q is set to 10^{-6} and to 10^{-10} in Eq. (16) and (17), respectively. P_n are the adjustable parameters. The third term used in Eq. (17) correctly fits experimental results when the concentration of solute is low. In this term $\hat{\gamma}_{S\infty}^I$ and $\hat{\gamma}_{S\infty}^{II}$ represent the solute activity coefficients calculated at infinite dilution in both phases and β_∞ the solute molar distribution ratio at infinite dilution.

The experimental data were correlated by fixing and without fixing this last parameter, β_∞, to an optimal value which is found by trial and error. This optimal value leads to the minimization of the mean error of the solute distribution ratio, $\Delta\beta$. This last parameter and the residual function, F, are used to evaluate the quality of the correlation:

$$F = 100\left[\sum_k min \sum_i \sum_j \frac{(x_{ijk}-\hat{x}_{ijk})^2}{6M}\right]^{0.5} \quad (18)$$

$$\Delta\beta = 100\left[\sum_k \frac{((\beta_k-\hat{\beta}_k)/\beta_k}{M}^2\right]^{0.5} \quad (19)$$

where M is the number of experimental tie-lines.

The binary interaction parameters, the residual function, and the mean error of the solute distribution ratio for the correlations of the ternary systems are showed in Tables 4.14 to 4.25. The experimental and correlated data are plotted together in Figures 4.1 to 4.12.

Table 4.14
Residual function (F), mean error of the solute distribution ratio ($\Delta\beta$) and binary interaction parameters for the correlations of the ternary system {[$C_6^{2,4}$mmpy][NTf_2] (1) + thiophene (2) + hexane (3)}.

NRTL

α = 0.2; not optimized

F	$\Delta\beta$	Components	Parameters	
		i-j	Δg_{ij} (J/mol)	Δg_{ji} (J/mol)
		1-2	-25581	2380.7
2.8428	8.4	1-3	679.37	17716
		2-3	25870	−22538

α = 0.2; optimized β_∞ = 5.00

F	$\Delta\beta$	Components	Parameters	
		i-j	Δg_{ij} (J/mol)	Δg_{ji} (J/mol)
		1-2	-22175	2447.5
2.8207	8.2	1-3	685.86	17341
		2-3	26686	−18929

UNIQUAC

Not optimized

F	$\Delta\beta$	Components	Parameters	
		i-j	Δu_{ij} (J/mol)	Δu_{ji} (J/mol)
		1-2	−1818.3	4122.1
0.2126	0.8	1-3	−741.27	5092.4
		2-3	−514.86	1802.5

Optimized β_∞ = 4.20

F	$\Delta\beta$	Components	Parameters	
		i-j	Δu_{ij} (J/mol)	Δu_{ji} (J/mol)
		1-2	−1845.6	4200.3
0.2137	0.6	1-3	−761.52	5250.5
		2-3	−558.31	1859.5

Table 4.15
Residual function (F), mean error of the solute distribution ratio ($\Delta\beta$) and binary interaction parameters for the correlations of the ternary system {[$C_6^{2,4}$mmpy][NTf_2] (1) + thiophene (2) + toluene (3)}.

NRTL

α = 0.3; not optimized

F	$\Delta\beta$	Components	Parameters	
		i-j	Δg_{ij} (J/mol)	Δg_{ji} (J/mol)
		1-2	820.54	763.40
7.1829	11.71	1-3	12181	-2189.1
		2-3	14296	−3311.8

α = 0.3; optimized β_∞ = 1.11

F	$\Delta\beta$	Components	Parameters	
		i-j	Δg_{ij} (J/mol)	Δg_{ji} (J/mol)
		1-2	197.65	351.15
3.3246	4.7	1-3	10679	-2740.9
		2-3	14394	−4182.2

UNIQUAC

Not optimized

F	$\Delta\beta$	Components	Parameters	
		i-j	Δu_{ij} (J/mol)	Δu_{ji} (J/mol)
		1-2	−1307.8	2888.5
0.5085	1.7	1-3	−1292.8	2783.6
		2-3	−64.869	65.928

Optimized β_∞ = 0.93

F	$\Delta\beta$	Components	Parameters	
		i-j	Δu_{ij} (J/mol)	Δu_{ji} (J/mol)
		1-2	−1313.4	2898.3
0.5065	1.7	1-3	−1292.2	2781.2
		2-3	−72.738	67.932

Table 4.16
Residual function (F), mean error of the solute distribution ratio ($\Delta\beta$) and binary interaction parameters for the correlations of the ternary system {[$C_6^{2,4}$mmpy][NTf_2] (1) + pyridine (2) + hexane (3)}.

NRTL

α = 0.1; not optimized

F	$\Delta\beta$	Components	Parameters	
		i-j	Δg_{ij} (J/mol)	Δg_{ji} (J/mol)
		1-2	-11185	5948.4
0.5011	29.6	1-3	-4780.3	22143
		2-3	10455	−3167.7

α = 0.1; optimized β_∞ = 16.7

F	$\Delta\beta$	Components	Parameters	
		i-j	Δg_{ij} (J/mol)	Δg_{ji} (J/mol)
		1-2	11506	8054.7
0.5165	29.3	1-3	−5077.6	23331
		2-3	9937.4	−2739.9

UNIQUAC

Not optimized

F	$\Delta\beta$	Components	Parameters	
		i-j	Δu_{ij} (J/mol)	Δu_{ji} (J/mol)
		1-2	1001.5	-1955.1
0.4799	31.2	1-3	1384.7	827.95
		2-3	136.23	1567.2

Optimized β_∞ = 12.8

F	$\Delta\beta$	Components	Parameters	
		i-j	Δu_{ij} (J/mol)	Δu_{ji} (J/mol)
		1-2	932.22	−1900.9
0.4801	29.6	1-3	1364.6	852.81
		2-3	131.25	1572.5

Table 4.17
Residual function (F), mean error of the solute distribution ratio ($\Delta\beta$) and binary interaction parameters for the correlations of the ternary system {[C_2mim][NTf_2] (1) + thiophene (2) + hexane (3)}.

NRTL

α = 0.2; not optimized

F	$\Delta\beta$	Components	Parameters	
		i-j	Δg_{ij} (J/mol)	Δg_{ji} (J/mol)
		1-2	-10916	30276
0.4988	8.6	1-3	6327.7	17727
		2-3	10588	-5695.6

α = 0.2; optimized β_∞ = 1.89

F	$\Delta\beta$	Components	Parameters	
		i-j	Δg_{ij} (J/mol)	Δg_{ji} (J/mol)
		1-2	-99690	30275
3.0491	8.3	1-3	23468	26105
		2-3	785.77	-96123

UNIQUAC

Not optimized

F	$\Delta\beta$	Components	Parameters	
		i-j	Δu_{ij} (J/mol)	Δu_{ji} (J/mol)
		1-2	-2216.6	5602.4
0.1474	1.6	1-3	1161.7	4286.1
		2-3	-104.72	1562.2

Optimized β_∞ = 1.96

F	$\Delta\beta$	Components	Parameters	
		i-j	Δu_{ij} (J/mol)	Δu_{ji} (J/mol)
		1-2	−2157.9	5423.2
0.1678	1.3	1-3	1259.4	3984.2
		2-3	126.50	1301.3

Table 4.18
Residual function (F), mean error of the solute distribution ratio ($\Delta\beta$) and binary interaction parameters for the correlations of the ternary system {[C_2mim][NTf_2] (1) + thiophene (2) + toluene (3)}.

NRTL

α = 0.3; not optimized

F	$\Delta\beta$	Components	Parameters	
		i-j	Δg_{ij} (J/mol)	Δg_{ji} (J/mol)
		1-2	892.31	285.52
0.9483	14.5	1-3	14193	-1927.4
		2-3	15006	-3738.0

α = 0.3; optimized β_∞ = 1.08

F	$\Delta\beta$	Components	Parameters	
		i-j	Δg_{ij} (J/mol)	Δg_{ji} (J/mol)
		1-2	-2.5411	90.062
1.3782	3.1	1-3	14179	-1922.0
		2-3	15019	-3572.8

UNIQUAC

Not optimized

F	$\Delta\beta$	Components	Parameters	
		i-j	Δu_{ij} (J/mol)	Δu_{ji} (J/mol)
		1-2	-2696.5	7009.3
0.1183	0.8	1-3	-2198.9	5694.4
		2-3	-344.38	429.23

Optimized β_∞ = 0.89

F	$\Delta\beta$	Components	Parameters	
		i-j	Δu_{ij} (J/mol)	Δu_{ji} (J/mol)
		1-2	-2697.0	7013.9
0.1198	0.6	1-3	-2209.8	5726.6
		2-3	-158.86	258.72

Table 4.19
Residual function (F), mean error of the solute distribution ratio ($\Delta\beta$) and binary interaction parameters for the correlations of the ternary system {[C_2mim][NTf_2] (1) + pyridine (2) + hexane (3)}.

NRTL

α = 0.3; not optimized

F	$\Delta\beta$	Components	Parameters	
		i-j	Δg_{ij} (J/mol)	Δg_{ji} (J/mol)
		1-2	-8698.6	7459.1
0.7358	27.9	1-3	10468	18369
		2-3	6740.5	1377.3

α = 0.3; optimized β_∞ = 7.14

F	$\Delta\beta$	Components	Parameters	
		i-j	Δg_{ij} (J/mol)	Δg_{ji} (J/mol)
		1-2	-5275.0	5244.8
0.9929	7.8	1-3	10808	21705
		2-3	7531.3	2150.2

UNIQUAC

Not optimized

F	$\Delta\beta$	Components	Parameters	
		i-j	Δu_{ij} (J/mol)	Δu_{ji} (J/mol)
		1-2	-7839.4	2812.4
0.5614	10.7	1-3	2848.5	1170.8
		2-3	355.46	-2786.1

Optimized β_∞ = 4.55

F	$\Delta\beta$	Components	Parameters	
		i-j	Δu_{ij} (J/mol)	Δu_{ji} (J/mol)
		1-2	8160.8	-4493.6
0.7246	7.2	1-3	3408.6	1094.3
		2-3	-323.42	2606.7

Table 4.20
Residual function (F), mean error of the solute distribution ratio ($\Delta\beta$) and binary interaction parameters for the correlations of the ternary system {[C_2mim][OAc] (1) + thiophene (2) + hexane (3)}.

NRTL

α = 0.2; not optimized

F	$\Delta\beta$	Components	Parameters	
		i-j	Δg_{ij} (J/mol)	Δg_{ji} (J/mol)
		1-2	-4751.2	15410
0.7914	5.0	1-3	9693.8	16369
		2-3	2603.8	-1278.0

α = 0.2; optimized β_∞ = 1.61

F	$\Delta\beta$	Components	Parameters	
		i-j	Δg_{ij} (J/mol)	Δg_{ji} (J/mol)
		1-2	-4749.6	15406
0.7913	4.9	1-3	9730.4	16377
		2-3	2591.4	-1264.0

UNIQUAC

Not optimized

F	$\Delta\beta$	Components	Parameters	
		i-j	Δu_{ij} (J/mol)	Δu_{ji} (J/mol)
		1-2	-1420.1	4007.2
0.3500	2.8	1-3	970.13	7250.4
		2-3	-1058.0	2620.6

Optimized β_∞ = 1.75

F	$\Delta\beta$	Components	Parameters	
		i-j	Δu_{ij} (J/mol)	Δu_{ji} (J/mol)
		1-2	-1387.2	3903.5
0.3564	2.1	1-3	913.26	7244.0
		2-3	-971.13	2436.3

Table 4.21
Residual function (F), mean error of the solute distribution ratio ($\Delta\beta$) and binary interaction parameters for the correlations of the ternary system {[C_2mim][OAc] (1) + thiophene (2) + toluene (3)}.

NRTL

α = 0.3; not optimized

F	$\Delta\beta$	Components	Parameters	
		i-j	Δg_{ij} (J/mol)	Δg_{ji} (J/mol)
		1-2	-2799.3	13506
0.5681	7.5	1-3	2756.7	12700
		2-3	348.58	-1681.1

α = 0.3; optimized β_∞ = 0.91

F	$\Delta\beta$	Components	Parameters	
		i-j	Δg_{ij} (J/mol)	Δg_{ji} (J/mol)
		1-2	-2630.3	12741
0.6945	4.6	1-3	2911.2	13464
		2-3	1241.9	-1467.3

UNIQUAC

Not optimized

F	$\Delta\beta$	Components	Parameters	
		i-j	Δu_{ij} (J/mol)	Δu_{ji} (J/mol)
		1-2	-1575.2	4464.6
0.3665	8.3	1-3	-655.72	3993.3
		2-3	-335.54	480.44

Optimized β_∞ = 0.95

F	$\Delta\beta$	Components	Parameters	
		i-j	Δu_{ij} (J/mol)	Δu_{ji} (J/mol)
		1-2	8160.8	-4493.6
0.4942	1.5	1-3	3408.6	1094.3
		2-3	-323.42	2606.7

Table 4.22
Residual function (F), mean error of the solute distribution ratio ($\Delta\beta$) and binary interaction parameters for the correlations of the ternary system {[C_2mim][OAc] (1) + pyridine (2) + hexane (3)}.

NRTL

α = 0.2; not optimized

F	$\Delta\beta$	Components	Parameters	
		i-j	Δg_{ij} (J/mol)	Δg_{ji} (J/mol)
		1-2	-51868	1765.7
1.4427	6.5	1-3	11477	15498
		2-3	15053	-53116

α = 0.2; optimized β_∞ = 2.05

F	$\Delta\beta$	Components	Parameters	
		i-j	Δg_{ij} (J/mol)	Δg_{ji} (J/mol)
		1-2	-51000	1624.5
1.4603	6.3	1-3	11582	15270
		2-3	15223	-52256

UNIQUAC

Not optimized

F	$\Delta\beta$	Components	Parameters	
		i-j	Δu_{ij} (J/mol)	Δu_{ji} (J/mol)
		1-2	-1863.6	4125.2
0.4886	3.1	1-3	1359.9	3288.5
		2-3	-321.46	1596.4

Optimized β_∞ = 2.27

F	$\Delta\beta$	Components	Parameters	
		i-j	Δu_{ij} (J/mol)	Δu_{ji} (J/mol)
		1-2	-1897.4	4292.3
0.4994	3.0	1-3	1377.5	3056.7
		2-3	-196.16	1409.6

Table 4.23
Residual function (F), mean error of the solute distribution ratio ($\Delta\beta$) and binary interaction parameters for the correlations of the ternary system {[C_2mim][DEP] (1) + thiophene (2) + hexane (3)}.

NRTL

α = 0.2; not optimized

F	$\Delta\beta$	Components	Parameters	
		i-j	Δg_{ij} (J/mol)	Δg_{ji} (J/mol)
		1-2	-46468	405.13
3.0229	11.4	1-3	7269.8	34435
		2-3	47521	-45696

α = 0.2; optimized β_∞ = 3.23

F	$\Delta\beta$	Components	Parameters	
		i-j	Δg_{ij} (J/mol)	Δg_{ji} (J/mol)
		1-2	-43573	724.61
3.0351	11.0	1-3	7171.4	27720
		2-3	46342	-42913

UNIQUAC

Not optimized

F	$\Delta\beta$	Components	Parameters	
		i-j	Δu_{ij} (J/mol)	Δu_{ji} (J/mol)
		1-2	-2632.4	6277.9
0.4314	2.0	1-3	-478.10	10940
		2-3	-1383.7	3628.6

Optimized β_∞ = 3.03

F	$\Delta\beta$	Components	Parameters	
		i-j	Δu_{ij} (J/mol)	Δu_{ji} (J/mol)
		1-2	-2745.3	6677.6
0.4288	1.9	1-3	-348.20	9555.8
		2-3	-1321.3	3474.6

Table 4.24
Residual function (F), mean error of the solute distribution ratio ($\Delta\beta$) and binary interaction parameters for the correlations of the ternary system {[C_2mim][DEP] (1) + thiophene (2) + toluene (3)}.

NRTL

α = 0.3; not optimized

F	$\Delta\beta$	Components	Parameters	
		i-j	Δg_{ij} (J/mol)	Δg_{ji} (J/mol)
		1-2	-4423.5	13726
0.6112	3.7	1-3	-445.04	16617
		2-3	-1394.2	459.90

α = 0.3; optimized β_∞ = 1.49

F	$\Delta\beta$	Components	Parameters	
		i-j	Δg_{ij} (J/mol)	Δg_{ji} (J/mol)
		1-2	-4451.5	13704
0.6502	2.1	1-3	5743.9	25720
		2-3	-3185.7	277.40

UNIQUAC

Not optimized

F	$\Delta\beta$	Components	Parameters	
		i-j	Δu_{ij} (J/mol)	Δu_{ji} (J/mol)
		1-2	-1628.6	4031.0
0.4321	4.5	1-3	-1814.5	9259.0
		2-3	-251.97	451.97

Optimized β_∞ = 1.18

F	$\Delta\beta$	Components	Parameters	
		i-j	Δu_{ij} (J/mol)	Δu_{ji} (J/mol)
		1-2	-1611.9	4031.8
0.6192	2.1	1-3	-1798.8	9498.4
		2-3	-746.74	1233.9

Table 4.25
Residual function (F), mean error of the solute distribution ratio ($\Delta\beta$) and binary interaction parameters for the correlations of the ternary system {[C_2mim][DEP] (1) + pyridine (2) + hexane (3)}.

NRTL

α = 0.1; not optimized

F	$\Delta\beta$	Components	Parameters	
		i-j	Δg_{ij} (J/mol)	Δg_{ji} (J/mol)
		1-2	-11213	16755
0.3748	3.0	1-3	-1588.8	19828
		2-3	5122.9	-2043.4

α = 0.1; optimized β_∞ = 6.25

F	$\Delta\beta$	Components	Parameters	
		i-j	Δg_{ij} (J/mol)	Δg_{ji} (J/mol)
		1-2	-10893	16658
0.3761	2.5	1-3	-1622.6	20149
		2-3	5027.3	-1759.8

UNIQUAC

Not optimized

F	$\Delta\beta$	Components	Parameters	
		i-j	Δu_{ij} (J/mol)	Δu_{ji} (J/mol)
		1-2	-1537.8	2507.5
0.5556	9.6	1-3	-320.21	8658.6
		2-3	-995.65	2463.0

Optimized β_∞ = 5.88

F	$\Delta\beta$	Components	Parameters	
		i-j	Δu_{ij} (J/mol)	Δu_{ji} (J/mol)
		1-2	-6277.2	-161.72
0.4066	3.6	1-3	577.16	2292.1
		2-3	2813.2	-6538.5

To establish a comparison, the correlations that best fitted the experimental data for each ternary system are presented in Table 4.26.

Table 4.26
Best-fitting correlations for the studied ternary systems.

IL	{IL+thiophene+ hexane}	{IL+thiophene+ toluene}	{IL+pyridine +hexane}
$[C_6^{2,4}mmpyr][NTf_2]$	UNIQUAC	UNIQUAC	NRTL α = 0.1
$[C_2mim][NTf_2]$	UNIQUAC	UNIQUAC	NRTL α = 0.3
$[C_2mim][OAc]$	UNIQUAC	UNIQUAC	UNIQUAC
$[C_2mim][DEP]$	UNIQUAC	UNIQUAC	NRTL α = 0.1

4.2. DESULFURIZATION OF SYNTHETIC FUELS

4.2.1. EXTRACTIVE DESULFURIZATION

4.2.1.1. SYNTHETIC GASOLINE

Figures 4.17 to 4.20 show the composition (%wt) of each component in the simulated gasoline and raffinate product after one, two and three extraction stages with each of the four ILs studied. It can be seen that the reduction of thiophene is stronger in the case of the pyridinium IL, achieving 84.9 wt% of extraction of this compound after three steps. In the case of the other ILs, the thiophene composition is reduced around 80.6 wt%, 79.3 wt%, and 61.1 wt% using [C_2mim][DEP], [C_2mim][OAc], and [C_2mim][NTf_2], respectively. The best performance of the pyridinium IL is probably due to the electronic π-π interactions of this ring with the aromatic sulfur specie, as it was previously explained in other works [148]. As expected from equilibria previously determined (section 4.1), an important dearomatization in the extraction process is also observed. The reduction of toluene content is around 67.0 wt%, 23.7 wt%, 14.2 wt%, and 32.8 wt% using [$C_6^{2,4}$mmpy][NTf_2], [C_2mim][DEP], [C_2mim][OAc], and [C_2mim][NTf_2], respectively. After three steps of extraction, the denitrogenation of the gasoline is total with the four ILs. In all the cases, no IL was found in the raffinate phases.

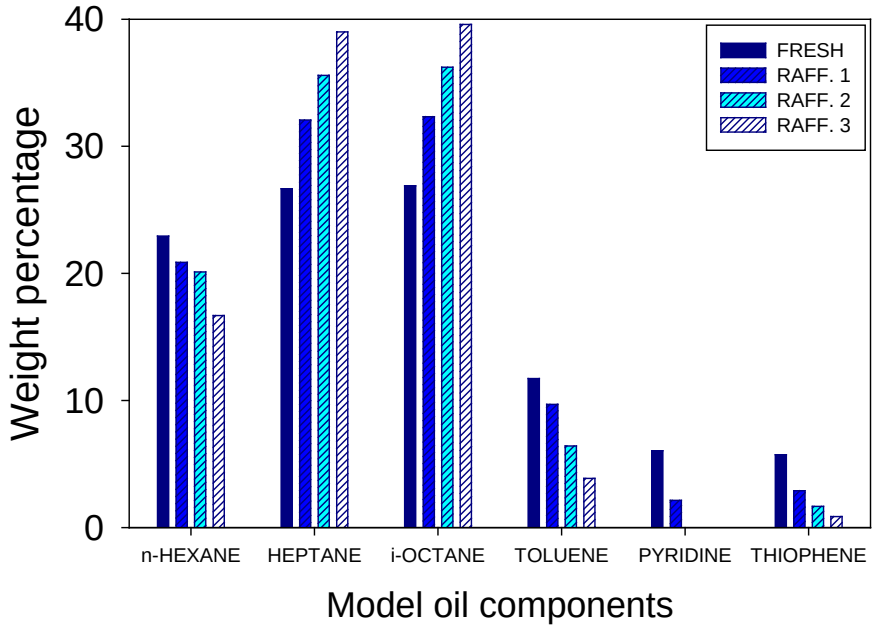

Figure 4.17. Three stages EDS of synthetic gasoline at 298.15 K and atmospheric pressure with the IL [$C_6^{2,4}$mmpy][NTf_2].

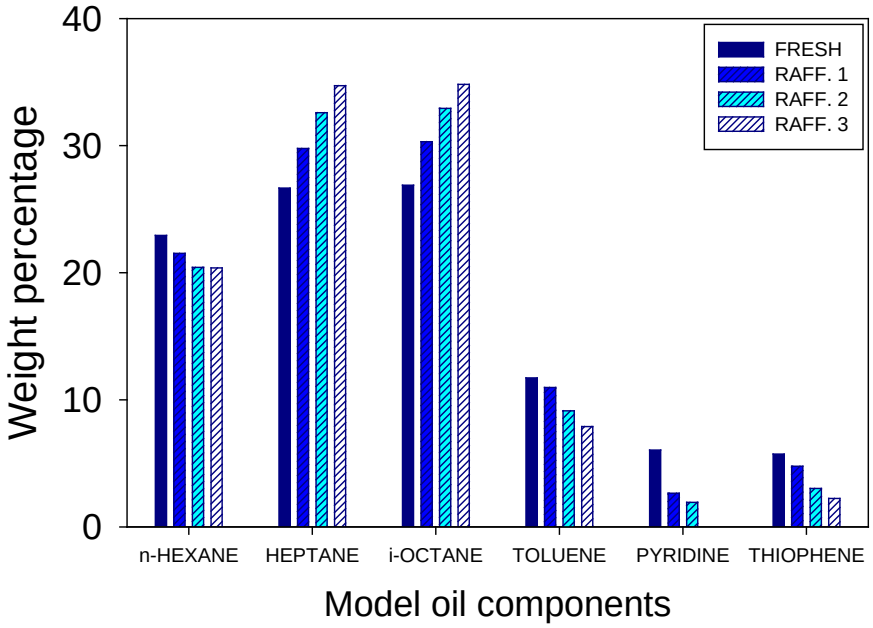

Figure 4.18. Three stages EDS of synthetic gasoline at 298.15 K and atmospheric pressure with the IL [C_2mim][NTf_2].

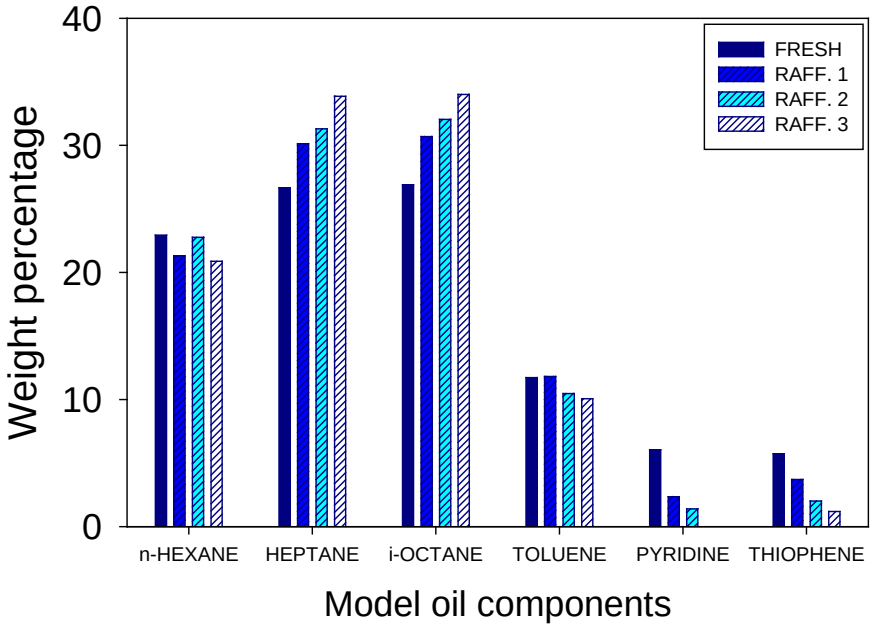

Figure 4.19. Three stages EDS of synthetic gasoline at 298.15 K and atmospheric pressure with the IL [C_2mim][OAc].

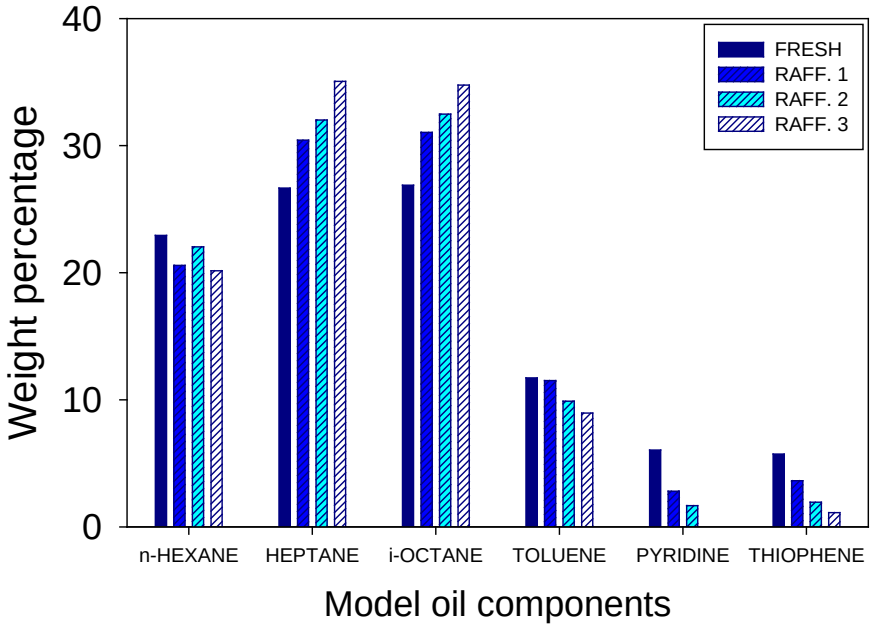

Figure 4.20. Three stages EDS of synthetic gasoline at 298.15 K and atmospheric pressure with the IL [C_2mim][DEP].

4.2.1.2. SYNTHETIC DIESEL OIL

In the case of the diesel oil model (see Figures 4.21-4.24) the desulfurization ability of these ILs follows the same tendency as in the case of the gasoline. Best results are found for [$C_6^{2,4}$mmpy][NTf_2], extracting more than the 90 wt% of thiophene and 98 wt% of dibenzothiophene. This IL also reduces around 78 wt% the toluene content. [C_2mim][OAc] extracts 87.2 wt% of thiophene, 88.0 wt% of dibenzothiophene and reduces around 53.2 wt% the toluene composition. [C_2mim][DEP] extracts 88.4 wt% of thiophene, 88.4 wt% of dibenzothiophene and reduces around 58.9 wt% the toluene composition. Finally, [C_2mim][NTf_2], that achieved the worst results, extracts 75.4 wt% of thiophene, 80.5 wt% of dibenzothiophene and reduces around 55.1 wt% the toluene composition. It must be highlighted that the extraction of dibenzothiophene is higher than that of thiophene, especially in the case of the pyridinium IL. The reason of this difference is the above-mentioned π-π interactions, which imply that the extraction increases with the electron density of the sulfur compounds [148]. One more time, denitrogenation is total for all the ILs after the three stages of extraction and no IL was found in the raffinate phases.

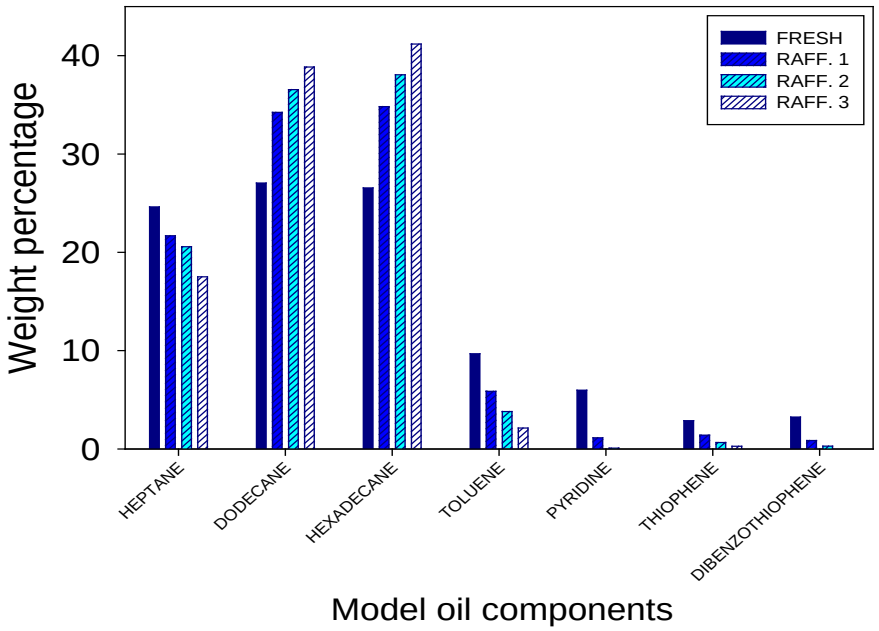

Figure 4.21. Three stages EDS of synthetic diesel oil at 298.15 K and atmospheric pressure with the IL [$C_6^{2,4}$mmpy][NTf_2].

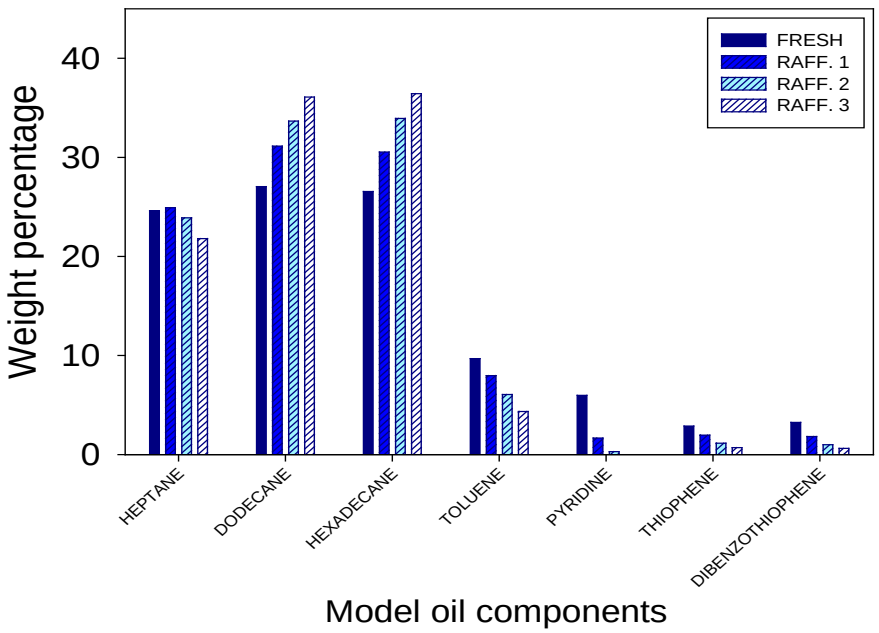

Figure 4.22. Three stages EDS of synthetic diesel oil at 298.15 K and atmospheric pressure with the IL [C_2mim][NTf_2].

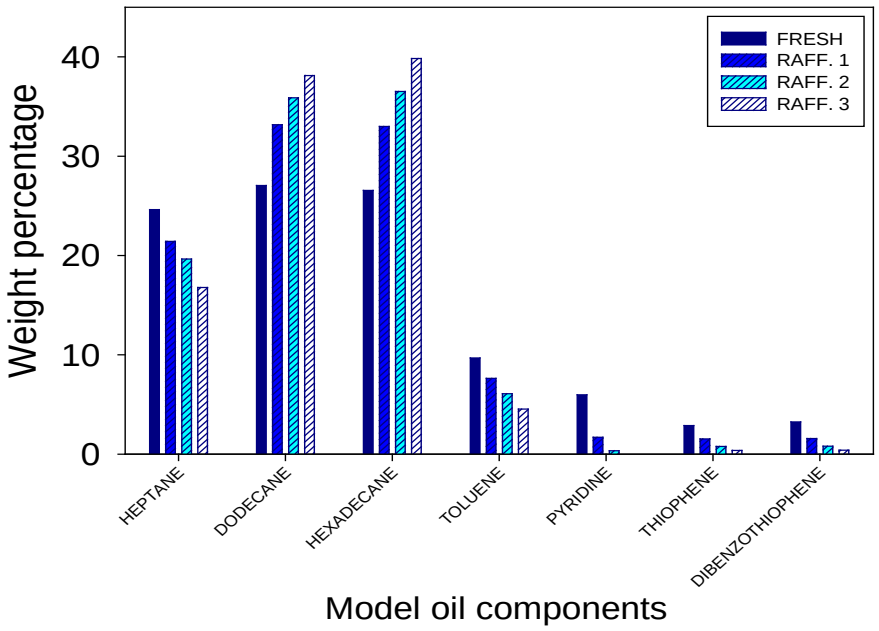

Figure 4.23. Three stages EDS of synthetic diesel oil at 298.15 K and atmospheric pressure with the IL [C_2mim][OAc].

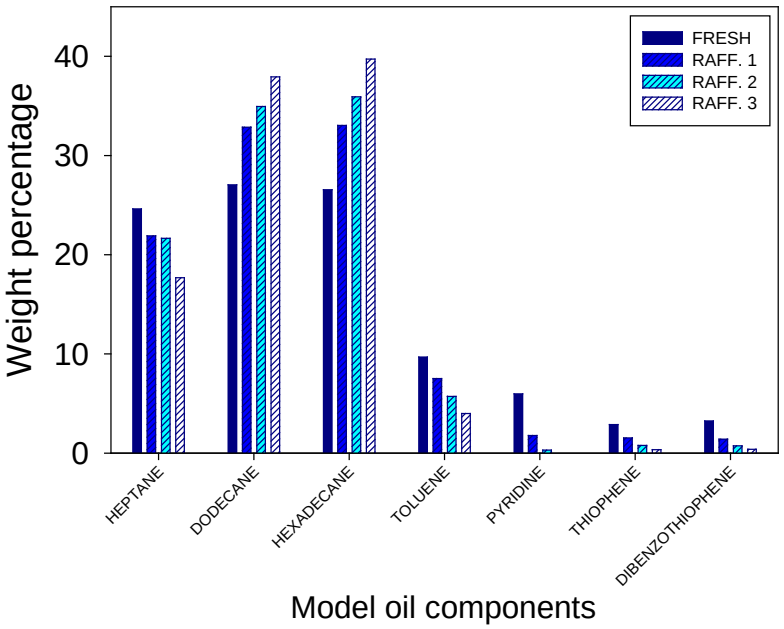

Figure 4.24. Three stages EDS of synthetic diesel oil at 298.15 K and atmospheric pressure with the IL [C_2mim][DEP].

4.2.2. OXIDATIVE DESULFURIZATION

4.2.2.1. SYNTHETIC GASOLINE

An ODS of the gasoline model oil was carried out working with H_2O_2 and AcOH, in several conditions and proportions, and results do not improve those obtained by simple extraction. This behavior was previously found in other works [130]. Thiophene has relatively low electron density and the reactivity of sulfur compounds for oxidation increases with this parameter.

4.2.2.2. SYNTHETIC DIESEL OIL

a) Optimization procedure

First, the optimization of the H_2O_2-AcOH oxidizing-catalytic system was carried out. Figure 4.25 shows the removal (%wt) of thiophene and dibenzothiophene when the synthetic diesel oil was mixed with the same quantity of $[C_6^{2,4}mmpy][NTf_2]$ with a fixed content of catalyst (n_{AcOH}/n_S=10) and at several ratios of oxidant (n_{H2O2}/n_S) after one oxidative extraction stage. The chosen ratio was 9 mol H_2O_2/ mol S, value from which the dibenzothiophene removal starts to keep almost constant.

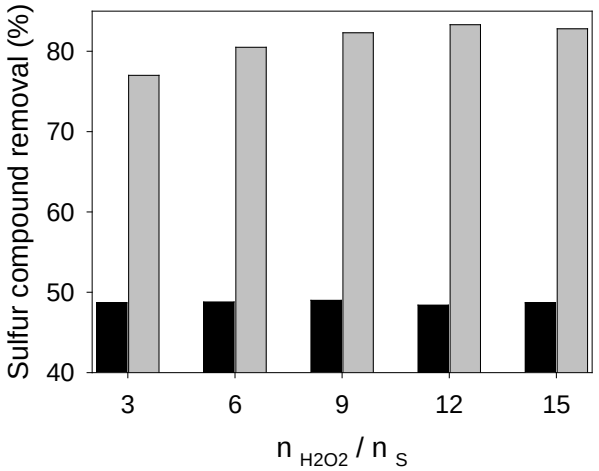

Figure 4.25. Removal of thiophene (black) and dibenzothiophene (grey) from synthetic diesel oil using the IL $[C_6^{2,4}mmpy][NTf_2]$ and n_{AcOH}/ n_S =10, at several ratios of oxidant.

Then, with the ratio of oxidizing agent fixed to 9, the influence of the amount of catalyst was evaluated (Figure 4.26) and the selected value for this ratio was also 9. With more catalyst the desulfurization achieved is slightly higher, but this increase does not compensate the manipulation of a major proportion of acid.

It must be highlighted that in the case of the ILs with $[NTf_2]$ anion, since they are water-immiscible, three phases appear during the settling down: the synthetic fuel phase, the oxocatalytic phase (with the hydrogen peroxide and acetic acid), and the IL phase. Nonetheless,

the ILs [C_2mim][OAc] and [C_2mim][DEP] are miscible with water, and after stirring the mixture, it splits in two different phases (the raffinate one and the other formed by the IL with the acetic acid and the hydrogen peroxide).

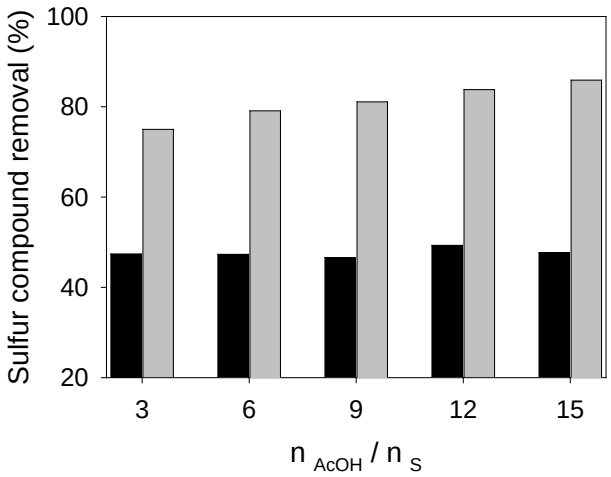

Figure 4.26. Removal of thiophene (black) and dibenzothiophene (grey) from synthetic diesel oil oil using the IL [$C_6^{2,4}$mmpy][NTf_2]: and n_{H2O2} / n_S = 9, at several ratios of catalyst.

Secondly, the H_2O_2-oxide nanoparticles oxidizing-catalytic system was tested. The nanoparticles synthesized by both dissolution/reprecipitation and spark discharge methods were characterized and compared (Figure 4.27). As it can be seen, the material obtained by the first method is not agglomerated and has a smaller size, what implies a higher specific surface area and a better catalytic activity. For this reason, this method was selected for the synthesis of the ionanofluids.

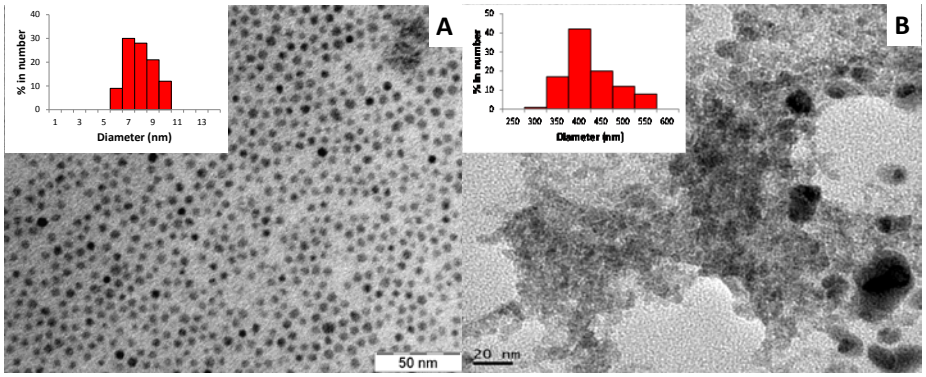

Figure 4.27. Transmission electron microscope photograph of the synthesized TiO_2 nanoparticles and distribution of sizes of the nanoparticles: a) dissolution/reprecipiatation method; b) spark discharge method.

Figure 4.28 shows the removal (%wt) of thiophene and dibenzothiophene when the synthetic diesel oil was mixed with the same quantity of ionanofluid (oxide nanoparticles dispersed within the IL [$C_6^{2,4}$mmpy][NTf_2]) at a fixed content of oxidant agent (n_{H2O2}/n_S=9), after one oxidative extraction stage. The ionanofluids were prepared by the dissolution-reprecipitation method, as it was explained above. The best desulfurization rates were found when using the Al_2O_3 and Cr_2O_3 nanoparticles, being the alumina option the most favorable due to its lower toxicity.

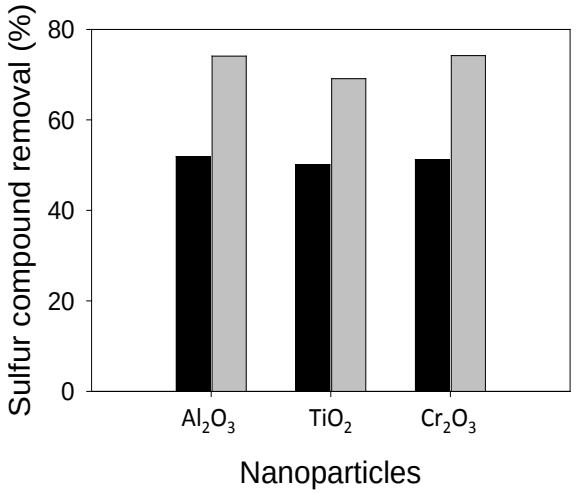

Figure 4.28. Removal of thiophene (black) and dibenzothiophene (grey) from synthetic diesel oil using the IL [$C_6^{2,4}$mmpy][NTf_2] (n_{H2O2} / n_S = 9) with different nanocatalyst prepared by dissolution/reprecipitation.

Nevertheless, the desulfurization rate is not enhanced in comparison to the use of a classical oxidative-catalytic system (H_2O_2 + AcOH), and thus the use of ionanofluids to improve the ODS technique was dismissed.

Following with the IL [$C_6^{2,4}$mmpy][NTf_2] and the H_2O_2-AcOH as oxidizing-catalytic system, the effect of the temperature in the ODS was tested. Figure 4.29 shows the removal (%wt) of thiophene and dibenzothiophene when the stirring and settle down processes are carried out at 298.15 K and 323.15K (no higher temperatures were tested due to the possible evaporation of the more volatile compounds of diesel oil). As it can be seen, an enhancement was found when working at 323.15 K (from 92.1 wt% to 99.0 wt% of dibenzothiophene reduction).

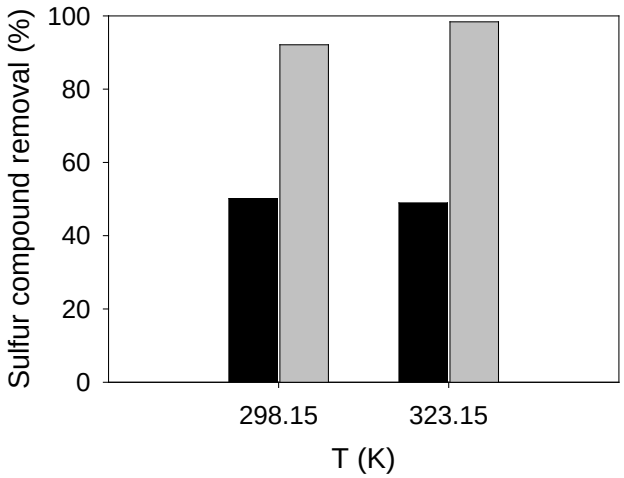

Figure 4.29. Removal of thiophene (black) and dibenzothiophene (grey) from synthetic diesel oil using the IL [$C_6^{2,4}$mmpy][NTf_2] (n_{H2O2} / n_S = 9, n_{AcOH} / n_S = 9) at different temperatures.

Figure 4.30 shows the removal of the diesel oil sulfur compounds when one-pot or two-step operation is used. When the model, the IL, and the oxidizing system is mixed at once the extraction of sulfur compounds is higher than when carrying out a normal EDS and oxidizing the mixture afterwards.

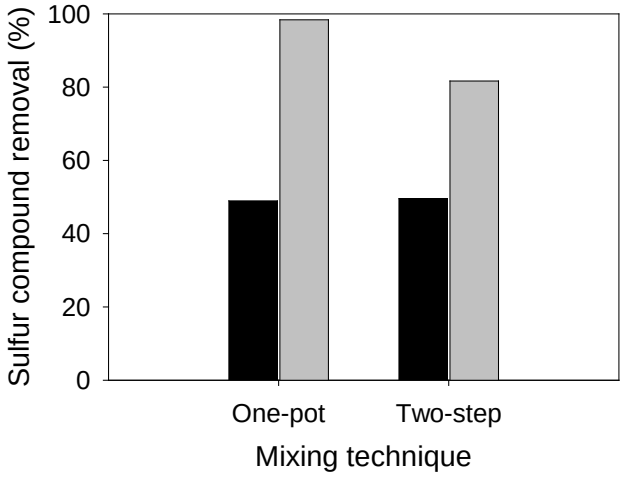

Figure 4.30. Removal of thiophene (black) and dibenzothiophene (grey) from synthetic diesel oil using the IL [$C_6^{2,4}$mmpy][NTf_2] (n_{H2O2} / n_S = 9, n_{AcOH} / n_S = 9, 323.15 K) at different number of steps for the process.

Working in EDS, previous tests [156] showed that 12h stirring and 12h settle down ensured the equilibrium achievement. For this reason, all the previous tests were carried out with these times. Nonetheless, as oxidation is a kinetic process, we finally followed the

evolution in time of the desulfurization in the optimized system (one-pot mixing, 323.15 K, m_{IL} / m_{model} = 1, n_{H2O2} / n_S = 9, n_{AcOH} / n_S = 9) at different stirring and settle down times (Figures 4.31 and 4.32).

Figure 4.31 shows the evolution of thiophene removal and the behavior corresponds to that found in the usual phase equilibria. Stirring 12h the extraction is higher than when less time is used (higher stirring times do not show any change in the curve), and settle down times of 12h are needed to do not appreciate variation in thiophene extraction.

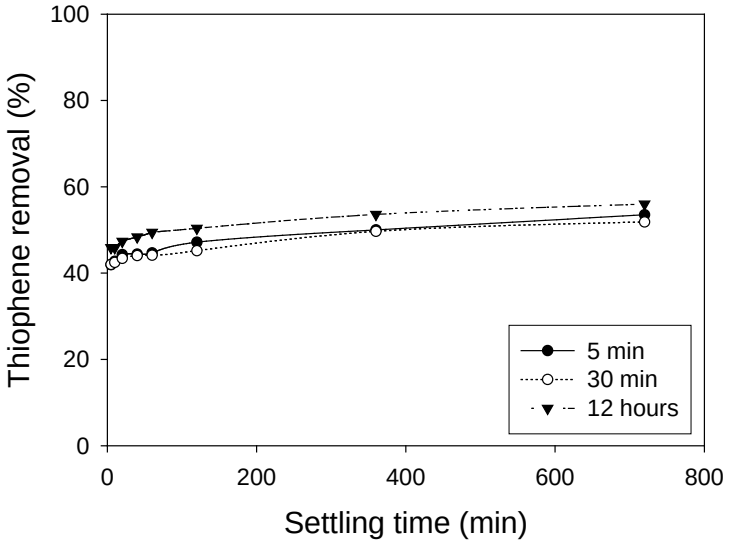

Figure 4.31. Removal of thiophene from synthetic diesel oil using the IL [$C_6^{2,4}$mmpy][NTf_2] at 323.15 K (n_{H2O2} / n_S = 9, n_{AcOH} / n_S = 9) and different mixing times.

A very different behavior is found for dibenzothiophene (Figure 4.32) where 12h of good mixing are needed to achieve the highest extraction, having the posterior settle down time little effect. To ensure the best effectiveness in the extraction of light and heavy sulfur compounds, 12h stirring and 12h settle down were fixed to all the desulfurization experiments.

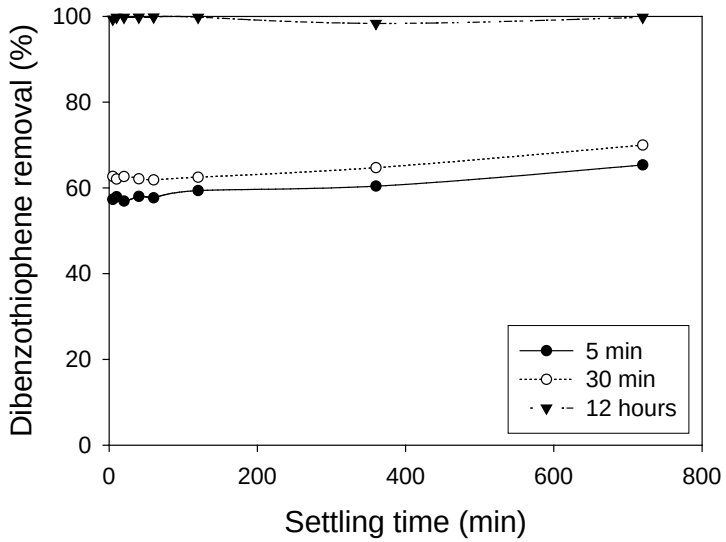

Figure 4.32. Removal of dibenzothiophene from synthetic diesel oil using the IL [$C_6^{2,4}$mmpy][NTf_2] at 323.15 K (n_{H2O2} / n_S = 9, n_{AcOH} / n_S = 9) and different mixing times.

b) Results

Figures 4.33 to 4.36 show the composition (%wt) of each component in the simulated diesel oil and raffinate products after one, two and three ODS stages, carriedo out with the previously optimized conditions, and with each of the four studied ILs. The best oxidesulfurization was achieved using the IL [$C_6^{2,4}$mmpy][NTf_2], extracting more than the 94 wt% of thiophene and all the dibenzothiophene. This IL also reduces around 66.1 wt% the toluene content. [C_2mim][NTf_2] extracts 87.1 wt% of thiophene, all the dibenzothiophene and reduces around 42.2 wt% the toluene composition. [C_2mim][DEP] extracts 59.8 wt% of thiophene, 61.6 wt% of dibenzothiophene and reduces around 48.4 wt% the toluene composition. Finally [C_2mim][OAc], that achieved the worst results, extracts 58.6 wt% of thiophene, 59.5 wt% of dibenzothiophene and reduces around 36.7 wt% the toluene composition. One more time, denitrogenation is total for all the ILs after the three stages of extraction and no IL was found in the raffinate phases.

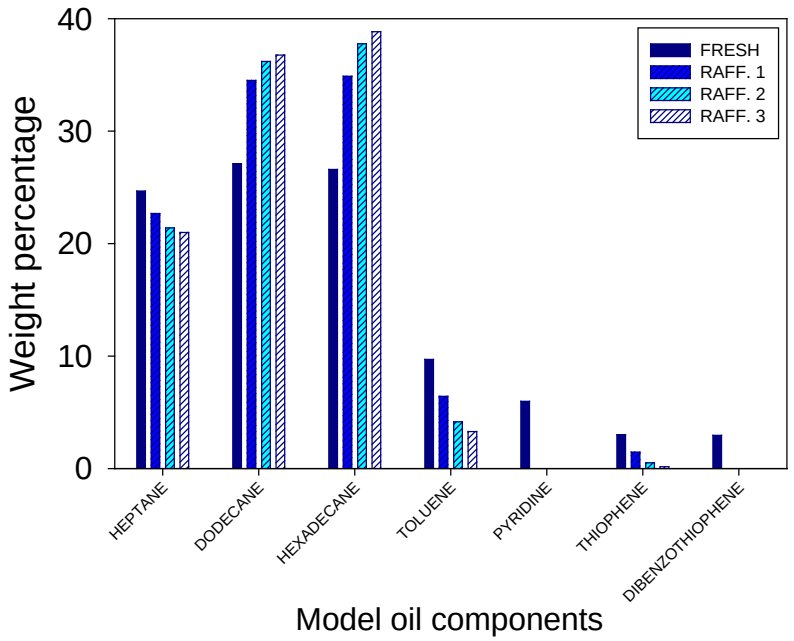

Figure 4.33. Three stages ODS of synthetic diesel oil at 323.15 K and atmospheric pressure with the IL [$C_6^{2,4}$mmpy][NTf_2].

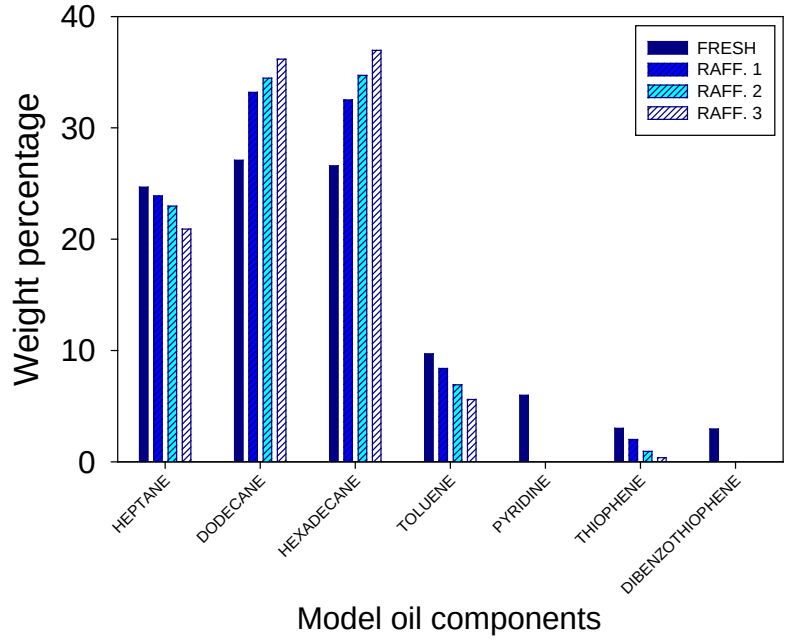

Figure 4.34. Three stages ODS of synthetic diesel oil at 323.15 K and atmospheric pressure with the IL [C_2mim][NTf_2].

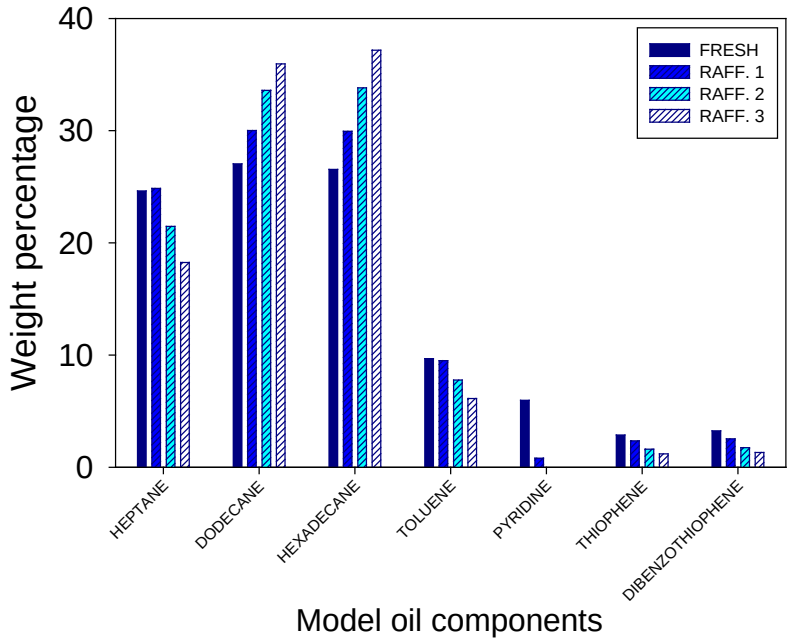

Figure 4.35. Three stages ODS of synthetic diesel oil at 323.15 K and atmospheric pressure with the IL [C_2mim][OAc].

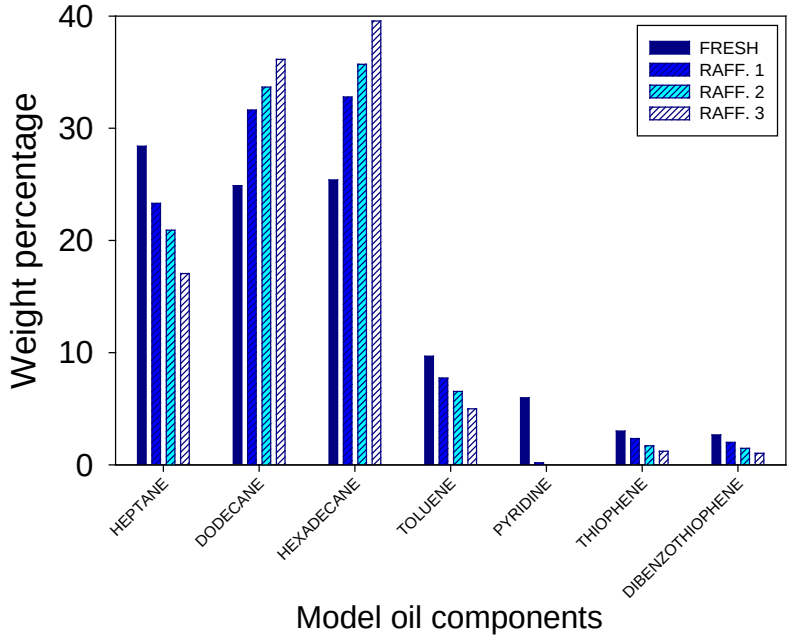

Figure 4.36. Three stages ODS of synthetic diesel oil at 323.15 K and atmospheric pressure with the IL [C_2mim][DEP].

In the case of [$C_6^{2,4}$mmpy][NTf_2] and [C_2mim][NTf_2], best results were found than when using simple extraction. This is in agreement with usual behavior found in bibliography [224,225]. Once the sulfur compounds are extracted to the IL-phase they are oxidized, and then the IL is able to keep on extracting more thiophene and dibenzothiophene. Nonetheless, it seems that desulfurization ability of the two water-miscible ILs ([C_2mim][DEP] and [C_2mim][OAc]) is diminished when acetic acid and hydrogen peroxide are solved within them. This behavior had been previously found for water-miscible ILs, such us [C_4mim][BF_4] [226] or the [C_2mim][DEP] itself [173]. The worsening in the extraction ability of ILs can be strongly affected by their water content. Since these two hydrophilic ILs are mixed with water, their efficiency in the ODS process is lower than when working with dry ILs in a simpler EDS.

A case in point is [C_2mim][NTf_2], when the cell was left to go down to room temperature after having taken the sample, a white crystalline precipitate started to appear. It was filtered out and washed several times with distilled water. Then, it was dried under soft vacuum for one day and the collected crystals (Figure 4.37) were analyzed by X-ray powder diffraction. The pattern of the sample matches with the diffractogram of dibenzothiophene dioxide, what means that the oxidation product could be separated from the IL-phase without the need of other extracting agents

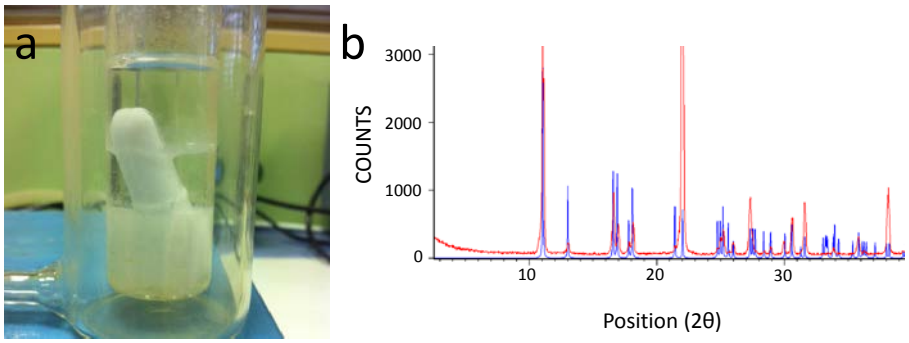

Figure 4.37. Precipitate after the ODS with [C_2mim][NTf_2]: a) Image of the crystals in the cell; b) X-ray powder diffraction of the collected crystals (red line) and of dibenzothiophene dioxide (blue line).

4.3. DESULFURIZATION OF REAL FUELS

4.3.1. EXTRACTIVE DESULFURIZATION

4.3.1.1. GASOLINE

Figure 4.38 shows how total sulfur concentration diminishes when a real gasoline is submitted to the same multistage extraction performed for the synthetic fuel. According to the results obtained for synthetic fuel, the expected ranking in the extraction capacity would be $[C_6^{2,4}mmpy][NTf_2]$ > $[C_2mim][DEP]$ ≈ $[C_2mim][OAc]$ > $[C_2mim][NTf_2]$. Nonetheless, in the case of the real fuel, desulfurization achieved with the IL $[C_2mim][OAc]$ is much more important (desulfurization yield of 38.7 wt% from the first stage) than the obtained for the other ILs. The ranking for the other ILs is maintained according to the synthetic gasoline.

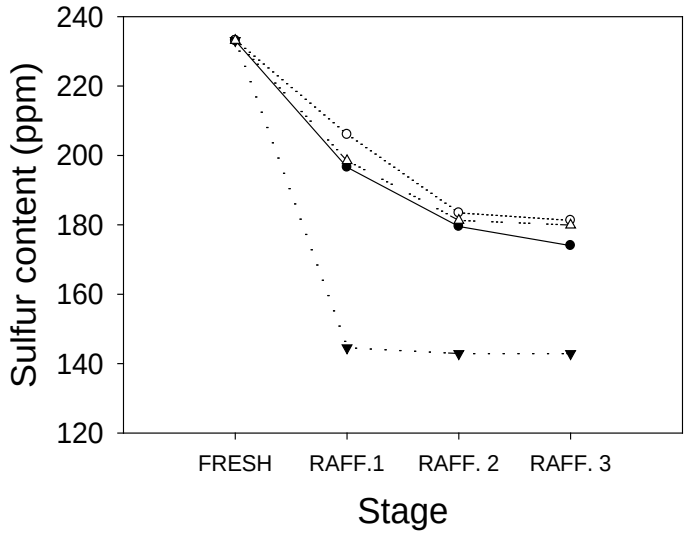

Figure 4.38. Three stages EDS of real gasoline at 298.15 K and atmospheric pressure: $[C_6^{2,4}mmpy][NTf_2]$ (●, solid line), $[C_2mim][NTf_2]$ (○, dotted line), $[C_2mim][OAc]$ (▼, dashed line), and $[C_2mim][DEP]$ (▽, dash-dotted line).

The difference between the studied gasoline model (based in thiophene) and the real gasoline (which contains derivatives of thiophene and small mercaptans) lies in the sulfur components. This fact leads to think that the acetate IL has better ability to extract compounds as mercaptans than the other ILs, and the desulfurization of the gasoline is increased for this reason. In order to corroborate this behavior, a mixture of a mercaptan (1-butanethiol) and $[C_2mim][OAc]$ was prepared and stirred. Then it was left to settle down and a sample of the upper phase (mercaptan) was analyzed by GC-MS. Results pointed out that the 1-butanethiol reacted in the presence of the IL to form dibutylsulfide and/or dibutyldisulfide, which would be easier to

extract from the gasoline. This interaction could explain the high desulfurization ability of this IL in comparison with the other ones.

4.3.1.2. DIESEL OIL

The desulfurization ability of the ILs by EDS of the real diesel oil is ranked as for the synthetic fuel: $[C_6^{2,4}mmpy][NTf_2]$ > $[C_2mim][DEP]$ > $[C_2mim][OAc]$ > $[C_2mim][NTf_2]$. The pyridinium IL achieved a good desulfurization (37.8 wt% after three steps) in comparison with the imidazolium ones. The obtained desulfurization evolution is showed in Figure 4.39.

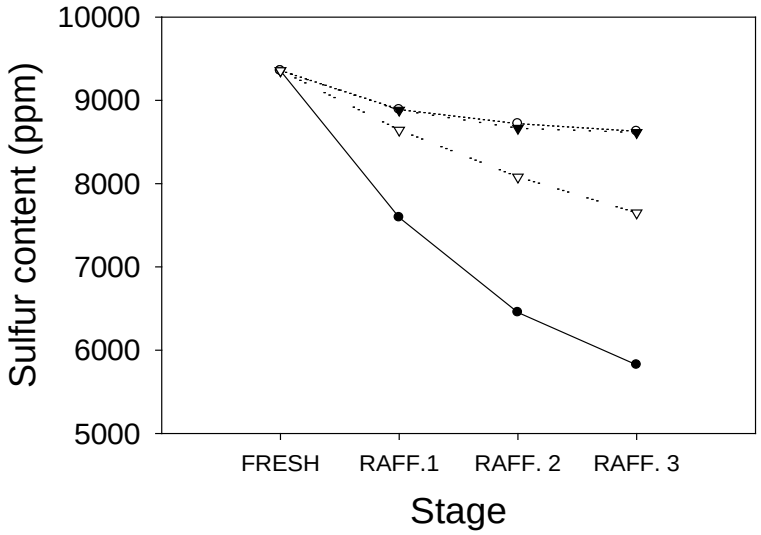

Figure 4.39. Three stages EDS of real diesel oil at 298.15 K and atmospheric pressure: $[C_6^{2,4}mmpy][NTf_2]$ (●, solid line), $[C_2mim][NTf_2]$ (○, dotted line), $[C_2mim][OAc]$ (▼, dashed line), and $[C_2mim][DEP]$ (▽, dash-dotted line).

4.3.2. OXIDATIVE DESULFURIZATION

4.3.2.1. GASOLINE

Since no improvement was observed with respect to the EDS technique with the synthetic gasoline, no ODS experiments were carried out with real gasoline.

4.3.2.2. DIESEL OIL

In Figure 4.40 it can be seen the ability of the four studied ILs to extract sulfur by ODS from real diesel oil, which can be ranked as follows: $[C_6^{2,4}mmpy][NTf_2]$ > $[C_2mim][NTf_2]$ >> $[C_2mim][DEP]$ > $[C_2mim][OAc]$. The behavior is similar to that found with the synthetic diesel oil. The desulfurization ability is clearly higher in the case of the $[NTf_2]^-$ based ILs and lower for the other two. The pyridinium and

imidazolium $[NTf_2]^-$ based ILs are able to extract the 96.5 wt% and the 82.0 wt%, respectively, of sulfur from the fuel.

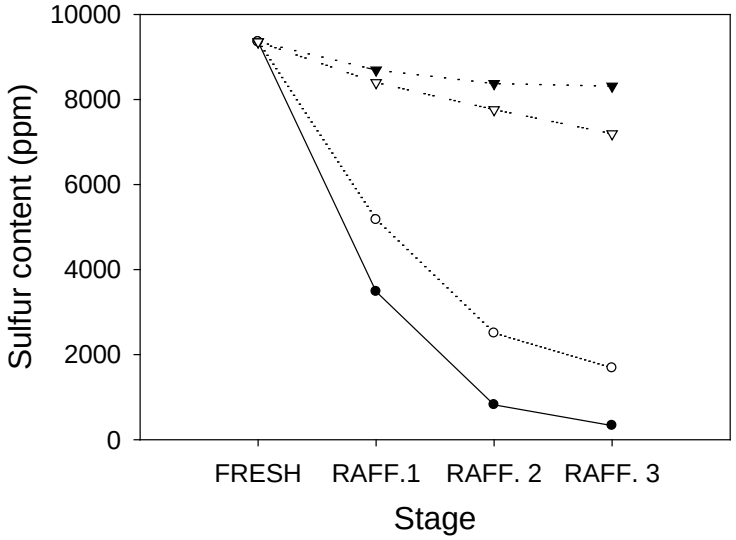

Figure 4.40. Three stages ODS of real diesel oil at 323.15 K and atmospheric pressure: $[C_6^{2,4}mmpy][NTf_2]$ (●, solid line), $[C_2mim][NTf_2]$ (○, dotted line), $[C_2mim][OAc]$ (▼, dashed line), and $[C_2mim][DEP]$ (▽, dash-dotted line).

5. CONCLUSIONS

In this thesis, in order to evaluate the ability of ILs to desulfurize fuels, four of them ([$C_6^{2,4}$mmpy][NTf_2], [C_2mim][NTf_2], [C_2mim][OAc] and [C_2mim][DEP]) were tested in extractive (EDS) and oxidative (ODS) desulfurization processes.

With that aim, the liquid-liquid equilibria for the systems {IL + thiophene + hexane}, {IL + thiophene + toluene} and {IL + pyridine + hexane} were obtained at 298.15 K and atmospheric pressure. These studies allow not only the analysis of the feasibility of these ILs to carry out the desulfurization of fuels by extraction, but also pay attention to simultaneous denitrogenation and dearomatization processes.

First conclusions can be established through the obtained solubilities and selectivities at low solute concentrations, in agreement with practical applications. The high values obtained of these parameters for the studied ILs indicate that all of them are able to separate thiophene and pyridine from hexane. Nevertheless, these thermodynamic parameters point out that the separation of thiophene from toluene will be more difficult, and higher amounts of solvent will be needed. This means that a certain dearomatization would take place simultaneously with the desired desulfurization and denitrogenation process.

After establishing a comparison between the ILs [$C_6^{2,4}$mmpy][NTf_2] and [$C_6^{3,5}$mmpy][NTf_2] (previously studied), it can be concluded that the asymmetry in the position of the methyl groups of the pyridinium cation slightly improves the desulfurization performance of the IL.

Taking into account the solute distribution ratio, the IL [$C_6^{2,4}$mmpy][NTf_2] would be chosen since it achieves the highest values in thiophene separation from hexane (lower solvent amount needed). However, the [C_2mim][OAc] is the one with the highest selectivities. Assuming that the recovery of ILs could be carried out, the selectivity can be considered as the criteria to select the best IL (always from a thermodynamic point of view), and in that case the [C_2mim][OAc] would be the best option.

In regards to the correlation of the ternary liquid-liquid equilibria, both tested models (UNIQUAC and NRTL) adequately fit the obtained data. As a general trend, it can be concluded that the systems with thiophene are better correlated using UNIQUAC, and the pyridine-containing ones with NRTL model (with the only exception of {[C_2mim][OAc] + pyridine + hexane} system).

To reinforce the conclusions established from equilibrium determinations, synthetic gasoline and diesel oil were prepared and used as model fuels for EDS (three stages) with the ILs. As it was expected, the IL [$C_6^{2,4}$mmpy][NTf_2] showed the highest desulfurization capacity (84.9 wt% of thiophene reduction in the case of gasoline, and 90.3 wt% of thiophene reduction and 98.4 wt% of dibenzothiophene reduction in the case of diesel oil). Nonetheless, this IL can not be proposed as the best candidate due to the enormous level of dearomatization found (67.0 wt% in the case of gasoline and 78 wt%

in the case of diesel oil). It would cause difficulties in the implementation of the process in a refinery. For this reason, it can be concluded that the IL [C_2mim][OAc] with only slightly lower results in desulfurization (79.3 wt% of thiophene reduction in the case of gasoline, and 87.2 wt% of thiophene reduction and 88.0 wt% of dibenzothiophene reduction in the case of diesel oil) and with significantly minor dearomatization (14.2 wt% in the case of gasoline and 53.2 wt% in the case of diesel oil) would be most preferable. With all the ILs, the denitrogenation (after the three steps) is total and no IL was found in the raffinate phases.

In an attempt to increase the desulfurization efficiency of the extraction with ILs, an ODS was also tested. The relatively lower electron density of thiophene made this process ineffective when attempting to desulfurize gasoline. In the case of diesel oil, besides trying the classical oxocatalytic system (H_2O_2 and acetic acid), the use of metal oxide nanoparticles as a catalyst was also studied.

For that purpose, a new method for the synthesis of stable ionanofluids was developed, the dissolution-reprecipitation method. This method was found to be useful for the synthesis of nanoparticles and ionanofluids. It avoids the use of reactants and allows work with moderate temperatures and atmospheric pressure. In comparison, the spark discharge method did not enhance the concentration of nanomaterial in the IL, and big agglomerates were obtained. Nevertheless, the combination of H_2O_2 as an oxidizing agent and the metal oxide nanoparticles as a catalyst did not improve the performance of the classical oxidative-catalytic system H_2O_2 and acetic acid.

With the H_2O_2-AcOH oxocatalytic system, at molar ratios n_{H2O2}/n_S = 9 and n_{AcOH}/n_S = 9, in a one-pot operation at 323.15 K, studies in synthetic diesel resulted in higher desulfurization levels by ODS than that obtained by EDS when using the $[NTf_2]^-$ based ILs. The IL [$C_6^{2,4}$mmpy][NTf_2] extracted more than 94 wt% of thiophene and all the dibenzothiophene, and the IL [C_2mim][NTf_2] extracted 87.1 wt% of thiophene and the totality of dibenzothiophene. With this last IL, easy removal of the oxidized sulfur compounds could be easily carried out by allowing the system cool down to room temperature in order to precipitate them. In comparison, the results were worse for the other two ILs. In all cases the degree of dearomatization decreased with respect to the EDS.

Finally, some experiments were also performed with real samples. For the EDS, the IL [C_2mim][OAc] showed the highest desulfurization ability of gasoline (38.7% of sulfur removal from the first stage), likely due to the reactive transformation of small mercaptans to more easily extractable compounds. It is proposed that this IL would be the optimal for EDS of gasoline at 298.15 K. The behavior in the EDS and ODS experiments with real diesel oil mimicked those with the synthetic one, although lower levels of desulfurization were found with the real diesel as a result of its higher degree of complexity. When

studying the ODS process with real diesel oil, the ILs $[C_6^{2,4}mmpy][NTf_2]$ and $[C_2mim][NTf_2]$ clearly showed the highest desulfurization rates (96.5% and 82.0% of sulfur removal from the fuel, respectively). Since $[C_2mim][NTf_2]$ led to a lower dearomatization of the fuel and its cost would be much lower than the one of $[C_6^{2,4}mmpy][NTf_2]$, it is proposed that $[C_2mim][NTf_2]$ would be the optimal IL for ODS of diesel oil with the above cited operation conditions.

These studies shed light to the process of desulfurization of fuels with ILs. It is important to note, however, that there is not a unique solution to this problem, and that sulfur extraction is not the only parameter to take into account. Co-extraction of (un)desired compounds, pilot plant experiments, integration of the process in the refinery, and life cycle analyses, among others, are further aspects to consider in the decision-making process prior to the implementation of the proposed alternatives.

LIST OF SYMBOLS

Symbols

a	*activity*
APILs	aprotic ionic liquids
CAS	chemical abstracts service
EDS	extractive desulfurization
F	residual function
F_a	objective function (activities)
F_b	objective function (compositions)
FRESH	fresh model, gasoline or gasoil
G	Gibbs energy
HDS	hydrodesulfurization
IL	ionic liquid
l	parameter in the UNIQUAC model
LLE	liquid-liquid equilibrium
M	number of tie-lines
n	number of moles
n_D	refractive index
NMR	nuclear magnetic resonance
NRTL	Non-Random Two Liquid
ODS	oxidative desulfurization
P	pressure
P_n	binary interaction parameter
PILs	protic ionic liquids
POM	polyoxometalate
q	area molecular-structure constant in the UNIQUAC model

Q	empirical constant, 10^{-6} in Eq. (16) and 10^{-10} in Eq. (17)
r	volume molecular-structure constant in the UNIQUAC model
R	universal constant of gases
RAFF.	Raffinate
RTILs	room-temperature ionic liquids
S	selectivity
S	sulfur
T	temperature
TSILs	task-specific ionic liquids
UNIQUAC	UNIversal QUAsiChemicaL
ωt	weight
x	mole fraction
z	lattice coordination number

Greek letters

α	non-randomness parameter in the NRTL model
β	solute distribution ratio; partition coefficient
γ	activity coefficient
$\Delta\beta$	mean error of the solute distribution ratio
Δg	binary energy interaction parameter in the NRTL model
Δu	binary energy interaction parameter in UNIQUAC model
θ	area fraction in the UNIQUAC model
ρ	density
τ	parameter in the NRTL or UNIQUAC models
υ	standard uncertainty

ϕ	segment fraction in the UNIQUAC model
ω_{H2O}	water content

Subscripts

a	activity
i=1,2,…,n	component
j=1,2,…,n	component
j	counter for phases
k=1,2,…,n	component
k	counter for tie-lines
m	phase
P	constant pressure
S	solute
T	constant temperature
∞	infinite dilution

Superscripts

I	raffinate phase
II	IL phase
m=1,2,…,n	phase

Symbols on top

^	calculated value

REFERENCES

[1] J. D. Holbrey, R. D. Rogers, *Ionic Liquids in Synthesis*, Ed. P. Wasserscheid, T. Welton, Wiley-VCH, Weinheim **2002**, 41-55.

[2] K. R. Seddon, *The International George Papatheodorou Symposium: Proceedings*, Ed. S. Boghosian, V. Dracopoulos, C. G. Kontoyannis, G. A. Voyiatzis, Patras **1999**, 131-135.

[3] J. H. Davis Jr., *Chemistry Letters* **2004**, 33, 1072-1077.

[4] C. Baudequin, D. Brégon, J. Levillain, F. Guillen, J. C. Plaquevent, A. C. Gaumont, *Tetrahedron: Asymmetry* **2005**, 16, 3921-3945.

[5] M. Y. Machado, R. Dorta, *Synthesis* **2005**, 15, 2473-2475.

[6] M. Freemantle, *An Introduction to Ionic Liquids*, Ed. The Royal Society of Chemistry, Cambridge **2010**, 1-11.

[7] J. S. Wilkes, J. A. Levisky, R. A. Wilson, C. L. Hussey, *Inorganic Chemistry* **1982**, 21, 1263-1264.

[8] J. S. Wilkes, M. Zaworotko, *Journal of the Chemical Society, Chemical Communications* **1992**, 13, 965-966.

[9] P. Benhôte, A. P. Dias, N. Papageorgiou, K. Kalyanasundaram, M. Grätzel, *Inorganic Chemistry* **1996**, 35, 1168-1178.

[10] C. Friedel, J. M. Crafts, *Comptes Rendues* **1877**, 84, 1392 & 1450.

[11] N. Nambu, N. Hiraoka, K. Shigemura, S. Hamanaka, M. Ogawa, *Bulletin of the Chemical Society of Japan* **1976**, 49, 3637-3640.

[12] P. Walden, *Bulletin de l'Academie Imperiale des Sciences de Saint-Pétersbourg* **1914**, 8, 405–422.

[13] S. Werner, M. Haumann, P. Wasserscheid, *Annual Review of Chemical and Biomolecular Engineering* **2010**, 1, 203–230.

[14] Y. Patell, K. R. Seddon, L. Dutta, A. Fleet, *Green Industrial Applications of Ionic Liquids*, Ed. R. D. Rogers, K. R. Seddon, S. Volkov, NATO Science Series, Dordtrecht **2002**, 499-510.

[15] M. J. Earle, K. R. Seddon, *Pure and Applied Chemistry* **2000**, 72, 1391-1398.

[16] S. P. Ong, O. Andreussi, Y. Wu, N. Marzari, G. Ceder, *Chemistry of Materials* **2011**, 23, 2979-2986.

[17] G. P. Smith, A. S. Dworkin, R. M. Pagni, S. P. Zingg, *Journal of the American Chemical Society* **1989**, 111, 5075-5077.

[18] T. Welton, *Chemical Reviews* **1999**, 99, 2071-2083.

[19] R. Giernoth, *Topics in Current Chemistry* **2007**, 276, 1-23.

[20] D. Coleman, N. Gathergood, *Chemical Society Reviews* **2010**, 39, 600–637.

[21] T. P. Thuy Pham, C. W. Cho, Y. S. Yun, *Water Research* **2010**, 44, 352–372.

[22] K. Fukumoto, M. Yoshizawa, H. Ohno, *Journal of the American Chemical Society* **2005**, 127, 2398–2399.

[23] N. Gathergood, P. J. Scammells, M. T. Garcia, *Green Chemistry* **2006**, 8, 156-160.

[24] R. Ferraz, L. C. Branco, C. Prudencio, J. P. Noronha, Z. Petrovski, *ChemMedChem* **2011**, 6, 975-985.

[25] T. Sato, T. Maruo, S. Marukane, T. Takagi, *Journal of Power Sources* **2004**, 138, 253-261.

[26] B. Garcia, S. Lavallée, G. Perron, C. Michot, M. Armand, *Electrochimica Acta* **2004**, 49, 4583-4588.

[27] S. Zein El Abedin, N. Borissenko, F. Endres, *Electrochemistry Communications* **2004**, 6, 510-514.

[28] J. D. Wadhawan, U. Schröder, A. Neudeck, S. J. Wilkins, R. G. Compton, F. Marken, C. S. Consorti, R. F. de Souza, J. Dupont, *Journal of Electroanalytical Chemistry* **2000**, 493, 75-83.

[29] W. Lu, A. G. Fadeev, B. Qi, B. R. Mattes, *Journal of the Electrochemical Society* **2004**, 151, 33-39.

[30] J. Ding, D. Zhou, G. Spinks, G. Wallace, S. Forsyth, M. Forsyth, D. MacFarlane, *Chemistry of Materials* **2003**, 15, 2392-2398.

[31] T. Brinz, U. Simon, *DE 2002-10245337* **2004**.

[32] Y. G. Lee, T. C. Chou, *Biosensors and Bioelectronics* **2004**, 20, 33-40.

[33] C. F. Poole, *Journal of Chromatography A* **2004**, 1037, 49-82.

[34] J. L. Anderson, D. W. Armstrong, *Analytical Chemistry* **2003**, 75, 4851-4858.

[35] K. Nobuoka, *JP 2004277351* **2004**.

[36] S. G. Cull, J. D. Holbrey, V. Vargas-Mora, K. R. Seddon, G. J. Lye, *Biotechnology and Bioengineering* **2000**, 69, 227-233.

[37] M. Seiler, C. Jork, A. Kavarnou, W. Arlt, R. Hirsch, *AIChE Journal* **2004**, 50, 2439-2454.

[38] F. Kubota, M. Goto, *Solvent Extraction Research and Development* **2006**, 13, 23-36.

[39] M. L. Dietz, *Separation Science and Technology* **2006**, 41, 2047-2063.

[40] A. B. Pereiro, J. M. M. Araujo, J. M. S. S. Esperanca, I. M. Marrucho, L. P. N. Rebelo, *Journal of Chemical Thermodynamics* **2012**, 46, 2-28.

[41] S. Oppermann, F. Stein, U. Kragl, *Applied Microbiology and Biotechnology* **2011**, 89, 493-499.

[42] A. E. Visser, R. P. Swatloski, S. T. Griffin, D. H. Hartman, R. D. Rogers, *Separation Science and Technology* **2001**, 36, 785-804.

[43] A. E. Visser, R. D. Rogers, *Journal of Solid State Chemistry* **2003**, 171, 109-113.

[44] J. A. Whitehead, G. A. Lawrence, A. McCluskey, *Green Chemistry* **2004**, 6, 313-315.

[45] N. Muhammad, Z. Man, K. Bustam, A. Mohamad, *European Journal of Wood and Wood Products* **2012**, 70, 125-133.

[46] P. Maeki-Arvela, I. Anugwom, P. Virtanen, R. Sjoeholm, J. P. Mikkola, *Industrial Crops and Products* **2010**, 32, 175-201.

[47] R. G. Reddy, Z. Zhang, M. F. Arenas, D. M. Blake, *High Temperature Materials and Processes* **2003**, 22, 87-94.

[48] C. J. Rao, K. A. Venkatesan, K. Nagarajan, T. G. Srinivasan, *Radiochimica Acta* **2008**, 96, 403-409.

[49] C. J. Rao, K. A. Venkatesan, K. Nagarajan, T. G. Srinivasan, P. R. V. Rao, *Journal of Nuclear Materials* **2011**, 408, 25-29.

[50] C. M. Jin, C. Ye, B. S. Phillips, J. S. Zabinsky, X. Liu, W. Liu, J. M. Shreeve, *Journal of Materials Chemistry* **2006**, 16, 1529-1535.

[51] C. Ye, W. Liu, Y. Chen, L. Yu, *Chemical Communications* **2001**, 21, 2244-2245.

[52] H. Rodríguez, M. Williams, J. S. Wilkes, R. D. Rogers, *Green Chemistry* **2008**, 10, 501-507.

[53] L. F. Vega, O. Vilaseca, F. Llovell, J. S. Andreu, *Fluid Phse Equilibria* **2010**, 294, 15-30.

[54] J. S. Andreu, L. F. Vega, *Journal of Physical Chemistry B* **2008**, 112, 15398-15406.

[55] A. Yokozeki, M. B Shiflett, *Energy & Fuels* **2009**, 23, 4701-4708.

[56] A. M. Pinto, H. Rodríguez, Y. J. Colón, A. Arce Jr., A. Arce, A. Soto, *Industrial & Engineering Chemistry Research* **2013**, 52, 5975-5984.

[57] S. Lago, H. Rodríguez, M. K. Khoshkbarchi, A. Soto, A. Arce, *RSC Advances* **2012**, 2, 9392-9397.

[58] G. J. Hirasaki, C. A. Miller, O. G. Raney, M. K. Poindexter, D. T. Nguyen, J. Hera, *Energy & Fuels* **2011**, 25, 555-561.

[59] K. W. Kim, B. Song, M. Y. Choi, M. J. Kim, *Organic Letters* **2001**, 3, 1507-1509.

[60] J. Fraga-Dubreuil, K. Bourahla, M. Rahmouni, J. P. Bazureau, J. Hamelin, *Catalysis Communications* **2002**, 3, 185-190.

[61] P. Lozano, T. De Diego, D. Carrie, M. Vaultier, J. L. Iborra, *Biotechnology Letters* **2001**, 23, 1529-1533.

[62] Y. Gu, C. Ogawa, J. Kobayashi, Y. Mori, S. Kobayashi, *Angewandte Chemie, International Edition* **2006**, 45, 7217-7220.

[63] C. Wheeler, K. west, C. Liotta, C. Eckert, *Chemical Communications* **2001**, 10, 887-888.

[64] M. Maase, *Multiphase Homogeneous Catalysis*, Ed. B. Cornils, W. A. Herrmann, I. T. Horvath, W. Leitner, S. Mecking, H. Olivier-Bourbigou, D. Vogt, Wiley-VCH, Weinheim, **2005**, 2, 560-566.

[65] H. Olivier-Bourbigou, F. Hugues, *Green Industrial Applications of Ionic Liquids*, Ed. R. D. Rogers, K. R. Seddon, S. Volkov, NATO Science Series II: Mathematics, Physics and Chemistry, Dordrecht, **2002**, 92, 67-84.

[66] J. D. Holbrey, N. V. Plechkova, K. R. Seddon, *Green Chemistry* **2006**, 8, 411–414.

[67] M. Abai, M. P. Atkins, K. Y. Cheun, J. D. Holbrey, P. Nockemann, K. R. Seddon, G. Srinivasan, Y. Zou, *WO Pat. Appl. PCT/WO 2012/046057* **2012**.

[68] N. Taniguchi, *Proceedings of the International Conference on Production Engineering*, *Part II*, Ed. Japan Society of Precision Engineering, Tokyo, **1974**.

[69] R. P. Feynman, *Caltech Engineering and Science* **1960**, 23, 22-36.

[70] K. E. Drexler, *Engines of Creation: The Coming Era of Nanotechnology*, Anchor Books, New York, **1986**.

[71] R. W. Kelsall, I. W. Hamley, M. Geoghegan, *Nanoscale Science and Technology*, John Wiley & Sons, **2005**.

[72] M. Zhao, R. M. Crooks, *Angewandte Chemie, International Edition* **1999**, 38, 364-366.

[73] A. Corma, H. García, *Chemical Society Reviews* **2008**, 37, 2096-2126.

[74] W. P. McConnell, J. P. Novak, L. C. III Brousseau, R. R. Fuierer, R. C. Tenent, D. L. Feldheim, *Journal of Physical Chemistry B* **2000**, 104, 8925-8930.

[75] W. J. Stark, *Angewandte Chemie, International Edition* **2011**, 50, 1242-1258.

[76] P. R. Srinivas, M. Philbert, T. Q. Vu, Q. Huang, J. L. Kokini, E. Saos, H. Chen, C. M. Peterson, K. E. Friedl, C. McDade-Ngutter, V. Hubbard, P. Starke-Reed, N. Miller, J. M. Betz, J. Dwyer, J. Milner, S. A. Ross, *Journal of Nutrition* **2010**, 140, 119-124.

[77] K. M. Lee, P. Y. Chen, C. P. Lee, K. C. Ho, *Journal of Power Sources* **2009**, 190, 573-577.

[78] F. Zipp, H. Juergen, *DE 102011116342 B3 20130314* **2013**.

[79] Y. Lv, H. Liu, Z. Wang, S. Liu, L. Hao, Y. Sang, D. Liu, J. Wang, I. R. Boughton, *Journal of Membrane Science* **2009**, 331, 50-56.

[80] S. A. Wissing, R. H. Muller, *International Journal of Pharmaceutics* **2003**, 254, 65-68.

[81] R. Dastjerdi, M. Montazer, *Colloids and Surfaces, B: Biointerfaces* **2010**, 79, 5-18.

[82] Y. Li. H. Li, R. Cao, *Journal of the American Ceramic Society* **2009**, 10, 2188-2191.

[83] Y. K. Jung, J. II Kim, J. K. Lee, *Journal of the American Chemical Society* **2010**, 132, 178-184.

[84] G. Audoit, J. S. Kulkarni, M. A. Morris, J. D. Holmes, *Journal of Materials Chemistry* **2007**, 17, 1608-1613.

[85] E. Coronado, A. Ribera, J. García-Martínez, N. Linares, L. M. Liz-Marzán, *Journal of Materials Chemistry* **2008**, 18, 5682-5688.

[86] J. H. Yu, J. Joo, H. M. Park, S. II Baik, Y. W. Kim, S. C. Kim, T. Hyeon, *Journal of the American Chemical Society* **2005**, 127, 5662-5670.

[87] U. S. Choi, *Enhancing Thermal Conductivity of Fluids with Nanoparticles, Developments and Applications of Non-Newtonian Flows*, Ed. D.A. Siginer, H.P. Wang, ASME, New York **1995**, 99-105.

[88] P. Keblinski, S. R. Phillpot, S. U. S. Choi, J. A. Eastman, *International Journal of Heat and Mass Transfer* **2002**, 45, 855-863.

[89] J. A. Eastman, S. U. S. Choi, S. Li, W. Yu, L. J. Thompson, *Applied Physics Letters* **2001**, 78, 718-720.

[90] P. Keblinski, J. A. Eastman, D. G. Cahill, *Materials Today* **2005**, 8, 36-44.

[91] S. K. Das, N. Putra, P. Thiesen, W. Roetzel, *Journal of Heat Transfer* **2003**, 125, 567-574.

[92] H. E. Patel, S. K. Das, T. Sundararajan, A. S. Nair, B. George, T. Pradeep, *Applied Physics Letters* **2003**, 83, 2931-2933.

[93] Z. Zhang, Q. Xue, J. Zhang, *Wear* **1997**, 209, 1-8.

[94] S. Huang, W. Yan, G. Hu, L. Wang, *Journal of Physical Chemistry C* **2012**, 116, 20558-20563.

[95] M. Antonietti, D. Kuang, B. Smarsly, Y. Zhou, *Angewandte Chemie, International Edition* **2004**, 43, 4988-4992.

[96] C. A. Nieto de Castro, M. J. V. Lourenço, A. P. C. Ribeiro, E. Langa, S. I. C. Vieira, P. Goodrich, C. Hardacre, *Journal of Chemical. Engineering Data* **2010**, 55, 653-661.

[97] B. Wang, X. Wang, W. Lou, J. Hao, *Journal of Physical Chemistry C* **2010**, 114, 8749-8754.

[98] T. Fukushima, A. Kosaka, Y. Ishimura, T. Yamamoto, T. Takigawa, N. Ishii, T. Aida, *Science* **2003**, 300, 2072-2074.

[99] F. Endres, S. Z. E. Abedin, *Chemical Communications* **2002**, 8, 892-893.

[100] B. Wanga, X. Wanga, W. Loua, J. Haoa, *Journal of Colloid and Interface Science* **2011**, 362, 5-14.

[101] M. Swadźba-Kwaśny, L. Chancelier, S. Ng, H. G. Manyar, C. Hardacre, P. Nockemann, Dalton Transactions **2012**, 41, 219-227.

[102] http://www.epa.gov/acidrain/what/index.html (last accessed on 01/10/2013).

[103] Directive of the European Parliament and of the Council 2003/17/EC. http://eur-lex.europa.eu/LexUriServ/LexUriServ.do?uri=CELEX:32003L0017:EN:HTML (last accessed on 01/10/2013).

[104] Directive of the European Parliament and of the Council 2009/30/EC. http://eur-lex.europa.eu/LexUriServ/LexUriServ.do?uri=OJ:L:2009:140:0088:0113:EN:PDF (last accessed on 01/10/2013).

[105] Regulatory Impact Analysis of the United States Environmental Protection Agency EPA420-R-00-026. http://www.epa.gov/otaq/regs/hd-hwy/2000frm/420r00026.pdf (last accessed on 01/10/2013).

[106] H. Tøpsoe, B. S. Clausen, F. E. Massoth, *Science and Technology*, Ed. J. R. Anderson, M. Boudart, Springer-Verlag Berlin **1996**, 11.

[107] X. Ma, K. Sakanishi, I. Mochida, *Industrial & Engineering Chemistry Research* **1994**, 33, 218-222.

[108] Z. Zhang, X. Guo, S. Liu, X. Zhu, L. Xu, *Fuel Processing Technology* **2008**, 89, 1135-1141.

[109] D. D. Whitehurst, T. Isoda, I. Mochida, *Advances in Catalysis* **1998**, 42, 345-471.

[110] I. V. Babich, J. A. Moulijn, *Fuel* **2003**, 82, 607-631.

[111] C. Song, *Catalysis Today* **2003**, 86, 211-263.

[112] C. Song, X. Ma, *Applied Catalysis B: Environmental* **2003**, 41, 207-238.

[113] G. A. Huff, O. S. Owen, B. D. Alexander, D. N. Rundell, W. J. Reagan, J. S. Yoo, *WO 9909117* **1999**.

[114] M. Arias, D. Laurenti, C. Geantet, M. Vrinat, I. Hideyuki, Y. Yoshimura, *Catalysis Today* **2008**, 130, 190-194.

[115] V. Meille, E. Shulz, M. Vrinat, M. Lemaire, *Chemical Communications* **1998**, 3, 305-306.

[116] A. Milenkovic, E. Shulz, V. Meille, D. Lofferda, M. Forissier, M. Vrinat, P. Sautet, M. Lemaire, *Energy & Fuels* **1999**, 13, 881-887.

[117] Y. Shiraishi, Y. Taki, T. Hirai, I. Komasawa, *Industrial & Engineering Chemistry Research* **2001**, 40, 1213-1224.

[118] R. M. Acheson, D. R. Harrison, *Journal of the Chemical Society D* **1969**, 13, 724-724.

[119] R. M. Acheson, D. R. Harrison, *Journal of the Chemical Society C* **1970**, 13, 1764-1784.

[120] K. A. Gray, O. S. Pogrebinsky, G. T. Mrrachko, L. Xi, D. J. Monticello, C. H. Squires, *Nature Biotechnology* **1996**, 14, 1705-1709.

[121] F. Kargi, J. M. Robinson, *Applied and Environmental Microbiology* **1982**, 44, 878-883.

[122] M. F. Luo, J. M. Xing, Z. X. Gou, S. Li, H. Z. Liu, J. Y. Chen, *Biochemical Engineering Journal* **2003**, 13, 1-6.

[123] T. Ohshiro, Y. Izumi, *Bioscience, Biotechnology and Biochemistry* **1999**, 63, 1-9.

[124] V. Selvavathi, V. Chidambaram, A. Meenakshisundaram, B. Sairam, B. Sivasankar, *Catalysis Today* **2009**, 141, 99-102.

[125] J. H. Kim, X. Ma, A. Zhou, C. Song, *Catalysis Today* **2006**, 111, 74-83.

[126] Z. Y. Zhang, T. B. Shi, C. Z. Jia, W. J. Ji, Y. Chen, M. Y. He, *Applied Catalysis B: Environmental* **2008**, 82, 1-10.

[127] I. Funakoshi, T. Aida, *US 5753102* **1998**.

[128] P. Forte *US 5582714* **1996**.

[129] M. Te, C. Fairbridge, Z. Ring, *Applied Catalysis A: General* **2001**, 219, 267-280.

[130] S. Otsuki, T. Nonaka, N. Takashima, W. Qian, A. Ishihara, T. Imai, T. Kabe, *Energy & Fuels* **2000**, 14, 1232-1239.

[131] J. M. Campos-Martin, M. C. Capel-Sanchez, P. Perez-Presas, J. L. G. Fierro, *Journal of Chemical Technology and Biotechnology* **2010**, 85, 879-890.

[132] E. Torres-García, A. Galano, G. Rodriguez-Gattorno, *Journal of Catalysis* **2011**, 282, 201-208.

[133] M. F. Ali, A. Al-Malki, B. El-Ali, G. Martinie, M. N. Siddiqui, *Fuel* **2006**, 85, 1354-1363.

[134] L. Chen, S. Guo, D. Zhao, *Chinese Journal of Chemical Engineering* **2007**, 15, 520-523.

[135] V. Toteva, A. Georgiev, L. Topalova, *Fuel Processing Technology* **2009**, 90, 965-970.

[136] F. A. Duarte, P. A. Mello, C. A. Bizzi, M. A. G. Nunes, E. M. Moreira, M. S. Alencar, H. N. Motta, V. L. Dressler, E. M. M. Flores, *Fuel* **2011**, 90, 2158-2164.

[137] H. Lü, Y. Zhang, Z. Jiang, C. Li, *Green Chemistry* **2010**, 12, 1954-1958.

[138] M. A. Ramos-Luna, L. Cedeño-Caero, *Industrial and Engineering Chemistry Research* **2011**, 50, 2641-2649.

[139] L. Cedeño-Caero, M. Ramos-Luna, M. Méndez-Cruz, J. Ramírez-Solís, *Catalysis Today* **2011**, 172, 189-194.

[140] W. Guo, C. Wang, P. Lin, X. Lu, *Applied Energy* **2011**, 88, 175-179.

[141] X. M. Yan, P. Mei, J. Lei, Y. Mi, L. Xiong, L. Guo, *Journal of Molecular Catalysis A: Chemical* **2009**, 304, 52-57.

[142] A. Bösmann, L. Datsevich, A. Jess, A. Lauter, C. Schmitz, P. Wasserscheid, *Chemical Communications* **2001**, 23, 2494-2495.

[143] N. H. Ko, J. S. Lee, E. S. Huh, H. Lee, K. D. Jung, H. S. Kim, M. Cheong, *Energy & Fuels* **2008**, 22, 1687-1690.

[144] R. Schmidt, *Energy & Fuels* **2008**, 22, 1774-1778.

[145] S. Zhang, Z. C. Zhang, *Green Chemistry* **2002**, 4, 376-379.

[146] S. Zhang, Q. Zhang, Z. C. Zhang, *Industrial and Engineering Chemistry Research* **2004**, 43, 614-622.

[147] C. Xuemei, H. Yufeng, L. Jiguang, L. Qianqing, L. Yansheng, Z. Xianming, P. Xiaoming, Y. Wenjia, *Chinese Journal of Chemical Engineering* **2008**, 16, 881-884.

[148] H. S. Gao, M. F. Luo, J. M: Xing, Y. Wu, Y. G: Li, W. L. Li, Q. F. Liu, H. Z. Liu, *Industrial and Engineering Chemistry Research* **2008**, 47, 8384-8388.

[149] R. P. Swatloski, J. D. Holbrey, R. D. Rogers, *Green Chemistry* **2003**, 5, 361-363.

[150] J. Eber, P. Wasserscheid, A. Jess, *Green Chemistry* **2004**, 6, 316-322.

[151] Y. Mochizuki, K. Sugawara, *Energy & Fuels* **2008**, 22, 3303-3307.

[152] C. C. Cassol, A. P. Umpierre, G. Ebeling, B. Ferrera, S. S. X. Chiaro, J. Dupont, *International Journal of Molecular Science* **2007**, 8, 593-605.

[153] L. Alonso, A. Arce, M. Francisco, A. Soto, *Journal of Chemical Engineering Data* **2007**, 52, 2409-2412.

[154] L. Alonso, A. Arce, M. Francisco, A. Soto, *Journal of Chemical Engineering Data* **2008**, 53, 1750-1755.

[155] L. Alonso, A. Arce, M. Francisco, A. Soto, *Fluid Phase Equilibria* **2008**, 263, 176-181.

[156] A. Arce, M. Francisco, A. Soto, *Journal of Chemical Thermodynamics* **2010**, 42, 712-718.

[157] C. Asumana, G. Yu, X. Li, J. Zhao, G. Liu, X. Chen, *Green Chemistry* **2010**, 12, 2030-2037.

[158] G. Yu, X. Li, X. Liu, C. Asumana, X. Chen, *Industrial & Engineering Chemistry Research* **2011**, 50, 2236-2244.

[159] A. R. Hansmeier, G. W. Meindersma, A. B. de Haan, *Green Chemistry* **2011**, 13, 1907-1913.

[160] M. M. Taib, T. Murugesan, *Asia-Pacific Journal of Chemical Engineering* **2012**, 7, 469-473.

[161] J. D. Holbrey, I. López-Martín, G. Rothenberg, K. R. Seddon, G. Silveiro, X. Zheng, *Green Chemistry* **2008**, 10, 87-92.

[162] M. Królikowski, K. Walczak, U. Domanska, *Journal of Chemical Thermodynamics* **2013**, 65, 168-173.

[163] K. Kedra-Królik, F. Mutelet, J: N. Joubert, *Industrial & Engineering Chemistry Research* **2011,** 50, 2296-2306.

[164] A. Marciniak, M Królikowski, *Journal of Chemical Thermodynamics* **2012,** 49, 154-158.

[165] M. Francisco, A. Arce, A. Soto, *Fluid Phase Equilibria* **2010**, 294, 39-48.

[166] L. Alonso, A. Arce, M. Francisco, O. Rodríguez, A. Soto, *Journal of Chemical Engineering Data* **2007**, 52, 1729-1732.

[167] L. Alonso, A. Arce, M. Francisco, A. Soto, *Journal of Chemical Thermodynamics* **2008**, 40, 966-972.

[168] L. Alonso, A. Arce, M. Francisco, O. Rodríguez, A. Soto, *AIChE Journal* **2007**, 53, 3108-3115.

[169] L. Alonso, A. Arce, M. Francisco, A. Soto, *Journal of Solution Chemistry* **2008**, 37, 1355-1363.

[170] L. Alonso, A. Arce, M. Francisco, A. Soto, *Fluid Phase Equilibria* **2008**, 270, 97-102.

[171] H. Rodríguez, M. Francisco, A. Soto, A. Arce, *Fluid Phase Equilibria* **2010**, 298, 240-245.

[172] J. Feng, C. X. Li, H. Meng, Z. Wang, *Petrochemical Technology* **2006**, 3, 272-276.

[173] Y. Nie, C. Li, A. Sun, H. Meng, Z. Wang, *Energy & Fuels* **2006**, 20, 2083-2087.

[174] X. Jiang, Y. Nie, C. Li, Z. Wang, *Fuel* **2008**, 87, 79-84.

[175] C. Yansheng, L. Changping, J. Qingzhu, L. Qingshan, Y. Peifang, L. Xiumei, U. Welz-Biermann, *Green Chemistry* **2011**, 13, 1224-1229.

[176] C. Jiang, J. Wang, S. Wang, H. Guan, X. Wang, M. Huo, *Applied Catalysis B: Environmental* **2011**, 106, 343-349.

[177] J. Wang, D. Zhao, K. Li, *Energy & Fuels* **2010**, 24, 2527-2529.

[178] H. Li, L. He, J. Lu, W. Zhu, X. Jiang, Y. Wang, Y. Yan, *Energy & Fuels* **2009**, 23, 1354-1357.

[179] L. Chuang, J. Huang, W. Lo, G. Wei, *Journal of the Chinese Chemical Society* **2012**, 59, 324-330.

[180] W. Zhu, H. Li, Q. Gu, P. Wu, G. Zhu, Y. Yan, G. Chen, *Journal of Molecular Catalysis A: Chemical* **2011**, 336, 16-22.

[181] H. Lü, J. Gao, Z. Jiang, F. Jing, Y. Yang, G. Wang, C. Li, *Journal of Catalysis* **2006**, 239, 369-375.

[182] W. Huang, W. Zhu, H. Li, H. Shi, G. Zhu, H. Liu, G. Chen, *Industrial & Engineering Chemistry Research* **2010**, 49, 8998-9003.

[183] J. Ge, Y. Zhou, Y. Yang, M. Xue, *Industrial & Engineering Chemistry Research* **2011**, 50, 13686-13692.

[184] J. Zhang, A. Wang, X. Li, X. Ma, *Journal of Catalysis* **2011**, 279, 269-275.

[185] D. Xu, W. Zhu, H. Li, J. Zhang, F. Zou, H. Shi, Y. Yan, *Energy & Fuels* **2009**, 23, 5929-5933.

[186] D. Liu, J. Gui, J. Ding, J. Ma, J. Lee, Z. Sun, *Reaction Kinetics, Mechanisms and Catalysis* **2011**, 104, 111-123.

[187] E. Lissner, W. F. de Souza, B. Ferrera, J. Dupont, *ChemSusChem* **2009**, 2, 962-964.

[188] D. Zhao, Z. Sun, F. Li, R. Liu, H. Shan, *Energy & Fuels* **2008**, 22, 3065-3069.

[189] D. S. Zhao, H. W. Ren, J. L. Wang, Y. Yang, Y. Zhao, *Energy & Fuels* **2007**, 21, 2543-2547.

[190] W. Zhu, J. Zhang, H. Li, Y. Chao, W. Jiang, S. Yin, H. Liu, *Royal Society of Chemistry Advances* **2012**, 2, 658-664.

[191] H. Li, W. Zhu, Y. Wang, J. Zhang, J. Lu, Y. Yan, *Green Chemistry* **2009**, 11, 810-815.

[192] J. Zhang, W. Zhu, H. Li, W. Jiang, Y. Jiang, W. Huang, Y. Yan, *Green Chemistry* **2009**, 11, 1801-1807.

[193] D. Zhao, J. Wang, E. Zhou, *Green Chemistry* **2007**, 9, 1219-1222.

[194] J. Wang, D. Zhao, K. Li, *Energy & Fuels* **2009**, 23, 3831-3834.

[195] L. Lu, S. Cheng, J. Gao, G. Gao, M. He, *Energy & Fuels* **2007**, 21, 383-384.

[196] W. Zhang, K. Xu, Q, Zhang, D. Liu, S. Wu, F. Verpoort, X.-M. Song, *Industrial & Engineering Chemical Research* **2010**, 49, 11761-11763.

[197] G. Yu, J. Zhao, D. Song, C. Asumana, X. Zhang, X. Chen, *Industrial & Engineering Chemical Research* **2011**, 50, 11690-11697.

[198] B. Zhang, Z. Jiang, J. Li, Y. Zhang, F. Lin, Y. Liu, C. Li, *Journal of Catalysis* **2012**, 287, 5-12.

[199] H. Gao, C. Guo, J. Xing, J. Zhao, H. Liu, *Green Chemistry* **2010**, 12, 1220-1224.

[200] D. Zhao, Z. Sun, F. Li, H. Shan, *Journal of Fuel Chemistry and Technology* **2009**, 37, 194-198.

[201] W. Keim, W. Korth, P. Wasserscheid, *WO Pat. WO 0016902* **2000**.

[202] J. A. Riddick, W. B. Bunger, T. K. Sakano, Organic Solvents. Physical Properties and Methods of Purification, 4th ed., John Wiley & Sons, **1986**.

[203] M. Fermeglia, G. J. Toriano, *Chemical Engineering Data* **1999**, 44, 965-969.

[204] B. Luo, G. C. Benson, B. C.-Y. Lu, *Journal of Chemical Thermodynamics* **1988**, 20, 267-271.

[205] T. E. Daubert, R. P. Danner, *Physical and thermodynamic properties of pure components: Data compilation*, Hemisphere Publishing Corporation, **1989**.

[206] D. R. Lide, *CRC Handbook of Chemistry and Physics, 87th ed.*; Taylor and Francis: Boca Raton, FL, **2007**.

[207] E. Guillet, D. Imbert, R. Scopelliti, J. C. G. Bunzil, *Chemistry of Materials* **2004**, 16, 4063-4070.

[208] M. Tariq, P. A. S. Forte, M. F. Costa Gomes, J. N. Canongia Lopes, L. P. N. Rebelo, *Journal of Chemical Thermodynamics* **2009**, 41, 790-798.

[209] M. G. Freire, A. R. R. Teles, M. A. A. Rocha, B. Schroder, C. M. S. S. Neves, P. J. Carvalho, D. V. Evtuguin, L. M. N. B. F. Santos, J. A. P. Coutinho, *Journal of Chemical Engineering Data* **2011**, 56, 4813-4822.

[210] A. P. Fröba, M. H. Rausch, K. Krzeminski, D. Assenbaum, P. Wasserscheid, A. Leipertz, *International Journal of Thermophysics* **2010**, 31, 2059-2077.

[211] J. Wang, C. Li, C. Shen, Z. Wang, *Fluid Phase Equilibria* **2009**, 279, 87-91.

[212] L. Hadlich de Oliveira, M. Aznar, *Journal of Chemical Engineering Data* **2011**, 56, 2005-2012.

[213] E. Kuhlmann, S. Himmler, H. Giebelhaus, P. Wasserscheid, *Green Chemistry* **2007**, 9, 233-242.

[214] A. Arce Arce, A. Soto Campos, E. Rodil Rodríguez, B. Rodríguez Cabo, *WO 2012013852 A2 20120202* **2012**.

[215] S. Schwyn, E. Garwin, A. Schmidt-Ott, *Journal of Aerosol Science* **1988**, 19, 639-642.

[216] N. S. Tabrizi, M. Ullmann, V. A. Vons, U. Lafont, A. Schmidt-Ott, *Journal of Nanoparticle Research* **2009**, 11, 315-332.

[217] N. S. Tabrizi, Q. Xu, N. M. van der Pers, A. Schmidt-Ott, *Journal of Nanoparticle Research* **2010**, 12, 247-259.

[218] H. Renon, J.M. Prausnitz, *AIChE Journal* **1968**, 14, 135-144.

[219] D. S. Abrams, J. M. Prausnitz, *AIChE Journal* **1975**, 21, 116-128.

[220] J. M. Prausnitz, T. F. Anderson, E. A. Grens, C. A. Eckert, R. Hsieh, J. P. O´Connel, *Computer Calculations for Multicomponent Vapor–Liquid and Liquid–Liquid Equilibria*, Prentice Hall, Englewood Cliffs, New York, **1980**.

[221] Z. Lei, J. Zang, Q. Li, B. Chen, *Industrial & Engineering Chemical Research* **2009**, 48, 2697-2704.

[222] R. Kato, J. Gmehling, *Journal of Chemical Thermodynamics* **2005**, 37, 603-619.

[223] J. M. Sørensen, W. Arlt, *Liquid-Liquid Equilibrium Data Collection,* DECHEMA Chemistry Data Series, Frankfurt, **1980**.

[224] L. W. Lo, H. Y. Yang, G. T. Wei, *Green Chemistry* **2003**, 5, 639-642.

[225] D. Zhao, Y. Wang, E. Duan, J. Zhang, *Fuel Process Technology* **2010**, 91, 1803-1806.

[226] H. Zhang, J. Gao, H. Meng, C. X. Li, *Industrial & Engineering Chemical Research* **2012**, 51, 6658-6665.

APPENDIX A (List of publications)

PUBLICATIONS

1. P. Verdía, E. J. González, **B. Rodríguez-Cabo** and E. Tojo.
Synthesis and characterization of new polysubstituted pyridinium-based ionic liquids: application as solvents on desulfurization of fuel oils.
Green Chemistry 2011, 13, 2768-2776.

2. B. Rodríguez-Cabo, E. Rodíl, H. Rodríguez, A. Soto and A. Arce.
Direct preparation of sulfide semiconductor nanoparticles from the corresponding bulk powders in an ionic liquid.
Angewandte Chemie International Edition 2012, 51, 1424-1427.

3. B. Rodríguez-Cabo, M. Francisco, A. Soto and A. Arce.
Hexyl dimethylpyridinium ionic liquids for desulfurization of fuels. Effect of the position of the alkyl side chains.
Fluid Phase Equilibria 2012, 314, 107-112.

4. B. Rodríguez-Cabo, E. Rodíl, A. Soto and A. Arce.
Preparation of metal oxide nanoparticles in ionic liquid medium.
Journal of Nanoparticle Research 2012, 14, 939/1-939/9.

5. B. Rodríguez-Cabo, A. Soto and A. Arce.
Desulfurization of fuel-oils with $[C_2mim][NTf_2]$: A comparative study.
Journal of Chemical Thermodynamics 2013, 57, 248-255.

6. I. Rodríguez-Palmeiro, **B. Rodríguez-Cabo**, E. Rodíl, A. Arce, J. M. Saiz-Jabardo and A. Soto.
Synthesis and characterization of highly concentrated AgI-$[P_{6,6,6,14}]$Cl ionanofluids.
Journal of Nanoparticle Research 2013, 15, 1881/1-1881/8.

7. B. Rodríguez-Cabo, A. Arce and A. Soto.
Desulfurization of fuels by liquid-liquid extraction with 1-ethyl-3-methylimidazolium ionic liquids.
Fluid Phase Equilibria 2013, 356, 126-135.

8. B. Rodríguez-Cabo, H. Rodríguez, E. Rodíl, A. Arce and A. Soto.
Extractive and oxidative-extractive desulfurization of fuels with ionic liquids.
Fuel 2014, 117, 882-889.

PATENTS

1. A. Arce Arce, A. Soto Campos, E. Rodíl Rodríguez and **B. Rodríguez-Cabo**.
Process for preparation of nanoparticles in ionic liquids.
PCT Int. Appl. 2012, WO 2012013852 A2 20120202.

APPENDIX B (Summary in Spanish, Resumen)

El principal objetivo de este trabajo es definir un sistema de desulfuración de combustibles mediante extracción líquido-líquido con líquidos iónicos (LIs) como disolventes. En concreto se estudiarán dos operaciones: desulfuración extractiva y desulfuración oxidativa.

Parejos a la industrialización y desarrollo de muchos países, los episodios de contaminación atmosférica se han propagado a nivel global. Suele ser habitual presuponer que la única causa de esta contaminación procede de las grandes industrias, pero lo cierto es que las emisiones de los automóviles contribuyen en gran manera a este fenómeno. Sus emisiones son las responsables de uno de los problemas de contaminación más conocidos, la lluvia ácida. Por ello, se hace obvia la necesidad de reducir el contenido en azufre de los combustibles, y muchos países ya han establecido legislaciones para conseguirlo.

El proceso industrial que actualmente se usa para la desulfuración de combustibles es la hidrodesulfuración (HDS). Sin embargo, no todos los compuestos azufrados presentes en los combustibles son igualmente reactivos frente a esta técnica, siendo las especies más pesadas (tales como dibenzotiofenos) las más difíciles de extraer. Para resolver estas limitaciones y mejorar la extracción de azufre de los combustibles, durante los últimos años se han estudiado nuevas técnicas para reemplazar o incluso acoplar al proceso de HDS. Los métodos más estudiados son la alquilación reactiva, métodos de precipitación, biodesulfuración, adsorción, desulfuración extractiva y desulfuración oxidativa. De entre todas estas técnicas, las más estudiada es probablemente la desulfuración extractiva (EDS), consistente en una extracción líquido-líquido. Sin embargo, la ausencia de un disolvente con las características apropiadas implica que, a día de hoy, ninguna de estas técnicas sea aún una realidad industrial.

Los LIs pueden definirse como sales con un punto de fusión por debajo de 373.15 K. Esta breve definición no arroja demasiada luz acerca de sus propiedades o características, pero sí sobre su naturaleza: al ser sales líquidas, están formadas por al menos un catión y un anión. Hay muchas posibles combinaciones de estos dos iones, lo que implica la existencia de un enorme número de LIs, con la posibilidad de ser diseñados a medida para una aplicación dada. Sus propiedades, tanto físicas como químicas, hacen que los LIs sean considerados como posible alternativa a los disolventes orgánicos tradicionales para mejorar el rendimiento de distintos procesos industriales a la vez que disminuyen sus episodios de contaminación. De entre todas sus características, destaca su presión de vapor despreciable, que evita fenómenos de contaminación atmosférica.

Desde que en 2001 Wassercheid publicó la extracción selectiva de azufre presente en combustibles usando LIs, se han presentado muchos trabajos en los que se estudia la idoneidad de distintos LIs para tal fin. Se propusieron diversos cationes (piridinios, imidazolios, amonios) y un gran número de aniones (alquilsulfatos,

tetrafluoroboratos, hexafluorofosfatos, cloruros, etc.). Un hito a destacar es la publicación por parte de Holbrey en 2008 de un ranking de cationes para la desulfuración de combustibles (basándose en la extracción de dibenzotiofeno presente en dodecano): alquilpiridinio ≥ piridinio ≈ imidazolio ≈ pirrolidinio.

Sin embargo, existe una llamativa ausencia de estudios publicados en los que se tenga en cuenta cómo evolucionan los otros compuestos presentes en los combustibles durante el proceso de extracción. La mayoría de estudios bibliográficos se basan simplemente en la solubilidad de un compuesto azufrado (normalmente dibenzotiofeno) en el LI. No se considera la desnitrogenación, que en el proceso HDS se produce simultáneamente a la desulfuración, ni la desaromatización que afecta directamente a las propiedades del combustible.

Con el propósito de mejorar la eficacia del proceso de extracción, se puede añadir un sistema oxocatalítico. Su función es oxidar los compuestos azufrados a sulfonas y sulfóxidos, de manera que el disolvente empleado como agente extractor es capaz de extraer más compuesto azufrado del combustible. Esta técnica recibe el nombre de desulfuración oxidativa (ODS). No han sido muchos los oxidantes estudiados (en la inmensa mayoría de trabajos se emplea H_2O_2), sin embargo los posibles catalizadores propuestos son bastante más numerosos (polioxometalatos, sólidos, LIs ácidos o coordinados…). El uso de uno de los sistemas oxidantes más empleados, H_2O_2 y AcOH, parece ser una de las mejores alternativas para la desulfuración oxidativa con LIs. No obstante, se hace necesario sopesar si la mejora alcanzada al utilizar estos sistemas difíciles de manejar y de recuperar justifica su uso frente a una EDS con LIs.

En la primera parte de este trabajo, se estudió la viabilidad de usar varios LIs para la desulfuración de combustibles mediante extracción líquido-líquido. Se completa así un trabajo previo, desarrollado en este grupo de investigación, en el que el LI bis(trifluorometilsulfonil)imida de 1-hexil-3,5-dimetilpiridinio, $[C_6^{3,5}mmpy][NTf_2]$, se propuso para tal fin, al mismo tiempo que se dejaban una serie de cuestiones sin resolver. Surgió la necesidad de analizar el efecto de la posición de las sustituciones del anillo catiónico sobre la desulfuración. Por tanto, se seleccionó el LI bis(trifluorometilsulfonil)imida de 1-hexil-2,4-dimetilpiridinio $[C_6^{2,4}mmpy][NTf_2]$, para realizar los ensayos de desulfuración. Por otra parte, estudios incipientes realizados en el grupo apuntaban al LI bis(trifluorometilsulfonil)imida de 1-etil-3-metilimidazolio como un candidato adecuado para nuestro fin. La selección de este segundo LI permite analizar la influencia del catión en el proceso. Con el objetivo de analizar la influencia del anión, se seleccionaron LIs con el mismo catión, 1-etil-3-metilimidazolio, y diferentes aniones. Un factor clave a la hora de elegirlos fue la ausencia de azufre en su estructura, lo que evitaría el incremento del contenido en azufre del combustible en caso de mínimas contaminaciones del mismo por el LI en los procesos de extracción. Por tanto, los dos últimos LIs seleccionados para esta

investigación fueron el acetato de 1-etil-3-metilimidazolio, [C_2mim][OAc], y el dietilfosfato de 1-etil-3-metilimidazolio, [C_2mim][DEP].

EQUILIBRIO LÍQUIDO-LÍQUIDO

Se determinó el equilibrio líquido-líquido de los sistemas {LI + hexano + tiofeno}, {LI + tolueno + tiofeno}, y {LI + hexano + piridina} con cada uno de los LIs seleccionados. Para determinar las rectas de reparto correspondientes al equilibrio de cada sistema ternario, se introdujeron en una celda termostatizada, de 30 ml, mezclas de los tres componentes en la región inmiscible. La temperatura se mantuvo constante a 298.15 K y las mezclas se agitaron durante 2 horas. Después, se dejaron reposar durante 4 horas y se tomaron muestras de ambas fases con una jeringa para ser analizadas por cromatografía de gases.

Los sistemas que contienen tiofeno se ajustan a un diagrama ternario tipo II, con dos pares de compuestos parcialmente miscibles entre sí. Para los sistemas con piridina, los diagramas obtenidos presentan comportamiento tipo I, con sólo un par de componentes inmiscibles.

Para evaluar la bondad como disolventes de los LIs seleccionados se emplearon dos parámetros termodinámicos (la razón de distribución de soluto, β, y la selectividad, S), analizando la desulfuración y los posibles procesos de desnitrogenación y desaromatización que pueden tener lugar. Tras comparar los resultados obtenidos para los LIs [$C_6^{2,4}$mmpy][NTf_2] y [$C_6^{3,5}$mmpy][NTf_2] (estudiado previamente), se observa que la asimetría en la posición de los grupos metilos del catión mejora levemente el poder de desulfuración del LI.

En los sistemas con tiofeno y hexano, para todos los LIs las solubilidades y selectividades son mayores que la unidad, lo que implica que estos disolventes son buenos candidatos para la desulfuración. El ranking de solubilidades es [$C_6^{2,4}$mmpy][NTf_2] > [C_2mim][DEP] > [C_2mim][NTf_2] > [C_2mim][OAc], lo que concuerda con lo establecido por Holbrey *et al.* en 2008. Considerando que el LI puede ser recuperado, la selectividad se convierte en un parámetro decisivo para la selección del LI más adecuado como disolvente. El ranking de selectividades para la extracción de tiofeno del hexano es [C_2mim][OAc] > [C_2mim][NTf_2] ≈ [C_2mim][DEP] > [$C_6^{2,4}$mmpy][NTf_2]. Los mejores valores de selectividad se obtienen con el LI [C_2mim][OAc], convirtiéndolo en la opción más prometedora. En este caso el LI con piridinio presenta los peores resultados.

Para la separación tiofeno-tolueno, las solubilidades decrecen en el orden [C_2mim][DEP] ≈ [$C_6^{2,4}$mmpy][NTf2] > [C_2mim][NTf_2] ≈ [C_2mim][OAc], estando todos los valores muy próximos a la unidad. Esto significa que se necesitaría una cantidad sustancial de disolvente para llevar a cabo la extracción. En el caso de la selectividad, el ranking de LIs es [C_2mim][OAc] > [C_2mim][DEP] > [C_2mim][NTf_2] >

[$C_6^{2,4}$mmpy][NTf_2]. Las selectividades son mayores que la unidad, aunque muy próximas en el caso de los dos LIs con anión bis(trifluorometilsulfonil)imida. Una vez más, apoyándose en la facilidad de recuperación del LI, [C_2mim][OAc] puede considerarse la mejor opción.

Por último, tanto los valores de solubilidad como los de selectividad son claramente mayores que la unidad al estudiar la separación piridina-hexano con todos los LIs. Estos resultados implican que se producirá una desnitrogenación simultáneamente al proceso de desulfuración. La solubilidad de la piridina en el LI sigue la tendencia [$C_6^{2,4}$mmpy][NTf_2] > [C_2mim][NTf_2] ≈ [C_2mim][DEP] > [C_2mim][OAc]. La capacidad de los LIs para extraer preferentemente piridina es [C_2mim][OAc] > [C_2mim][NTf_2] ~ [C_2mim][DEP] > [$C_6^{2,4}$mmpy][NTf_2].

Los datos experimentales obtenidos se correlacionaron para facilitar su uso en el diseño y simulación del proceso. Para tal fin se emplearon los modelos NRTL y UNIQUAC, obteniendo ajustes satisfactorios. Los sistemas que contienen tiofeno se correlacionaron mejor usando UNIQUAC; sin embargo, cuando el sistema contiene piridina, las mejores correlaciones se obtuvieron con el modelo NRTL, excepto en el caso del sistema {[C_2mim][OAc] + piridina + hexano}, que es el único con comportamiento solutrópico.

DESULFURACIÓN DE COMBUSTIBLES SINTÉTICOS

Con el fin de simular el comportamiento de combustibles reales, se prepararon modelos de gasolina y diésel, que se usaron para estudiar la desulfuración mediante extracción con LIs. La gasolina sintética se simuló mediante una mezcla de hexano (26% en masa), heptano (26% en masa), isooctano (26% en masa), tolueno (10% en masa), piridina (6% en masa) y tiofeno (6% en masa). En el caso del modelo de diésel, los alcanos se hacen más pesados y la carga de azufre está repartida con una especie más refractaria, resultando la siguiente mezcla: heptano (26% en masa), dodecano (26% en masa), hexadecano (26% en masa), tolueno (10% en masa), piridina (6% en masa), tiofeno (3% en masa) y dibenzotiofeno (3% en masa).

Para estudiar la desulfuración extractiva de los modelos de combustible con LIs se llevaron a cabo tres etapas de extracción. En cada una de ellas, se introdujo el combustible sintético en una celda termostatizada con el correspondiente LI a 298.15 K y presión atmosférica. Tras 12 horas de agitación y 12 horas de reposo, la composición de los refinados se analizó por cromatografía de gases. Se siguió el mismo protocolo experimental para los modelos de gasolina y de diésel.

En el caso de la gasolina sintética, después de tres etapas de desulfuración, la mayor reducción de tiofeno alcanzada se consigue con el LI piridinio, (84.9 % de extracción en masa). También se produce una importante desaromatización (67 %), como se predecía a

partir de los equilibrios previamente determinados. Por ello, y coincidiendo con los resultados obtenidos en el estudio de los equilibrios, parece mejor opción el uso del LI [C_2mim][OAc], que alcanza la segunda mejor eficacia de desulfuración (79.3 %) mientras que la desaromatización que implica es mucho menor (14.2 %) tras tres etapas de extracción. La desnitrogenación de la gasolina sintética es completa para los cuatro LIs, y en ningún caso se encontró LI en la fase del refinado.

En el caso del diésel sintético, la capacidad de los LIs para desulfurar sigue la misma tendencia que en la gasolina. El mejor resultado se obtuvo para el LI [$C_6^{2,4}$mmpy][NTf_2], que extrajo más del 90 % de tiofeno y 98 % de dibenzotiofeno, siendo la desaromatización del 78 %. Cabe destacar que la extracción de dibenzotiofeno es mayor que la de tiofeno para todos los LIs, pero especialmente para el piridinio. Esto se justifica debido a las interacciones electrónicas π-π del anillo catiónico con el compuesto azufrado aromático. El LI [C_2mim][OAc] produce una desaromatización del diésel sintético mucho menor (entorno al 53 %) que el piridinio, mientras que la desulfuración alcanzada es muy similar (87.2 % de tiofeno y 88.0 % de dibenzotiofeno). Por ello, de nuevo este LI podría ser la opción más adecuada para la desulfuración del diésel sintético mediante EDS. Una vez más, la desnitrogenación es total para los cuatro LIs después de tres etapas de extracción, y no se encontró LI en la fase de refinado.

Además de la desulfuración extractiva de los modelos, se ensayó un proceso de desulfuración oxidativa, con el propósito de aumentar la extracción de los compuestos azufrados. Los resultados obtenidos con el modelo de gasolina no mejoraron los de una extracción convencional. Este comportamiento, previamente encontrado en la bibliografía, se justifica debido a la baja densidad electrónica del tiofeno (la reactividad de los compuestos azufrados para la oxidación aumenta con este valor). Sin embargo, los resultados de desulfuración en el caso del diésel son diferentes cuando se aplica un proceso de ODS frente a la EDS.

Se procedió en primer lugar a la optimización de los diversos parámetros del proceso de oxidación. Para analizar la posibilidad de usar como oxidante H_2O_2 y como catalizador nanopartículas de óxidos metálicos, se puso a punto una técnica de síntesis de ionanofluidos, también válida para la síntesis de nanopartículas en LIs. Esta técnica, que permite trabajar a temperaturas moderadas y presiones atmosféricas, evita el uso de otros disolventes o reactivos de partida. Además es un método muy sencillo y no genera subproductos de reacción. Nuestra técnica se comparó con el método de chispa disruptiva, con el fin de seleccionar el método de fabricación de ionanofluidos que más favoreciese el proceso de desulfuración oxidativa. Dado que las nanopartículas formadas por la primera técnica no estaban aglomeradas y eran de menor tamaño (lo que implica un aumento en su actividad catalítica al tener una mayor área específica) se seleccionó la disolución-reprecipitación como método de

fabricación de los ionanofluidos. Se sintetizaron dispersiones de nanopartículas de Al_2O_3, TiO_2, y Cr_2O_3 en el LI $[C_6^{2,4}mmpy][NTf_2]$ (1% en masa) y se usaron como agente extractor-catalítico. Sin embrago, el uso de ionanofluidos no mejoró los resultados obtenidos con un sistema oxocatítico clásico (H_2O_2 y AcOH), por lo que se decidió trabajar con este último sistema.

Así, en el sistema H_2O_2-AcOH, se optimizaron las relaciones molares de catalizador y de agente oxidante por mol de azufre en el modelo. Las condiciones de oxidación que proporcionaron mejores resultados en cuanto a la extracción implican el uso de catalizador (AcOH) y agente oxidante (H_2O_2) en una relación molar de 9 con respecto al azufre del modelo. Con dicho sistema oxocatalítico, se optimizaron la temperatura y los tiempos de agitación y reposo, obteniéndose el mayor grado de desulfuración a 323.15 K, tras 12 horas de agitación y 12 horas de separación de las fases. Además, se extrae mayor cantidad de compuestos azufrados cuando se trabaja mezclando todo el sistema a la vez, en lugar de hacerlo en dos pasos.

Una vez optimizado el sistema, se realizó la desulfuración del diésel sintético con los LIs. Nuevamente, la mayor desulfuración se alcanzó con el LI $[C_6^{2,4}mmpy][NTf_2]$, extrayendo más del 94 % de tiofeno y todo el dibenzotiofeno. El LI $[C_2mim][NTf_2]$ mostró eficacias muy similares de desulfuración, mientras que su precio es mucho menor. Además, como en el caso de la EDS, la desaromatización que implica el LI imidazolio es mucho menor que la del piridinio (42.2 % frente al 66.1 %). Por ello, este segundo LI es en principio más favorable para la ODS del diésel sintético. Cabe mencionar que en el caso de los LIs miscibles con agua ($[C_2mim][OAc]$ y $[C_2mim][DEP]$) la eficacia de desulfuración se ve reducida con respecto al proceso de EDS. Esto se debe a que al llevar a cabo un proceso de ODS con H_2O_2, aumenta el contenido en agua de los LIs, lo que provoca que su habilidad para extraer los compuestos azufrados sea menor.

DESULFURACIÓN DE COMBUSTIBLES REALES

Para corroborar la eficacia de desulfuración de los LIs testada en los combustibles sintéticos, se llevaron a cabo las correspondientes EDS y ODS con combustibles reales. El procedimiento experimental seguido fue el mismo que en el caso de los modelos, con la diferencia de que se empleó un analizador de azufre total para medir el contenido en azufre de los combustibles reales tras cada etapa de extracción, debido a la dificultad de analizar el elevadísimo número de componentes de un combustible real.

De acuerdo con los resultados obtenidos para el modelo de gasolina, la capacidad de desulfuración de los LIs debería seguir el orden $[C_6^{2,4}mmpy][NTf_2]$ > $[C_2mim][DEP]$ ≈ $[C_2mim][OAc]$ > $[C_2mim][NTf_2]$. Sin embargo, al trabajar con gasolina real, el grado de desulfuración alcanzado por el LI $[C_2mim][OAc]$ es mucho mayor (desulfuración del 38.7 % en masa en la primera etapa) que el conseguido con otros LIs. Se comprobó que este incremento en la

extracción de azufre podía ser debido a la transformación de pequeños mercaptanos presentes en la gasolina real a dialquilsulfuros y dialquildisulfuros, que se extraen con mayor facilidad. Este comportamiento no se observó en la gasolina sintética debido a que el único compuesto azufrado del modelo era el tiofeno. La tendencia para el resto de LIs sigue el mismo orden que en el caso de muestras sintéticas.

La eficacia de los LIs en una EDS con diésel real sigue el siguiente orden: $[C_6^{2,4}mmpy][NTf_2]$ > $[C_2mim][DEP]$ > $[C_2mim][OAc]$ > $[C_2mim][NTf_2]$, que coincide con los resultados obtenidos para el modelo sintético de diésel. En comparación con los LIs con catión imidazolio, el LI basado en piridinio consigue una buena desulfuración (37.8 % en tres etapas).

Para la desulfuración oxidativa del diésel real se emplearon los parámetros de oxidación (catalizador, tiempos, temperatura…) seleccionados como óptimos al estudiar la desulfuración oxidativa de las muestras sintéticas. La capacidad extractiva de los LIs se ordena del siguiente modo: $[C_6^{2,4}mmpy][NTf_2]$ > $[C_2mim][NTf_2]$ >> $[C_2mim][DEP]$ > $[C_2mim][OAc]$. La tendencia es la misma que en el caso de la muestra sintética, extrayéndose, tras tres etapas, un 96.5 % del azufre total usando el LI piridinio y un 82 % con el imidazolio.

Es necesario remarcar que los valores de extracción de compuestos azufrados, aun siguiendo la misma tendencia que en los modelos, son menores en el caso de los combustibles reales debido a la mayor complejidad de estos últimos.

CONCLUSIONES

Teniendo en cuenta los datos de equilibrio determinados, se puede concluir que todos los LIs probados son buenos agentes desulfurantes. Además, se observa un altísimo grado de desnitrogenación. La mayor cantidad de disolvente requerida para la separación de los compuestos azufrados de los aromáticos, se traduce en que además de la desulfuración se producirá una importante desaromatización que tendrá que ser considerada en la integración del proceso en una refinería. Atendiendo a los datos de equilibrio, y priorizando los valores de la selectividad, se concluye que el LI más idóneo para la desulfuración es el acetato de1-etil-3-metilimidazolio, $[C_2mim][OAc]$.

Tras estudiar la EDS de gasolina sintética se deduce que el LI con mayor eficacia de desulfuración es el piridinio. Sin embargo, como se predecía a partir del equilibrio, la extracción de compuestos azufrados va acompañada de una importante desaromatización. Por ello, se propone el LI $[C_2mim][OAc]$, con porcentajes muy próximos de desulfuración y una desaromatización mucho menor, como óptimo para la desulfuración de gasolinas. En el caso del diésel sintético, el comportamiento encontrado es el mismo, y las conclusiones idénticas.

El proceso de ODS se muestra inefectivo para la desulfuración de gasolina sintética debido a la baja densidad electrónica del tiofeno. Sin embargo, este proceso optimizado (n_{H2O2}/n_S = 9 y n_{AcOH}/n_S = 9, 323.15 K, 12 horas de agitación y 12 horas de reposo) puede mejorar los resultados de la EDS en el caso del diésel. Los LIs con anión [NTf_2] son los más efectivos para la ODS, alcanzando altísimos valores de desulfuración. De entre estos dos LIs se propone como mejor disolvente el [C_2mim][NTf_2], que tiene un coste mucho menor que el piridinio e implica una menor desaromatización del combustible.

Finalmente, los ensayos con combustibles reales soportan, y en el caso de la gasolina refuerzan, las conclusiones establecidas a partir de los datos de equilibrio y desulfuración de combustibles sintéticos, permitiendo proponer para la desulfuración de gasolina un sistema EDS a 298.15 K con [C_2mim][OAc] y en el caso del diésel un sistema ODS con las condiciones optimizadas citadas anteriormente y utilizando el LI [C_2mim][NTf_2].

Este estudio aporta nueva y valiosa información al proceso de desulfuración de combustibles con LIs. Es importante señalar, no obstante, que no existe una única solución a este problema, y que la extracción de azufre no es el único parámetro a tener en cuenta. La co-extracción de otros compuestos, experimentos en planta piloto, la integración del proceso en una refinería y el análisis de ciclo de vida son, entre otros, aspectos a tener en cuenta en la decisión previa a la implementación de las alternativas aquí propuestas.